Role of nuclear progesterone receptor during bovine oocyte growth and maturation

This thesis is submitted to University College Dublin in fulfilment of the requirements for the degree of Doctor of Philosophy in the School of Agricultural and Food Science

By Julieta Maria D'Augero

(Student number: 20208404)

Head of School: Professor Frank Monahan

Supervisor: Professor Trudee Fair

Table of Contents

List of Figures

List of Tables

Abbreviations

Assisted Reproduction Techniques	ART
In-vitro embryo production	IVP
In-vitro fertilisation	IVF
Progesterone	P4
Progesterone receptors	PR
Nuclear progesterone receptors	nPR
Deoxyribonucleic acid	DNA
Ribonucleic acid	RNA
Messenger ribonucleic acid	mRNA
Ribosomal ribonucleic acid	rRNA
Cumulus-oocyte complex	COC
Germinal Vesicle	GV
Germinal vesicle breakdown	GVBD
Luteinising hormone	LH
Cyclin-dependent kinase 1	CDK1
Cyclic adenosine monophosphate	cAMP
Maturation-promoting factor	MPF
Phosphodiesterase	PDE
Adenosine triphosphate	ATP
C/natriuretic peptide receptor 2	NPPC/NPR2
C-type natriuretic peptide	CNP
Cyclic guanosine monophosphate	cGMP
Subcortical Maternal Complex	SCMC
Cytoplasmic polyadenylation element-binding protein	CPEB
Electron transport chain	ETC
Reactive oxygen species	ROS
Early-antral follicles	EAFs
Germinal vesicle 0 configuration	GV0
Germinal vesicle 1 configuration	GV1
Germinal vesicle 2 configuration	GV2
Germinal vesicle 3 configuration	GV3
In-vitro oocyte culture	IVOC
long IVOC	L-IVOC
Follicular stimulating hormone	FSH
In-vitro growth	IVG
Gonadotrophin-releasing hormone	GnRH
Prostaglandin PF2α	PGF
Oestradiol	E2
Corpus luteum	CL
3-beta hydroxysteroid dehydrogenase/isomerase	3β-HSD

DNA-binding domain	DBD
ligand or hormone binding domain	LBD or HBD
Progesterone response elements	PRE
Membrane progesterone receptors	mPR
G protein-coupled receptors	GPCRs
P4 receptor membrane components 1	PGRMC1
P4 receptor membrane components 2	PGRMC2
Membrane associated P4 receptor protein family	MAPR
PR knockout	PRKO
Artificial insemination	AI
Nuclear progesterone receptor isoform A	nPR-A
Nuclear progesterone receptor isoform B	nPR-B
Insulin-like growth factor I	IGF-I
Interleukin 6	IL-6
Histone	H
Heterochromatin protein 1-γ	HP1γ
Brahma-related gene-1	BRG1
Ribonucleic acid polymerase II	RNA pol II
Metaphase plate II	MII
Metaphase plate I	MI
Aberrant	AB
Degenerated oocyte	DEG
3-isobutyl-1-methylxanthine	IBMX
Foetal calf serum	FCS
Mitochondria deoxyribonucleic acid	mtDNA
False discovery rate	FDR
Gene Ontology	GO

Abstract

The oocyte is the foundation of life, and its development is a meticulously coordinated process involving both nuclear and cytoplasmic maturation, ultimately leading to the acquisition of competence. A competent oocyte, often referred to as a high-quality oocyte, possesses the inherent potential to progress beyond the blastocyst stage and develop into an independent organism. Evidence suggests that increasing circulating progesterone levels during the growth of the dominant follicle can enhance pregnancy rates in sub-fertile cows. Progesterone receptors (PR) have been identified in fully-grown and mature bovine oocytes, implicating a functional role during oocyte maturation and competence acquisition. Despite these findings, the specific molecular and cellular pathways through which progesterone influences oocyte development and maturation remain poorly understood. Therefore, the aim of this thesis is to investigate the expression and functionality of the nuclear progesterone receptor (nPR) during bovine oocyte growth. This research provides crucial insights into nPR timing and functionality, revealing a novel association between nPR and mitochondria in growing bovine oocytes. A comprehensive descriptive analysis demonstrated continuous expression of nPR from the early to late stages of folliculogenesis in both follicle cells and oocytes, with an increase in nPR associated with oocyte size. Functional studies on growing bovine oocytes revealed that nPR negatively affects cumulus-oocyte complex survival and reduces the oocyte's ability to resume meiosis. Further in silico analysis highlighted the enrichment of nuclear and mitochondrial pathways regulated by nPR during oocyte growth. Notably, this research presents the first evidence of nPR and mitochondrial colocalisation in smaller oocytes. The findings of this thesis significantly enhance our understanding of nPR role in oocyte development, emphasizing its importance in determining oocyte quality. These insights could inform future strategies aimed at improving in vitro embryo production and fertility treatments.

Statement of original authorship

I hereby declare authorship of this submitted thesis, presenting my work as a registered PhD student at the University College Dublin.

This project has received funding from the European Union's Horizon 2020 Research and Innovation Programme under the Marie Sklodowska-Curie Grant Agreement N° 86960.

The functional analysis was conducted in collaboration with the Reproductive and Developmental Biology Laboratory (Red BioLab) at the University of Milan, Lodi, Italy.

I have not previously submitted this thesis for examination at University College Dublin or any other university. I authorise University College Dublin to make available, photocopy, or load this thesis for research proposes, upon request.

Candidate Name: Julieta Maria D'Augero.
Candidate ID: 20208404
Date: 04/09/2024

Acknowledgments

I would like to express my sincere thanks to the **Marie Sklodowska-Curie Grant** for providing the essential financial support needed to carry out this research, and to **University College Dublin** for creating an environment that has greatly nurtured my growth as a researcher. The university's facilities, resources, and community have been crucial to my academic journey.

A special thank you goes to my supervisor, **Professor Trudee Fair**. Your guidance, support, and patience have been key to my success. Our many discussions, and your ability to encourage me to find new solutions after each setback were invaluable.

I would also like to thank **Professor Valentina Lodde** for her constant support from the start of this project. Her advice was always helpful, and her kindness means a lot to me. My thanks also go to **Professor Patrick Lonergan** for his guidance, our coffee walks after his lectures, and for his daily humor.

I am incredibly grateful to **Lais Barbosa Latorraca**, who has been more than a friend—she has been my support and my family in Ireland. She was my right hand and my daily companion. I could not have done this without her. **Professor Belen Rabaglino** also deserves special mention; she became a dear friend whom I deeply admire. I am profoundly grateful for all that she has taught me and for her companionship throughout these years. I am also thankful to **Stella Galatidou**, who inspired me with new ideas and supported me through challenging times. I extend my sincere thanks to **Magdalena Ladrón de Guevara**, who not only opened her home to me during my time in Italy but also her heart.

I would like to extend my appreciation to my family: **Walter, Pamela, Milagros, Sol, Bautista** and **Ambar.**. They reminded me that I could reach this goal and recharged me with love every year. Two people deserve special mention: my daughter, **Maia Urioste D'Augero**, who has been my daily source of strength and inspiration. This PhD is dedicated to her, to show her that anything is possible in life. And **Gaston Santoni**, who came into my life at just the right time, giving me the love and support I needed to finish this PhD. His daily encouragement made all the difference in my life.

A big part of this PhD has also been the amazing ESR colleagues I met along the way, some of whom I have already mentioned. They made these years unforgettable: **Berta, Cristina, Aimilia, Rafaella, Andrea, Camilla, Sara, Giorgos, Leah, and Pritha**.

Finally, I want to acknowledge **myself**. This PhD has taught me that no matter what happens, you have to keep trying. Progress is not always straightforward, and true strength comes from overcoming challenges.

Chapter 1

Literature Review

1.1. Introduction

Oocyte biology is crucial to female fertility, involving a complex life cycle that begins with its formation during foetal development, continues through its growth and ovulation, and ends with its depletion at menopause. The oocyte has been extensively studied for a deeper understanding of this cell in female mammalian reproduction and to ultimately produce high-quality oocytes. In cattle, only one oocyte is ovulated per cycle, which limits reproductive success. Consequently, the quality of the oocyte is essential for successful fertilisation. A good quality oocyte is defined as an oocyte that has the capacity to undergo fertilisation, develop to the blastocyst stage, implant and achieve a successful pregnancy. The acquisition of this competence is acquired following a complex process of events which include oocyte growth and nuclear and cytoplasmic maturation.

Over many years, methodologies developed during experiments directed to better understand oocyte development have led to the advancement of Assisted Reproduction Techniques (ARTs), that are now in every day practice. The oocyte is at the centre of these technologies, thus the developmental competence of the oocyte is pivotal to the success of the reproductive intervention. For example, in bovine *in-vitro* embryo production (IVP), 90% of immature oocytes submitted to *in-vitro* maturation (IVM) reach metaphase II stage, and ~80% of those oocytes successfully fertilize *in-vitro* (IVF), followed by cleavage, to the two-cell stage. Typically, only 30 – 40% of oocytes submitted to IVP develop to the blastocyst stage (Lonergan et al., 2001; McGeady et al., 2017). Thus, the quality of the oocyte submitted to IVP is the key limiting factor (Rizos et al., 2002; Lonergan et al., 2003; Lonergan et al., 2006; McGeady et al., 2017).

In cattle, only fully grown oocytes contained within medium or large size antral follicles are routinely used in IVP (for a review see Fair, 2003). The remaining and most abundant store of female gametes in the ovary are the primordial follicles; they constitute the ovarian reserve. Growing oocytes in primary, secondary, and small antral follicles account for this store to a lesser extent. The development of efficient *in-vitro* culture protocols for early-antral follicle derived oocytes may expand the our potential to exploit the ovarian reserve, thus providing more oocytes suitable for ARTs. To this end, knowledge of the physiological requirements of

an oocyte's transition from the growing phase to the fully grown state are essential in order to recapitulate these events *in vitro* and to overcome the current limits of *in-vitro* culture of growing oocytes.

In cattle, evidence shows that supplementing systemic progesterone (P4) using a P4-releasing vaginal device during an oestrous synchronisation programme improves oocyte quality (Wiltbank et al., 2011). While the underlying signalling mechanisms have yet to be elucidated, it is known that fully-grown bovine oocytes and their surrounding cumulus cells express progesterone receptors (PR), moreover, evidence suggests an association with PR activity and oocyte maturation and subsequent potential to sustain embryo development (Luciano et al., 2010; Aparicio et al., 2011; O'Shea et al., 2013; Terzaghi et al., 2016).

1.2. Oogenesis

The mammalian ovary accommodates and drives oocyte and follicle development, maturation, and release of mature oocytes for fertilisation. However, oogenesis begins with the formation of these gonads during fetal life (for a review see Araujo et al., 2014). Primordial germ cells are the precursors of the germline in mammals, having the capacity to become either oocytes or spermatozoa depending on the gonadal environment (McLaren, 1991). In cattle, sexual differentiation occurs between days 40 and 45, when mitotic proliferation of the primordial germ cells commences within the gonad. Once these cells start mitotic divisions, there are referred to as oogonia. The number of oogonia increase up to approximately 2 million per animal before they enter meiosis and form oocytes (Marion & Gier, 1971). However, 95% of these oogonia degenerate before the heifer calf is born (Erickson, 1966). This decline in numbers is regulated by a combination of cell death/survival pathways at each stage of development that ultimately determines the size of the follicle population (Findlay et al., 2015).

Between days 75 and 80 post-conception oogonia enter the prophase of their first meiotic division and are subsequently referred to as primary oocytes. Oocytes progress through the sub- stages leptotene, zygotene, and pachytene of prophase I, eventually arresting at the diplotene stage by day 170 (Erickson, 1966, Baker & Hunter, 1978). Leptotene is characterised by the beginning of recombination and the condensation of chromatin around the developing chromosome axis. During zygotene, chromatin threads start to pair homologously, bringing the

chromosome axes closer together. By the pachytene stage, recombination is complete, and in diplotene, chromosomes begin to desynapse in preparation for the first meiotic division (Bolcun-Filas et al., 2018). The oocyte is then arrested at the diplotene/dictyate stage and will be enclosed within somatic (granulosa) cells to form primordial follicles which constitute the ovarian store of follicles.

1.3. Folliculogenesis and oocyte growth

Folliculogenesis describes the process by which a follicle grows through different stages of development, beginning with its recruitment from the follicular reserve and continuing until it either ovulates or becomes atretic. From day 170 onwards, the oocyte becomes surrounded by a single layer of 4 - 8 flattened granulosa cells and a basal membrane, giving rise to the first stage of follicle development, i.e., the resting primordial follicle. At this stage the pre-granulosa cells stop multiplying and remain in a resting phase until they are stimulated to grow.

During the initiation of follicular growth, in a phase known as primordial follicle activation, some primordial follicles are recruited to exit the reserve pool of quiescent follicles and to enter the growing pool of follicles (primary, secondary, early-antral, antral and preovulatory stage). This is a nonreversible step in folliculogenesis. In cattle, primordial follicles have a mean diameter of 35 µm and oocyte growth is only initiated upon the division and transformation of flatted granulosa cells into cuboidal shape, characteristic of the primary follicle (Hulshof et al., 1994; Fair et al., 1997; Fair, 2003; Aerts & Bols, 2010). A summary of key events and transitions during bovine oocyte growth is shown in Figure 1.1.

Given that primordial follicles lack functional gonadotropin receptors and have limited access to the blood supply, primordial follicle activation is believed to be controlled in a gonadotropin-independent manner, relying on paracrine signaling within the follicle and across the local environment (Oktay et al., 1997). Extensive research using genetically modified mice, *in-vitro* culture experiments, and transcriptomic analysis enabled the identification of master transcriptional factors in the process of granulosa proliferation and differentiation as well as intrafollicular signaling pathways regulating primordial follicle quiescence and entry into growth (for review see Telfer et al., 2023). Knock-out mice studies, revealed that follicles of mice deficient in *Figla*, *Sohlh1*, *Lhx8*, *Nobox*, *Stat3*, *Tbpl2*, *Dynll1* or *Sub1* were not able to

develop beyond the primordial follicle stage, leading to the identification of these transcription factors as critical for follicle activation (Joshi et al., 2007; Choi et al., 2008; Gallardo et al., 2007). Pan et al., 2005 reported that the transcriptome of mice primordial oocytes was unique compared to oocytes obtained from the subsequent stages of follicular development, describing an upregulation in the expression of members of the transforming growth factor (TGF)-β superfamily, including *Bmp15*, *Gdf9*, *Bmp5*, *Bmp6*, *Tgfb2* and *Tgfb3* during primordial follicle activation. Recent work by Hamazaki et al., 2021, identified a set of eight transcription factors (*Sox2*, *Oct4*, *Klf4*, *Myc*, *Prdm1*, *Nr5a2*, *Otx2*, Tfap2c) capable of inducing the transition from primordial to primary follicle stage in mice. The Authors demonstrate that oocyte growth and lineage-specific de novo DNA methylation can occur independently of earlier epigenetic reprogramming events typically seen in primordial germ cells. All this evidence suggests that the transition period between the primordial and primary follicle is a critical check point during oocyte growth. However, it is important to remember that in cattle, the development of these events occur over a much longer time frame as will be detail further.

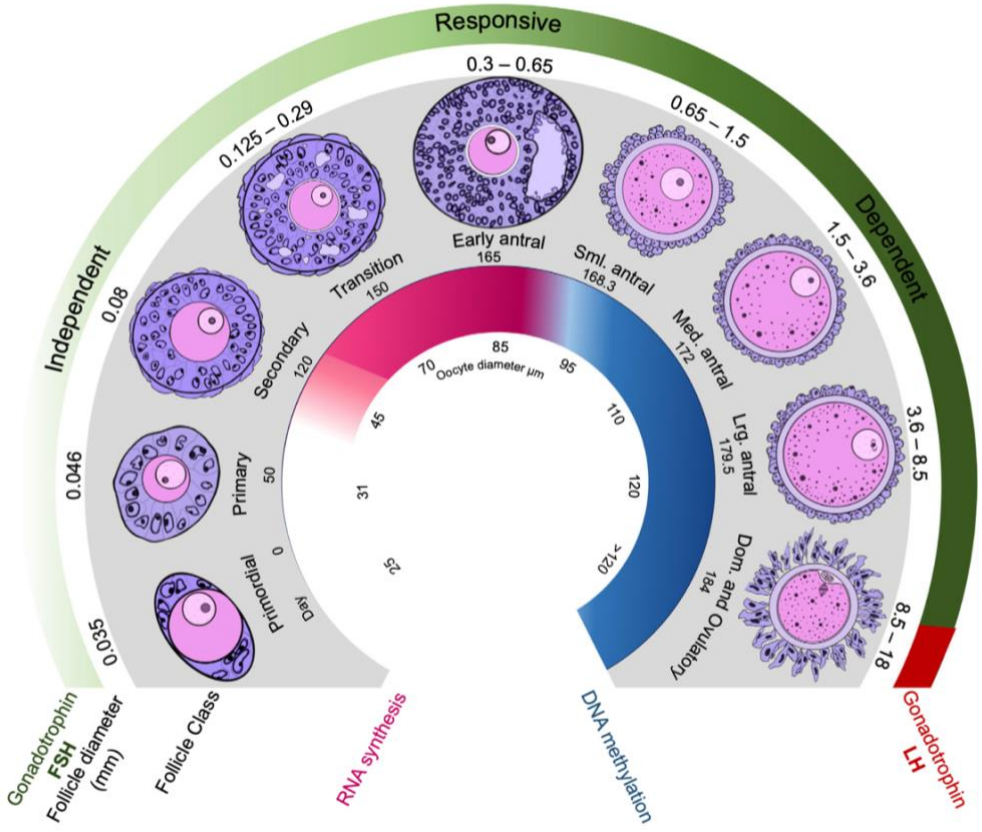

Figure 1.1. Schematic diagram describing oocyte growth and follicle classification in cattle. The schematic diagram illustrates oocyte growth and follicle classification in cattle, detailing the progression of oocyte diameter, RNA synthesis, and DNA methylation alongside follicle class and diameter. Abbreviations: Sml. Antral, small antral follicle; Med. Antral, medium antral follicle; Lrg. Antral, large antral follicle; Dom. and Ovulatory, dominant and ovulatory follicles. FSH, follicle stimulating hormone; LH, luteinising hormone (Fair & Lonergan, 2024).

Over a period of 30 days, progression to the secondary follicle stage is characterised by the appearance of a second layer of granulosa cells and an increase in oocyte volume (Lussier et al., 1987). At this stage, gap junctions appear between granulosa cells, as well as deposition of small patches of zona pellucida around the oocyte and the formation of cortical granules within the oocyte cytoplasm (Fair et al., 1997). Secondary follicles appear in the bovine foetal ovary in a range from 46 μm to 250 μm in diameter (from early to late secondary follicles), while the oocyte within these follicle measures starts in 30 μm and ends up in 70 μm (Lussier et al., 1987; for review see Fair & Lonergan, 2023). Recently single cell RNAseq analysis of individual bovine oocytes across the growth phase, revealed a higher expression of *BMP15*, *NLRP2*, *NLRP5*, *PADI6*, and *TLE6* in oocytes from 70 to 110 μm in diameter (Barbosa-Latorraca et al, 2024). As described before, *BMP15*, is an oocyte secreted factor critical for follicle development and cell proliferation (for review see Paulini & Melo, 2010). The events of the secondary follicle stage were previously proposed to correspond to the marked changes observed in the oocyte transcriptome during the primordial to primary follicle transition in mouse oocytes (Fair & Lonergan, 2023).

In the following growth stage, granulosa cells organise in several layers and an antral cavity filled with follicular fluid is formed among these cells. The formation of the antrum leads to the differentiation of the granulosa cells into two distinct populations, the mural granulosa cells which line the antrum, and the cumulus granulosa cells which surround the oocyte, forming the cumulus oocyte-complex (COC) (Fair et al., 1997). From this moment onwards, the follicles are called tertiary or early-antral follicles. In cattle, this stage is described by follicles measuring around 0.3 up to 1-3 mm in diameter, represented by oocytes from 80 – 110 μm of diameter (for review see Fair & Lonergan, 2023).

The transition from secondary to early-antral follicle includes the development of the internal and external theca cell layers; and as mentioned before, the differentiation of cumulus cells. These cumulus cells produce projections, called transzonal projections, that penetrate the zona pellucida, invaginate the oolemma, and establish bi-directional communications through gap junctional contact with the oocyte, called transzonal projections (for review see Clarke, 2022). This dialog allows granulosa cells to support oocyte growth and meiotic progression and to modulate their transcriptional activity (Brower & Schultz, 1982; Eppig, 1991). In turn, oocytes control granulosa cell proliferation and differentiation into steroid-secreting factors (Richani et al., 2021).

This period of oocyte growth is characterised by intensive messenger RNA (mRNA) and ribosomal RNA (rRNA) transcription, an increase in oocyte volume and further proliferation of the oocyte organelles (for review, see Fair 2003). The transcriptional activity of these oocytes in the early-antral follicles continues until the follicle reaches 2–3 mm within an oocyte corresponding a 110 μm of diameter (Fair et al., 1996). The accumulation of mRNAs, ribosomes and polypeptides by the oocyte during the growth phase is crucial to achieve competence. Some transcripts are immediately translated to support oocyte growth, while others, essential for future maturation and fertilisation, are stored for later translation (Susor et al., 2016). Continuous research on this subject provides new insights to the importance of this storing event. A study demonstrated that in the absence of MSY2, a germ cell-specific RNA-binding protein implicated in regulating mRNA stability, lead to compromised fertility in female mice (Medvedev et al., 2011). Additionally, Cheng et al., 2023 described a novel structure in mammalian oocytes called the mitochondria-associated ribonucleoprotein domain (MARDO), which serves as a storage site for maternal mRNA during the final stages of oocyte growth when oocytes are transcriptionally inactive. Recent data from Barbosa-Latorraca et al., 2024 from a single cell RNAseq transcriptomic analysis in growing bovine oocytes revealed a continuous increase of *ZAR1L* expression throughout oocyte growth. The proteins ZAR1 and ZAR2 (also known as ZAR1L) participate in mRNA storage and oocyte maturation (for review see Wu & Fan, 2022). Thus, the increase in *ZAR1L* expression suggests its role in mRNA storage towards the end of the bovine oocyte growth phase.

Follicle and oocyte grow in parallel until the follicle reaches a diameter of 3 mm, after that, the oocyte diameter plateaus at about 120-130 μm, while the follicle continues the growth up to 15-20 mm in diameter (Fair et al., 1995). Differential genes expression analysis between oocyte size groups revealed that at this stage of oocyte growth there is an upregulation of genes involved in chromatin condensation and suppression of transcription. One of these genes is *DPPA3* (also known as *STELLA*), which is essential for chromatin condensation (Liu et al., 2012; Barbosa-Latorraca et al., 2024).

Bovine oocytes achieve full meiotic competence at a diameter of 110 to 115 μm, and developmental competence is acquired at 120 μm oocyte diameter (Fair et al., 1997).

1.4. Oocyte maturation

Final oocyte maturation *in-vivo* takes place within the dominant follicle, which reaches its peak size just as the acute preovulatory surge of LH occurs, typically within six hours of standing estrus (Chenault et al., 1975). If the follicle remains as dominant and receive the luteinising hormone (LH) signal to ovulate, the final maturation of the oocyte occurs. LH stimulates oocyte maturation via its action on the theca and granulosa cells. This process is characterised by the breakdown of the large oocyte nucleus and release of its nucleoplasm into the cytoplasm, a process known as a germinal vesicle breakdown (GVBD). Subsequently, the chromosomes condense and progress through the final stages of meiosis I and arrest at metaphase of meiosis II. Additional ultrastructural changes occur within the oocyte, which include an increase in lipid content, a decrease in the size of the Golgi complexes and a more superficial location of the cortical granules (for review see Fair, 2003). These orchestred events can be categorised into nuclear and cytoplasmic maturation.

1.4.1. Nuclear maturation

The acquisition of meiotic competence is marked by the oocyte accumulation of maturation-promoting proteins, like cyclin-dependent kinase 1 (CDK1) and cyclin, which together form maturation-promoting factor (MPF; a heterodimer of CDK1 and cyclin B1, B2, and B3) (de Vant'ery et al., 1996; de Vant'ery et al., 1997). While growing, the accumulation of CDK1 and cyclin B1 increase, as well as their affinity to combine, therefore the MPF needs to be inhibited to prevent the premature resumption of meiosis (Masui & Markert, 1971). This arrest is maintained by elevated levels of cyclic adenosine monophosphate AMP (cAMP) within the oocyte and support from surrounding somatic cells (for review see Conti et al., 2002). When intracellular cAMP levels are elevated a cascade of events leads to the phosphorylation of CDK1 and its inhibition, thus making MPF inactive and holding the oocyte in meiotic arrest (Maller & Krebs, 1980).

The synthesis of cAMP originates with the adenosine triphosphate (ATP) via adenylyl cyclase, whereas cAMP degradation is ruled by phosphodiesterases (PDEs). Although oocyte production of cAMP is the major pathway in regulating meiotic arrest, somatic cells also have an indirect role in maintaining elevated cAMP levels within the oocyte. The granulosa cells

production of cyclic guanosine monophosphate (cGMP) inhibits the degradation of cAMP by inhibiting PDE3 activity in the oocyte. This is mediated via the natriuretic peptide C/natriuretic peptide receptor 2 (NPPC/NPR2) system. C-type natriuretic peptide (CNP) is produced in mural granulosa cells, and its receptor NPR2 (a member of the guanyl cyclase receptor family) is expressed within cumulus granulosa cells (Zhang et al., 2010).

Therefore, the LH signal reduces the cAMP level downregulating the NPPC/NPR2 system and closing gap junctions between the oocyte and cumulus cells. By affecting this system and disrupting cell-cell communication, cAMP and cGMP levels are reduced within the oocyte leading to the phosphorylation of PDE3A and the degradation of cAMP. This sequence of events results in the synthesis of MPF and phosphorylation of proteins such as the anaphase-promoting complex leading to the resumption of meiosis and driving the formation of the first meiotic spindle (Adhikari & Liu, 2013).

This marks the start of metaphase I with compaction of chromosomes and the homologs orient on the metaphase I plate and segregating at anaphase I leading to the extrusion of one set of chromosomes in the first polar body. This first division is an even division of chromosomes but uneven of cytoplasm. Following this division, a second spindle forms, and the chromosomes align on the spindle. Meiosis is arrested for a second time at metaphase II and will remain arrested until fertilisation or degeneration. Fertilisation initiates the resumption of meiosis and the separation of sister chromatids (for review see Telfer et al., 2023).

A recent study by Hu et al., using transcriptome and translatome sequencing of single-cell oocyte samples during human oocyte maturation revealed the functionality of oocyte secreted protein, OOSP2, as a maturation factor in this specie. Interestingly, Wang et al., 2023 described that long non-coding RNA in bovine oocytes participate in oocyte maturation, identifying several key pathways enrichment such as FoxO signaling, Wnt signaling and P4-mediated oocyte maturation. Mogessie & Schuh, 2017 also demonstrated that actin filaments play a critical role in ensuring the accurate alignment and segregation of chromosomes in mammalian eggs, thereby preventing aneuploidy during meiosis. Therefore, nuclear and cytoplasmic maturation are key processes in the final acquisition of oocyte competence.

1.4.2. Cytoplasmic maturation

The cytoplasmic maturation involves three key events: the molecular maturation, changes in cytoskeletal filament dynamics, and the redistribution of cytoplasmic organelles (Ferreira et al., 2009).

Molecular maturation involves the efficient production, storage and processing of the mRNA for posterior critical periods of fertilisation and early embryonic development. The Subcortical Maternal Complex (SCMC) is a multiprotein complex; the core components include: *NLRP5*, *TLE6*, *KHDC3L*, *OOEP*, *NLRP2*, and *PADI6*. These genes are expressed predominantly in oocytes and early embryos and play crucial roles in the stability of the oocyte cytoplasm and in the successful progression through early stages of development after fertilisation. Mutations or dysfunction in any of these genes can lead to early embryonic arrest or other reproductive issues (for review see Bebbere et al., 2021). Evidence demonstrated that these complexes are involved in organelle distribution, mRNA storage and spindle localisation (Fernandes et al., 2012; Yu et al., 2014; Liu et al., 2017). Recent work by Jentoft et al., 2023 showed that cytoplasmic lattices are filament structures where the oocyte stores essential proteins. The Authors demonstrated that peptidyl arginine SCMC proteins were contained in the lattices, and that knockout of these genes resulted in an early embryonic arrest in mice. Recent bovine transcriptomic data identified several maternal-effect genes associated with oocyte growth; the expression of *BMP15*, *NLRP2*, *NLRP5*, *PADI6*, and *TLE6* was increased in the mid-phase of oocyte growth (from 70 to 110 μm in diameter) (Barbosa-Latorraca et al., 2024). Another essential process for maintaining the integrity of the oocyte's cytoplasm was found by Zaffagnini et al., 2024. This group demonstrated that mouse oocytes accumulate protein aggregates in specialised compartments named endo-lysosomal vesicular assemblies (ELVAs). These super-organelles help manage and degrade misfolded or damaged proteins, thereby preventing their accumulation, which could otherwise lead to cellular dysfunction.

As mentioned above, the progression from GVBD to metaphase II is dependent on cytoskeleton dynamics. Chromosomes are segregated by a microtubule spindle, but in oocytes, this assembles in the absence of centrosomes. The structure usually serves as a microtubule nucleation which forms the two poles of meiotic spindles. Despite the absence of centrosomes, mammalian oocytes express centrosomal proteins, several of these proteins have been identified in the acentriolar microtubule organizing centers (Schuh & Ellenberg , 2007). A

study conducted by So et al., 2009 described that the acentrosomal spindle assembly is helped by a domain that contains multiple microtubule regulatory factors called liquid-like meiotic spindle domains. Nevertheless, formation of microtubules after the GVBD is delayed, an alternative chromosome migration and clustering mechanism was characterised at this stage: Actin cables form in the disassembling nucleus moving the chromosomes until a cage of stable microtubules, which drives the later stages of chromosome clustering (Harasimov et al., 2023). These findings were reported in human and mice oocytes, however the similar timeline of meiotic events suggests that could be applicable for bovine too. Additionally, Uzbekova et al. 2008 described that phosphorylation of cytoplasmic polyadenylation element-binding protein (CPEB) by Aurora-A kinase, modulates these cytoskeletal processes, ensuring the correct alignment and segregation of chromosomes during oocyte maturation.

During oocyte maturation several ultrastructural changes regarding morphology and redistribution were described in cytoplasmic organelles. These movements is guided by cytoskeletal microfilaments and microtubules, with their positions shifting according to the requirements of the oocyte at each stage of development. During the GV stage, when the nucleolus is active and ribosomal RNA transcription is ongoing, there is a production of ribosomes that supports mRNA translation. This contributes to a greater accumulation of ribosomes in oocytes at the metaphase I stage (Van Blerkom et al., 2000). It had been described that bovine oocytes in the GV stage present Golgi fragments that are transformed into vesicles during GVBD, nevertheless the dynamics of the Golgi membranes during maturation and fertilisation in mammals requires more study (Moreno et al., 2002; Payne & Schatten, 2003). A recent publication by Zhang et al., 2024 revealed that a small GTPase regulate retrograde and intra-Golgi transport and spindle organizsation during oocyte meiosis in mice. *In-vivo* studies of mouse oocytes at the GV stage have shown that the endoplasmic reticulum (ER) is uniformly distributed throughout the ooplasm. As the oocyte develops to the metaphase II stage, the ER relocates to the cortical regions and forms small clusters, 1–2 μm in size, dispersed throughout the cytoplasm (Kline, 2000; Stricker, 2006). The cortical granules are organelles exclusively found in oocytes and their composition includes a diverse population of proteins, structural molecules, enzymes, and glycosaminoglycans. In the GV stage, cortical granules are distributed in clusters throughout the cytoplasm, whereas at the end of the maturation period, the granules are distributed throughout the inner surface close to the plasma membrane. This pattern is strategically arranged for their exocytosis when the sperm reach the oocyte to prevent polyspermy (Hosoe & Shioya, 1997). Among all these organelles,

mitochondria had been extensively studied in oocytes. As mitochondria are a primary focus of this thesis, they are addressed in greater detail below.

1.5. Mitochondria

The movement of mitochondria to areas of high energy consumption is crucial for oocytes and embryo blastomeres during critical periods of the cell cycle. During oocyte maturation, mitochondria synthesizes the ATP necessary for the synthesis of proteins which, in turn, supports the completion of subsequent maturation processes and embryo development (Stojakovic et al., 2001, for review see van der Reest et al., 2021).

Mitochondria are maternally inherited organelles responsible for the production of most cellular energy in the form of ATP, through oxidative phosphorylation (Cummins, 2004). A series of large membrane protein complexes (I – V), in the inner mitochondrial membrane are responsible for this process, known as the electron transport chain (ETC). The ETC takes electrons from metabolites and uses their energy to build a proton gradient across the inner mitochondrial membrane, which in turn powers production of ATP (Sousa et al., 2008). The majority of the correct functioning of mitochondria is based on the large electrochemical proton gradient, whose component, the inner mitochondrial membrane potential, is strictly controlled by ion transport through mitochondrial membranes (Szabo & Szewczyk, 2023).

Mitochondrial ATP generation and reactive oxygen species (ROS) production are intimately related through the function of the ETC; thus, efficient measurement of ETC is required for a correct mitochondria functionality. Under normal physiological conditions, a small amount of ROS is produced in mitochondria owing to electron leakage from the ETC. However, mitochondria are highly susceptible to damage induced by ROS. In particular, the mitochondrial genomic DNA responsible for encoding core elements of the ETC lacks histone protection, antioxidant defenses, and effective DNA repair systems, therefore is prone to ROS damage (Nolfi-Donegan et al., 2020; Wang et al., 2021).

Although there is a substantial body of literature about mitochondria and the impact of ageing, research investigating the behavior of the mitochondria complex during oocyte growth is limited. Recent work from our group revealed that the expression of a cohort of genes related

to energy production through the ETC was negatively correlated with bovine oocyte size (Barbosa-Latorraca et al., 2024). These findings suggest that as the oocyte grows and increases in diameter, there is a decrease in mitochondrial activity. Additionally, data published by Rodriguez Nuevo et al., 2022 revealed that human primordial oocytes and *Xenopus* stage I oocytes (equivalents) do not present assembled or active mitochondrial complex I, suggesting this suppression as an evolutionarily conserved strategy that allows oocyte longevity by avoiding reactive oxygen species exposure.

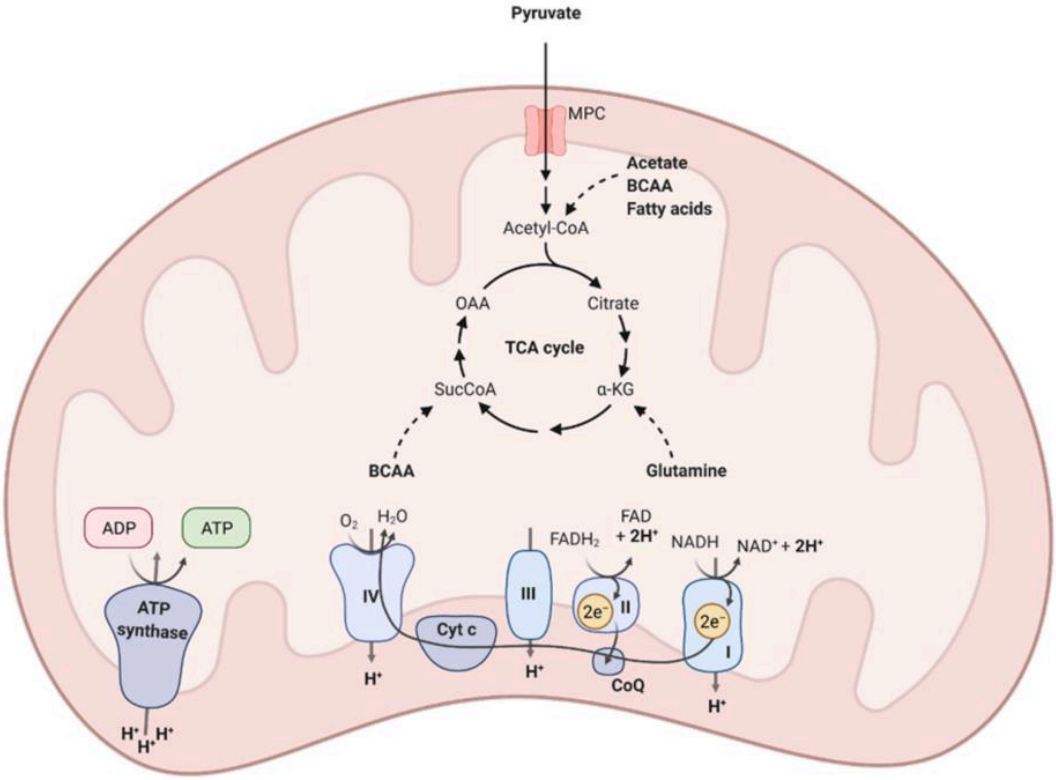

Figure 1.2. Representation of the electron transport chain that supports the process of oxidative phosphorylation in the mitochondria. Pyruvate produced from glucose in glycolysis is imported into the mitochondria and further oxidised in the TCA cycle to yield the electron carriers NADH and FADH2. The ETC complexes accept and transport electrons along the mitochondrial membrane, while pumping protons into the intermembrane space through the mitochondrial complex (I – V), which generates the electrochemical gradient that drives ATP production by ATP synthase. Abbreviations: MPC = mitochondrial pyruvate carrier, SucCoa = succinyl-CoA, OAA = oxaloacetate, α-KG = alpha-ketoglutarate, CoQ = coenzyme Q, Cyt c = cytochrome c. (see (van der Reest et al., 2021).

1.6. I*n-vitro* oocyte maturation

In-vitro oocyte maturation is the first step in the process of IVP in human and domestic species and provides the possibility to exploit what is a largely untapped biological resource (Lonergan & Fair, 2016).

Ultrastructural analysis of bovine oocytes matured *in-vitro* indicates their morphological changes closely resemble those occurring *in-vivo* with minor differences (Hyttel et al., 1986). Oocytes aspirated from their follicles can spontaneously resume meiosis and complete at least nuclear maturation when cultured in suitable media (Edwards, 1965). This was first demonstrated by Pincus and Enzmann, 1935 who showed the progression of oocytes from prophase I to metaphase II. Diakinesis occurs around 5-6hrs after placing bovine oocytes in culture (*Brackett*, 1985). The migration of cortical granules *in-vitro* was shown to be comparable to the *in-vivo* process (Hyttel et al., 1986).

The developmental ability of an oocyte to become an embryo depends on it having enough specific information in the form of mRNA or proteins. If these are missing or insufficient, *in vitro* development will be impacted (Machatkova et al., 2004). Some important factors have been identified which influence the fate of bovine oocyte maturation *in vitro*. These include the follicle size from which the oocyte is aspirated, the presence or absence of cumulus cells, and the morphology of the cumulus cells. While IVM is well-established for fully-grown bovine oocytes (>120 μm), smaller oocytes require an additional period of culture and/or prematuration, however, successful *in-vitro* culture of growing follicles or oocytes <120 μm is a challenge.

1.7. I*n-vitro* oocyte growth culture

Despite the mammalian ovary's potential to produce thousands of oocytes housed in follicles at different stages of development, only a small fraction mature to a stage where they can generate viable embryos and be effectively used in IVP. In cows, only fully grown oocytes from medium and large antral follicles are typically utilised in IVP (for review see Fair, 2003). The remaining and most abundant part constitutes oocytes enclosed in primordial follicles and, in a smaller proportion, growing oocytes in primary, secondary, and small antral follicles

(EAFs). However, the oocytes contained in these follicle populations are not equipped with the molecular, biochemical, and cellular machinery that allows meiosis resumption and the formation of an egg suitable for fertilisation and embryo development (Reviewed by Fair, 2003; Garcia-Barros et al., 2023).

Growing bovine oocytes isolated from EAFs (0.5–2 mm) display uncondensed and dispersed chromatin within the GV, characterised as the GV0 configuration (Lodde et al., 2007). At this stage, described in the folliculogenesis section, the oocytes are transcriptionally active and maintain functional connections with surrounding cumulus cells via gap junctions (Lodde et al., 2007, 2008). However, they lack the ability to spontaneously resume meiosis or support embryo development. Oocytes within mid-antral follicles (2–8 mm), undergo significant changes associated with the completion of their growth phase, including the shift from GV0 to more compact chromatin configurations, namely GV1, GV2, and GV3 (Luciano et al., 2014). This transition is marked by progressive transcriptional silencing, alterations in epigenetic markers, and redistribution of cytoplasmic organelles (Lodde et al., 2008; Lodde et al., 2009; Labrecque et al., 2015).

The *in-vitro* oocyte culture (IVOC) system from growing bovine isolated from EAFs provides the platform to support the progressive acquisition of meiotic and developmental competence and the possibility to understand this complex orchestic event. Luciano and co-workers developed a system called long IVOC (L-IVOC), which focuses on maintaining adequate cyclic nucleotides levels by combining low FSH levels and the PDE3 inhibitor cilostamide to promote functional gap junction-mediated communications between oocytes and their cumulus cells. With this approach, approximately 40% of oocytes that progressed through the IVOC protocol successfully resumed meiosis and achieved metaphase II after IVM (Garcia-Barros, 2023).

Similarly, Japanese researchers also developed an *in-vitro* growth (IVG) culture system for bovine oocytes. In their study, oocytes grew from approximately 92 to ~114 μm in diameter, using an 8-day IVG system divided into two phases. This system included supplementation with the antioxidant astaxanthin and with hypoxanthine, a purine catabolite known to inhibit meiotic resumption and a key component of follicular fluid. In the first phase, COCs were cultured under 5% oxygen for 4 days, followed by a shift to 20% oxygen for an additional 4 days (Chelenga et al., 2022). After IVG, COCs underwent a 5-hour pre-in vitro maturation

(pre-IVM) culture in the presence of IBMX, followed by 24 hours of in-vitro maturation (IVM). The researchers reported that the oocytes achieved a maturation II (MII) progression rate of nearly 70% after IVM, and the inclusion of a pre-IVM step resulted in a 22% in-vitro blastocyst development rate for IVG COCs (Chelenga et al., 2023).

The variations in oocyte survival and meiotic progression rates observed between these systems can likely be attributed to the inclusion of fetal calf serum in the Japanese system, in contrast to its exclusion in the Italian system. Establishing a reliable and consistent IVOC system would be highly valuable for research, enabling detailed studies of bovine oocyte growth and providing insight into the factors that regulate this process.

1.8. Estrous cycle and follicle growth

Cattle are polyoestrous animals and display oestrous behaviour approximately every 21 days. The cycle is divided into two distinct phases and four stages according to the dominant structure present in the ovary. The phases are the follicular and the luteal phase. In the follicular phase, the primary structure present in the ovary is a dominant follicle and is characterised to last from the regression of the corpus luteum to the ovulation of the dominant follicle. In the luteal phase, the dominant structure present in the ovary is the corpus luteum and is characterised from the time of ovulation until corpus luteum regression.

Estrous cycle stages are subdivisions of the follicular and luteal phases. Proestrus and estrus are part of the follicular phase and metestrus and diestrus comprise the luteal phase. Proestrus begins when P4 declines as a result of luteolysis (corpus luteum regression) and lasts about 3 days. Estrus is characterised by behavioural symptoms such as sexual receptivity and mating due to high oestradiol (E2) influence. It has a duration period that ranges from 6 to 24 h and ovulation occurs 24 to 32 h after onset of estrus. Metestrus is the period of corpus luteum formation after ovulation, and lasts 2 to 5 days. Diestrus is the longest stage of the estrous cycle (10 to 14 d) and is the period when the corpus luteum is fully functional and P4 concentration is high and ends with luteolysis process (Fortune, 1994).

The estrous cycle is regulated by the hormones of the hypothalamus (gonadotrophin-releasing hormone; GnRH), the anterior pituitary (FSH, and LH), the ovaries (P4, E2, and

inhibins) and the uterus (prostaglandin PF2α; PGF). These hormones function through a system of positive and negative feedback to govern the oestrous cycle of cattle (Roche, 1996). GnRHs control the oestrous cycle through its actions on the anterior pituitary which regulates LH and FSH secretion (Schally et. al, 1971). After transportation of GnRH from the hypothalamus to the pituitary gland, a series of signaling pathways respond to this stimulus and culminates in the release of FSH and LH from storage compartments (Weck et al., 1998).

During the follicular phase of the oestrous cycle there is a hormonal environment of basal P4 due to the regression of the corpus luteum (CL). Also, there is an increase in E2 concentrations from the rapid proliferation of the pre-ovulatory dominant follicle, concomitant with the decrease in circulating concentrations of P4, which induces a surge in GnRH and allows the display of behavioural oestrus during which heifers/cows are sexually receptive and will stand to be mounted (Frandson et al., 2003). This pre-ovulatory GnRH surge induces a coincidental LH and FSH surge (Sunderland et al., 1994). Only when serum P4 concentrations are basal and LH pulses occur every 40–70min for 2–3 days will the dominant follicle ovulate. Ovulation occurs 10–14 hours after oestrus and is followed by the luteal phase of the oestrous cycle (Roche, 1996).

The luteal phase is characterised by the formation of the CL from the collapsed ovulated follicle and an increase in P4 concentrations due to the formation of this structure. This luteinisation process is characterised by the transformation of the granulosa and theca cells to produce P4 in readiness for the establishment and maintenance of pregnancy and/or resumption of the oestrous cycle (Niswender, 1981). While P4 concentrations remain elevated, 2-3 consecutive waves of follicle growth are initiated in response to a rise in serum FSH concentration. FSH-sensitive follicles respond to the increased serum FSH concentrations by forming a cohort of growing follicles. Nevertheless, this occurs while P4 concentrations remain elevated, preventing the ovulation of these dominant follicles. The P4 dominant luteal phase of the oestrous cycle, through negative feedback, only allows the secretion of greater amplitude but lesser frequency LH pulses that are inadequate for ovulation of the dominant. Finally, in the absence of a pregnancy, the CL regresses in response to PGF secretion from the uterus and P4 concentrations decrease. However, in the presence of a pregnancy, the CL remains, as well as the P4 concentrations, decreasing gonadotrophin secretion and preventing behavioural oestrus occurring (Hansel & Convey, 1983).

1.9. Progesterone and progesterone receptors

Progesterone is a steroidal hormone synthesised by luteal cells of the CL present in the ovary during the luteal phase. As a steroidal hormone, the principle precursor for its synthesis is cholesterol, which is transported into the mitochondria inside the cell. In the inner mitochondrial membrane the cholesterol is cleaved to form pregnenolone, and then is converted to P4 by the enzyme 3beta-hydroxysteroid dehydrogenase/isomerase (3β-HSD) in the smooth endoplasmic reticulum (Niswender, 2002).

The role of P4 is the maintenance of pregnancy, preparing the reproductive tract for embryo implantation and the subsequent maintenance of the pregnant state (Lonergan et al., 2016; for review see Lonergan & Sanchez et al., 2020). Also, P4 inhibits the anterior pituitary gonadotropin secretion by acting on the hypothalamus; therefore, inhibiting follicular development (Hadley, 2000).

1.9.1. Nuclear Progesterone Receptor

Progesterone effects are primarily transduced through the classical signalling pathway via ligand binding to PRs. These ligand-bound PRs subsequently bind to gene regulatory regions including progesterone response elements to initiate transcription of progesterone-responsive genes. Classical progesterone actions are mediated by nuclear progesterone receptors (nPRs). There are two well described nPR isoforms: PR-A (94 kDa) and PR-B (120 kDa). Transcripts for both A and B isoforms encode an N-terminal A/B domain that regulates transcriptional efficiency, a C domain or DNA-binding domain (DBD), a D domain or hinge region, and the E/F domains responsible for ligand or hormone binding (LBD or HBD) (Wen et al., 1994). Both isoforms arise from differential promoter usage in a single gene, and PR-A differs from PR-B only in that it is 164 amino acids shorter at the amino-terminus.

There is a third isoform that is truncated in the N-terminally, named PR-C (45–50 kDa). This isoform lacks the first zinc finger of the DBD, consequently lacking DNA-binding activity but retained the ligand binding properties of full-length receptors. Thus, one mechanism of action of the C isoform is to antagonize PR-A or -B activation by sequestering progesterone (Garg, 2017; Gellersen, 2008) (Figure 1.3).

A less well-known isoform is the mitochondrial progesterone receptor (PR-M), which is smaller in size than both PR-A and PR-B (Saner et al., 2003). PR-M contains the hinge and HBD, however lacks the N-terminus A/B domains and the C domain for DNA binding. The lack of a DBD in PR-M precludes direct regulation of gene transcription. The unique N-terminus is hydrophobic with poor antigenicity, characteristic of a transmembrane domain. PR-M has been localised to the outer mitochondrial membrane and its functionality is to increase cellular respiration by enhancing oxidative phosphorylation and subsequent ATP production (Dai et al., 2013; Shaia et al., 2023).

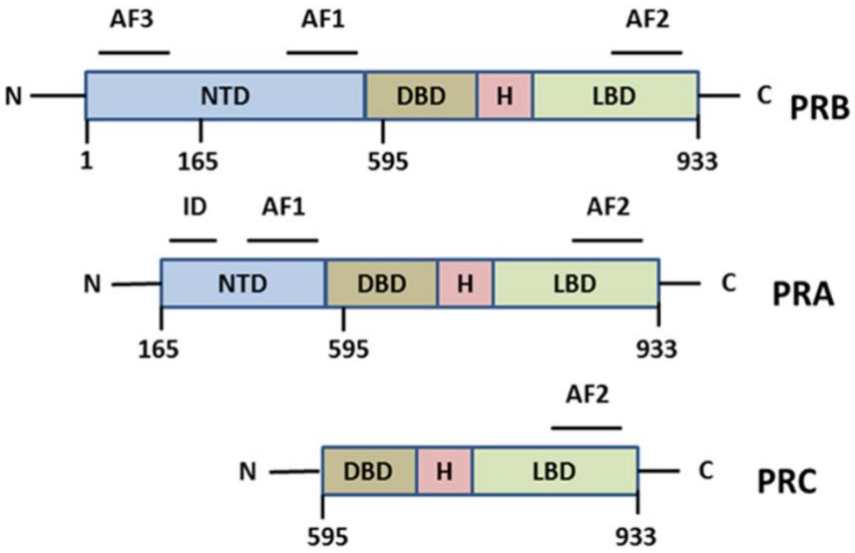

Figure 1.3. Structure of different isoforms of progesterone receptors. The PR consist of four different domains, NTD represents the N-terminal transactivation domain, DBD represents the DNA binding domain, a hinge region, and LBD represent the Ligand-binding domain. AF1, AF2, and AF3 are activation function domains (for review see Azeez et al., 2021).

1.9.1.1. Progesterone response element

The principal feature of nPR is their ability to interact with DNA in response to hormone binding or other signals and then to recruit multiprotein complexes that control gene expression. This classical activation of genomic receptors is a slow and complex process.

In the absence of P4, PRs reside in the cytoplasm, forming a complex with chaperone proteins. These chaperones hold the receptor in an inactive state, primed to bind to ligands

(Pratt & Toft, 1997). Upon ligand binding, PR undergoes a conformational change that triggers release from the chaperone complex and favors receptor dimerisation. The receptor/chaperone complex then travels along the cytoskeleton to the nucleus, a process called the "transportosome" (Pratt et al., 1999). In the nucleus, the complex dissociates, and chaperones help regulate the DNA binding and transcriptional activities of the steroid receptors (Davies et al., 2002; Thackray et al., 2003). The DBD of the receptor provides specificity for target genes, recognizing DNA sequences known as progesterone response elements (PREs) in the enhancer/promoter regions of those genes, which link the receptors to the cellular transcription machinery and regulate gene transcription (Qi-Liang et al., 2016).

Upon the binding of the receptor to the PRE, the activated receptor then interacts with co-activators, which will link the steroid hormone receptor to the basal transcriptional machinery of the cell. The co-activators not only link the receptor to the transcription machinery, but also facilitate transcription by modifying the chromatin to facilitate the transcription of specific genes. In mice, PR has a specific sequence motif consisting of a palindromic hormone response element “AGAACAnnnTGTTCT” (Ham et al., 1988). However, PR binding is not limited to the full PRE, it was demonstrated that PR can also bind to promoters of known progesterone target genes such as *Lifr*, *Gata2*, *Cyp26a1*, and *Ihh* with just half the sequence of the normal PRE (Rubel et al., 2012).

1.9.2. Membrane progesterone receptors

Recently, an alternative pathway that can be dependent or independent of transcriptional or genomic regulation was described (Mueck et al., 2014). In this non-classical pathway, various second messengers and signal transduction pathways play an important role to exert rapid hormonal effects mediated by non-classical signalling. Although non-classical P4-dependent actions may be rapid, the downstream consequences can be intense and sustained (for review see Thomas, 2022).

Specific membrane-bound PRs (mPRs), also called PAQRs (progestin and adipoQ receptors), have been implicated in non-genomic progesterone action and participate in the regulation of membrane-associated progesterone signalling event. There are three mPR isoforms, mPRα, mPRβ, and mPRγ, and recently two more were added to this category, mPRδ

and mPRε. All these receptors are characterised for having seven transmembrane domains, similarly to G protein-coupled receptors (GPCRs). P4 mediates its non-genomic effects P4 mediates its nongenomic effects through the nongenomic P4 receptor membrane components 1 and 2 (PGRMC1 and PGRMC2), which belong to the membrane associated P4 receptor (MAPR) protein family (Calhill, 2007; Garg et al., 2017).

Both, the non-genomic and genomic mechanisms of action are not only connected but work in conjunction to produce a cell-specific progesterone response.

1.10. Role of PR in the ovary

The role of PR in rodent reproduction was revealed through interrogation of the PR knockout (PRKO) mouse model, in which both isoforms of PR were not expressed. These animals displayed defects in all reproductive tissues, including impaired uterine hyperplasia, lack of mammary gland development, attenuated lordotic behavior and the inability to release the oocyte from the follicle, even after exogenous superovulation treatments (Lydon et al., 1995; Chappell et al., 1997).

In rodents, PR expression in the ovary is temporal. In the PRlacZ mouse model, where the lacZ reporter is placed within exon 1 of the PR gene, the expression of this receptor was detected within 4 h of the LH surge, specifically in the mural granulosa cells of preovulatory follicles (Ismail et al., 2002). Teilman et al. (2006) demonstrated the localisation of PR in the mural granulosa cells of mouse preovulatory follicles, transiently up regulated at 4 h and 8 h post-hCG (mimicking the LH surge), and undetectable by 12 h (Teilman et al., 2006). In response to the LH surge, PR is expressed at higher levels in the mural granulosa cells, but not in the cumulus cells (Teilman et al., 2006; Smith et al., 2022).

Unlike the transient pattern of PR described in rodents, primates and humans display more prolonged expression of PR in the ovary, due to the extended luteal phase in these species. In primates, PR expression was described in granulosa cells of primordial and primary follicles, but not in granulosa cells of follicles beyond this stage. However, PR expression in the thecal

layers is continuous during the menstrual cycle. Regarding the oocyte, no expression was described for the PR from primordial to small antral follicles (Hild-Petito et al., 1988).

There are few studies on PR expression in the human ovary. Consistent with the findings in other species, PR is expressed in the theca cells of the dominant follicle at the time of LH surge (Iwai et al., 1990; Suzuki et al., 1994). While Szuki et al. (1994) reported the absence of PR expression in granulosa cells from primordial to preantral follicles, this contrasted with the report of Revelli et al., 1996, which described PR expression in the granulosa cells from primordial to antral follicles, as well as in theca cells from preantral and antral follicles, suggesting a potential role of the P4 in follicular development and recruitment.

The two main isoforms of the progesterone receptor, PR-A and PR-B are present in a tissue-specific, tightly controlled ratio to transcriptionally regulate functions across the entire reproductive system (Peavey et al., 2021). Specifically, PR-A is highly expressed in preovulatory follicles in rats and mice, while the PR-B isoform is detected throughout the ovary (Robker, Akison & Russell, 2009). Mouse knockout experiments have also helped to elucidate the specific roles of individual PR isoforms in the ovulation process. Mice null for PR-A isoform (PRAKO) had anovulation phenotypes while PR-B null mice (PRAKO) were able to ovulate normally (Mulac-Jericevic et al., 2000; Mulac-Jericevic et al., 2003). Nevertheless, the definitive pathway explaining how PR regulates ovulation is still unknown in this species.

In mouse, PR expression is not detected in oocytes and does not appear to be essential for oocyte developmental competence (Conneely et al., 2001; Smith et al., 2022). However, mice PRKO oocytes showed subtle differences in mitochondrial activity, but no differences in granulosa cells respiration. Thus, these changes were explained due to alterations in PR-mediated granulosa cell responses (Smith et al., 2022).

In human, no relation was found between PR expression in cumulus cells from IVF patients and oocyte fertilisation or cleavage rate. However, the same study found an association between low PR expression and embryo quality (Haseguawa et al., 2005). Svensson et al. (2001) described that PR mediated effects are involved in regulating the susceptibility to apoptosis in luteinising granulosa cells from IVF patients. Additionally, a PR mutation was found to be more prevalent in women with unexplained infertility than in fertile controls (Pisarska et al., 2003).

These results suggest that P4 concentrations or PR expression in humans and primates are not associated with oocyte maturation and developmental competence.

1.11. Progesterone and PR in cattle

GnRH and LH pulsatility are regulated by circulating P4 concentrations during the oestrous cycle, where LH is the responsible factor that defines if a dominant follicles ovulates or undergoes atresia. Therefore, when high P4 concentration, low LH pulsatility induces follicle atresia of the dominant follicle; and on the opposite way when low P4 concentrations, high LH pulse frequency allows the growth of the dominant follicle (Roche et al., 1999; Ireland et al., 2000). Considering that each estrous cycle consists of 2 to 3 follicular waves and that this process is occurring during fluctuating P4 concentrations, this hormone had been a matter of study in various reproductive aspects in this specie.

1.11.1. Progesterone and follicular development

A study conducted with two hundred and twelve Holstein and Jersey cows showed that conception rate was affected by peripheral P4 concentration 12 days before first insemination for both breeds, demonstrating for one of the first times a relationship between P4 and reproductive performance (Fonseca et al., 1986)

Several subsequent studies addressed the underlying mechanism of embryonic death and P4 concentrations, demonstrating that the success or failure of the maintenance of pregnancy depends on circulating P4 concentrations at specific time points and changes in other hormones as consequence of P4 patterns (Inskeep, 2004).

Cunha et al. (2008) analyzed the effects of high P4 on fertility to a timed artificial insemination (AI) during a synchronisation program; they reported a significant increase in pregnancies at Day 29 in cows with high compared to cows with low -circulatory levels of P4. Although cows with low P4 had a higher double ovulation rate, their fertility was lower (37.1%), indicating that increasing P4 before timed AI resulted in higher fertility. These results also suggest that the lower fertility observed in lactating dairy cows could be partially attributed

to low P4 concentrations. Furthermore, Denicol et al. (2012) demonstrated that insemination of lactating cows induced to ovulate follicles of the first follicular wave results in lower pregnancy rates because the ovulatory follicles were exposed to a minimal P4 concentration (<1 ng/ml), whereas maximum pregnancy rates were observed when ovulatory follicles grew under P4 concentration >2 ng/ml, regardless of the follicular waves.

Wiltbank et al. (2011) reviewed the effects of changes in circulating P4 in lactating dairy cows and the potential reproductive challenges associated with these alterations, describing a model for the effects of P4 concentrations previous, near, and posterior to AI. This model explains that prior to AI, higher P4 concentrations lead to an increase in pregnancy rate; near AI, it is critical that P4 concentrations reach a base concentration for an adequate luteolysis, and following AI, again high P4 concentrations are required for embryo growth, and for the establishment and maintenance of pregnancy.

Consistent with these results, Rivera et al. (2011) studied the effect of P4 on embryo quality. The experiment consisted of superstimulating cows with FSH in the first follicular wave with or without P4 supplementation, or in the second follicular wave, followed by embryo collection post AI, categorisation of embryo quality and transfer or cryopreservation of the blastocyst. The resulting data showed that the percentage of embryos from the second follicular wave and the first follicular wave supplemented with P4 that were classified as excellent/good and fair was significantly higher than those from the first follicular wave. Their findings indicate that peripheral P4 concentrations of 1 ng/ml during the growth of ovulatory follicles reduces embryo quality by reducing oocyte quality or embryo development up to day 7. Similar results were shown in beef cows when P4 was supplemented during the first follicular wave (Nasser et al., 2011). In summary, these results suggest a relationship between concentrations of P4 and follicle growth and potential development after ovulation.

1.11.2. Progesterone and ovulation

Luteinising hormone is known to induce luteinisation, COC expansion, oocyte maturation, ovulation, and a change in the follicular fluid from E2 dominance to P4 dominance (Dieleman et al. 1983).

Jo, Komar & Fortune (2002) characterised the role of P4 and PR as time-dependent in the regulation of periovulatory events in cattle. This research revealed that there is a transient increase in levels of PR, with a peak at 6h after GnRH and a decline to the time 0 value by 12h, and a second increase at 24h (near the time of ovulation). This triphasic pattern of expression of PR reflects the changes in concentrations of P4 in the follicular fluid described by Dieleman et al. (1983). Also, this study showed that the LH surge is the mechanism regulating the transient increase in PR, matching the findings in rodents.

One of the main approaches to elucidate the role of P4 in ovulation was the inhibition of the synthesis of P4 with trilostane in bovine preovulatory follicles. This resulted in a significant decline in P4 production within the follicle. Nevertheless, it did not affect ovulation rate or CL function, and normal serum P4 concentrations were observed during subsequent luteal development. Although in this research oocyte maturation was not evaluated, the findings suggest that the preovulatory increase in intrafollicular P4 may not be obligatory for bovine follicle rupture (Li et al., 2007).

1.11.3. Progesterone and oocyte competence and maturation

Although a specific role for P4 and follicle rupture has not been determined, there is evidence to suggest that P4 may play a role in oocyte maturation. Aparicio et al. (2011), described the expression of genomic and non-genomic PRs in bovine oocyte cumulus complex (COCs) before and after *in vitro* maturation (IVM). PR-A, nPR-B, mPRα, mPRβ, PGRMC1, and PGRMC2 were detected in bovine cumulus cells, whereas only nPR-A, mPRα, and mPRβ were detected in bovine oocytes. The protein expression of nPR-A, nPR-B, mPRa, and mPRb increased in cumulus cells after IVM, whereas nPR-A, mPRa, and mPRb decreased in oocytes after IVM, suggesting a cell-dependent (oocyte vs cumulus) and receptor-specific manner of expression (Aparicio et al., 2011). The effect of pharmacological inhibition of cumulus cell P4 synthesis, with trilostane, was investigated in the same study. Although meiotic maturation and fertilisation were not affected, the blastocyst rate was significantly decreased. Moreover, the effect was completely reversed by supplementation with exogenous P4 or a P4 agonist. Similarly, nPR inhibition by RU 486 had no effect on meiotic resumption or fertilisation, but significantly impaired blastocyst development (Aparicio et al., 2011). These inhibitory studies

confirmed the functional relevance of P4 and PR during oocyte maturation to oocyte acquisition of developmental competence.

Further studies confirmed that cumulus cell P4 synthesis and PR signaling during oocyte maturation in cattle are essential to oocyte developmental competence, identifying AVEN (P4 regulated protein) as a key downstream mediator of P4 regulation of oocyte survival and protection from apoptosis (O'Shea et al., 2013). Additionally, Luciano et al. (2010) described the membrane bound receptor PGRMC1 involved in oocyte meiotic maturation and first mitosis, as intracytoplasmic injection of oocytes with an antibody against PGRMC1 affected chromosome segregation during oocyte meiotic maturation (Luciano et al., 2010). A few years later, the same group described the localisation of PGRMC1 in the nucleolus of both bovine granulosa cells and oocytes, suggesting that PGRMC1 has a role in regulating the function of the nucleolus of these two cell types (Terzaghi et al., 2016).

While the role of P4 in mammalian oocyte maturation and its potential impact on oocyte quality has been well defined, information on the expression and function of PRs in growing and fully grown bovine oocytes is less clear. Further studies are needed to achieve a better understanding of the molecular mechanisms underlying the effect of this steroid hormone on oocyte competence.

1.12. Aim

(1) To determine the critical timings/stages of progesterone and nuclear progesterone receptor signalling during COC growth and maturation.

(2) To determine the specific contribution of nuclear progesterone receptor-mediated progesterone signalling during oocyte growth and maturation to completion of oocyte meiotic maturation and oocyte acquisition of developmental competence.

(3) To identify the cellular organelles and molecular targets of nuclear progesterone receptor-mediated progesterone signalling during oocyte development.

Chapter 2

Localisation and Expression of Nuclear Progesterone Receptor in Growing Bovine Oocytes

2.1. INTRODUCTION

Numerous *in-vivo* studies in cattle have highlighted the link between circulating P4 and fertility, where higher or elevated systemic P4 concentrations were associated with increased pregnancy rates (Fonseca et al, 1983; Stevenson et al., 2006, 2008; Chebel et al., 2010; Binsotto et al., 2010) see also Wiltbank et al., 2011, for review). Similarly, P4 supplementation during superstimulation of the first follicular wave, improved the quality of resulting embryos in dairy (Rivera et al., 2011) and beef (Nasser et al., 2011) cows. These findings suggest that low serum P4 concentrations during the final week of follicle growth may impact oocyte quality or competence for embryo development up to day 7. Therefore, the use of a P4-releasing vaginal device during the synchronisation programme before AI was established as a routine protocol to improve oocyte quality (Wiltbank et al., 2011). The molecular mechanisms underlying this effect are still unknown.

The expression of the nuclear progesterone receptor (nPR) in immature and *in-vitro* matured (IVM) cumulus oocyte complexes (COCs) was previously described by our group Aparicio et al. (2011). Moreover, this study also described the detrimental impact of inhibiting progesterone (P4) synthesis, or blocking the nPR with the antagonist RU486 during IVM on the resulting blastocyst rate, suggesting a functional relevance for P4 and nPR activity during oocyte maturation to oocyte competence. Further studies confirmed the importance of cumulus cell P4 synthesis and PR signalling during IVM to bovine oocyte competence, and identified AVEN (P4 regulated protein), as a key downstream mediator of P4 regulation of oocyte survival and protection from apoptosis (O'Shea et al., 2013).

Nuclear PR isoforms nPR-A (94 kDa) and nPR-B (120 kDa) represent the two major isoforms in the reproductive tissues (Kastner et al, 1990; Wen et al., 1994; Leonhardt et al., 2003). Both isoforms are identical, except the A-receptor is lacking 164 amino acids at its N-terminus (Kastner et al., 1990). Bovine COCs express both nPR, in a cell-dependent (oocyte vs cumulus) and receptor specific manner. Bovine oocytes express only nPR-A both before and after IVM, with a decrease in expression during this process. In contrast, cumulus cells express

nPR-A before IVM and both isoforms after maturation, with an increase in their expression. This suggests different roles for each receptor in the process of acquiring oocyte competence (Aparicio et al., 2011).

Although the role of P4 during mammalian oocyte maturation and its potential impact on oocyte quality has been well defined, information on the expression and function of nPR in growing and fully grown bovine oocytes is less clear. The present study aimed to address this knowledge deficit by characterising the expression, localisation and function of nPR in growing bovine oocytes from primordial to early antral follicle stages.

2.2. MATERIALS AND METHODS

2.2.1. Bovine oocyte collection and processing

Cumulus oocyte complexes were obtained from ovaries collected at a local abattoir. The ovaries were submerged in dissection medium [TCM-199 with 0.4% BSA fraction V, 0.164 mM penicillin, 0.048 mM streptomycin, 1790 units/L heparin, and 5μM cilostamide (Sigma, Ireland)] and oocytes were liberated from their follicles by slicing. Good quality COCs were selected, denuded of their cumulus investment and the oocyte diameter was measured. Subsequently, oocytes were pooled and categorised into diameter groups: 60-100 μm, 100-110 μm, and >120 μm, then snap-frozen in liquid nitrogen for Western blotting; or groups 60-70μm, 70-80 μm, 80-90 μm, 90-100 μm, 100-110 μm and 120-130 μm and fixed in 4% paraformaldehyde for 25 minutes at room temperature (RT) for whole-mount immunocytochemistry. Cumulus cells from fully grown COCs (oocyte diameter >120 μm), recovered during denudation were also snap-frozen for protein analysis.

Additionally, COCs from aspirated oocytes were collected, in vitro matured and used as a positive control in the protein analysis. Briefly, good quality COCs were selected, washed and groups of up to 50 COCs were placed in 500 μl IVM media in a four-well dish and cultured at 39°C for 24 h in a humidified atmosphere containing 5% CO2. Matured COCs were washed four times in PBS, and snap-frozen in liquid N2 for western blot analysis.

2.2.2. Western Blotting

Five replicate pools of oocytes assigned to the three diameter groups 60-100 μm (100 oocytes); 100-110 μm (70 oocytes), and 120-130 μm (50 oocytes) were denuded by gentle pipetting and repeated washing in PBS-0.1% PVP. Oocyte samples were resuspended in lysis buffer (M-PER Mammalian Protein Extraction Reagent, Pierce #78503, Thermo Scientific, Rockford, IL) supplemented with Protease and Phosphatase Inhibitors Cocktail (Halt Protease Inhibitor Cocktail EDTA free and Halt Phosphatase Cocktail, Pierce #78415, #78420, respectively; Thermo Sicentific) frozen and thawed three times and centrifuged for 15 min at 10.000 *g* at 4°C. Cumulus cells from fully grown COCs, bovine endometrium and corpus luteum tissue samples were included as positive controls. Proteins were extracted from these samples through homogenisation with lysis buffer, followed by centrifugation at 10,000 g for 15 minutes at 4°C, and the resulting supernatant was centrifuged again at 10,000 g for 10 minutes at 4°C. Proteins were denatured by boiling for 5 min at 95°C in loading buffer. The protein content of the cumulus cells, positive controls and oocyte pools was calculated using the Bradford Assay. Twelve micrograms of protein were loaded and resolved by SDS-PAGE on a 4-12% Bis Tris gel (Invitrogen). Proteins were transferred into a nitrocellulose membrane and blocked with blocking buffer (5% BSA in Phosphatase buffered saline solution + Tween 20 [PBST] containing 10mM phosphate buffer, 137mM sodium chloride, 2.7mM potassium chloride, and 0.1% Tween 20) for 1h at RT. Immunoblotting was performed by incubating the membranes in blocking buffer overnight at 4°C with mouse anti-nPR antibody, at 1:250 dilution (Epredia #MS-298-P). Membranes were subsequently washed in PBST and incubated with secondary anti-mouse antibody (CellSignalling #7076S) at a 1:1000 dilution 1h at RT. Following which they were washed 3 times for 5 min each with PBST and the signal was visualised using SuperSignal West Pico Chemiluminescent Substrate Kit (Thermo Scientific #34077), according to the Manufacturer's instructions. Anti-GAPDH antibody was used as a loading control. Band intensity was quantified using the iBright analysis software (Invitrogen).

2.2.3. Ovary processing for immunohistochemistry

Bovine ovaries with surface visible antral follicles but lacking an active corpus luteum were selected from 9 animals. Small pieces (0.25 cm^3) of ovarian cortex were fixed in 4% paraformaldehyde at 4°C for 24 h. Following washing, they were embedded in paraffin wax and subsequently sectioned at 4 μm thickness and mounted on clean dry slides. Prior to immunohistochemical (IHC) labelling, the slides were deparaffinised with xylene, rehydrated

through a graded alcohol series, and exposed to heat-induced antigen retrieval in 10 mM citrate buffer for 10 minutes in a pressure cooker. The slides were then rinsed in PBST and blocked in PBST with 10% Goat serum in PBS for 1h at RT. Detection of nPR by IHC was performed using a 1:100 dilution of the monoclonal nPR antibody (Abcam aba191138) in blocking solution overnight at 4°C and a final incubation at 37°C for 1 h. Following which, the sections were washed with PBST prior to endogenous peroxidase blocking for 30 min at RT. After rinsing with PBST, the sections were incubated with a 1:100 dilution of biotinylated donkey anti-mouse antibody (Abcam #AB205724) for 1 h at 37°C, followed by incubation in 100 ul DAB chromogen substrate for 1 min., and counterstained with Mayer's haematoxylin. Finally, cover-slips were applied manually with DPX mounting media. The IHC-stained tissue slides were scanned and digitised using Aperio AT2 Digital Slide Scanner (Leica Biosystems) at 20X magnification and the images were viewed, annotated, and analysed with Aperio ImageScope 12.3 software (Leica Biosystems). A total of 118 follicles were classified according to their stage: primordial follicles (oocyte surrounded by flattened granulosa cells), primary follicles (oocyte surrounded by cuboidal granulosa cells), secondary follicles (oocyte surrounded by more than two layers of cuboidal granulosa cells and some deposition of theca cells) and early-antral follicles (oocyte surrounded by cumulus cells and starting formation of the antral cavity); annotations were performed in each cell type: oocyte, granulosa, theca and cumulus -cells. Positive and negative controls were included in each replicate; they included an IgG control for each animal's ovary sections and bovine endometrium sections as positive controls. The number of nPR stained cells per annotation were identified using a Nuclear v9 algorithm and the diameter of the follicles was measured. Oocyte nPR labelling was assessed visually. In the case of weakly labelled samples, the intensity of DAB staining was calculated in ImageJ using the colour deconvolution plugin, and the mean was used to include them or exclude them from the nPR stained group (Schneider et al., 2012). A total of three replicates, comprised of ovarian tissue from three animals per replicate, were performed.

2.2.4. Whole-mount Immunofluorescence

Fixed oocytes and COCs were incubated in PBS containing 0.1% Triton X100 (PBSTx) for 1h under gentle rocking, followed by blocking in PBSTx containing 20% donkey serum at RT for 3h and subsequently incubated overnight at 4°C with the nPR antibody diluted 1:50 in PBSTx containing 10% donkey serum. After incubation, samples were washed four times for 15 min each in PBSTx at 300 rpm and labelled with Alexa Fluor 488 goat anti-mouse secondary

antibody in a dilution of 1:500 (Invitrogen #A11029) for 40 min at RT. Finally, the samples were washed for four times for 15 min each in PBSTx at 300 rpm and 1h in PBS at 300 rpm. Cellular DNA was stained with 4′,6-diamidino-2-phenylindole (DAPI, 1:1000 dilution) for 30 min and washed repeatedly with PBS. Oocytes were placed on a glass slide with mounting medium and covered with a glass coverslip. Immunolabeled oocytes were visualised using a Carl Zeiss LSM 800 Airy confocal microscopy system at 64X magnification (Carl Zeiss, Jena, Germany). The resulting z-stack images were convoluted in a 3D image and analysed in IMARIS software to quantify nPR expression, oocyte and nuclear volume. A total of four replicates were performed, each containing 10 oocytes per group.

2.2.5. Statistical Analysis

Statistical analysis was carried out using R studio version 4.2.1 software package for MacOS 11. Differences between groups were considered significant at $p<0.05$. The percentage of nPR-stained cells were evaluated in follicular granulosa cells using the Kruskal-Wallis test, and in theca cells using Wilcoxon sum rank test. The correlation between the percentage of nPR for somatic cells and the diameter of the follicle was determined by Spearman rank correlation coefficient. Additionally, statistical analysis of oocyte labelling was performed by chi-squared analysis. The densitometry data from the Western blots were analysed using ANOVA. Data from the immunolabelled oocytes were analysed by Poisson regression to determine the correlation between number of nPR foci and oocyte diameter. Furthermore, the nPR foci/μm^3 and the oocyte diameter was evaluated by ANOVA followed by a Kruskal-Wallis test.

2.3. RESULTS

2.3.1. Expression of nPR in growing bovine oocytes

The specification of the antibody used to study the expression of nPR-A and nPR-B was confirmed by immunoprecipitation of immature and *in- vitro* matured oocytes and cumulus cell resulting in two protein bands corresponding to nPR-A (80kDa) and nPR-B (120kDa) (Figure 2.1.A). Genomic nPR-A was detected in luteal and endometrial control samples; in fully grown (120 μm) and growing (60-100 μm) -oocyte groups, as shown in Figure 2.1.B. The expression of nPR-A protein was not statistically different ($p<0.9$) between groups ($n = 5$) (Figure 2.1.C).

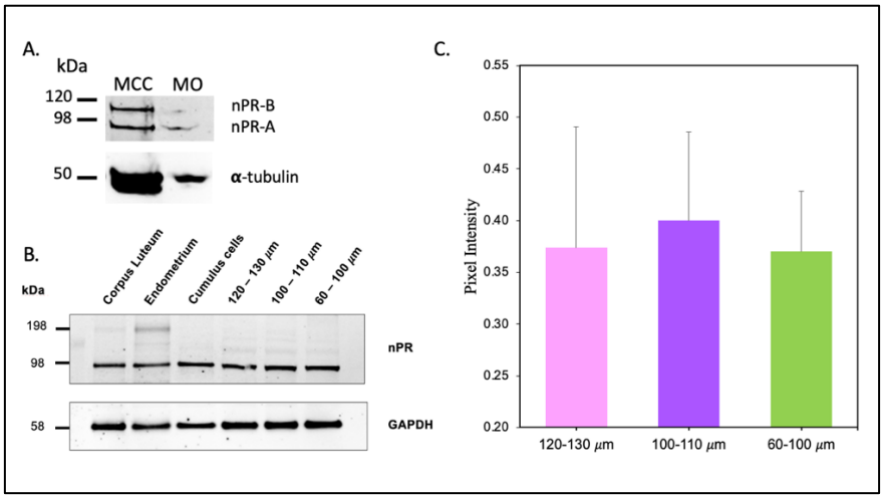

Figure 2.1. Expression of nPR in bovine COCs. Proteins were resolved by SDS-PAGE and immunoblotting was performed using a monoclonal antibody against nPR-A (80 kDa) and nPR-B (120 kB). A) The specificity of the antibody against nPR was tested by immunoprecipitation of mature fully grown bovine oocytes (MO) and mature cumulus cells (MCC) proteins. Lane 1. Cumulus cells from fully growth oocytes after 24hs of IVM. Lane 2. Oocytes after 24hs of IVM. B) Protein lysates from corpus luteum, endometrium, cumulus cells, and bovine oocytes were resolved per lane. Lane 1. Corpus luteum. Lane 2. Endometrium. Lane 3. Cumulus cells. Lane 4. Pool of 50 oocytes 120-130 µm. Lane 5. Pool of 70-75 oocytes 100-110 µm. Lane 7. Pool of 100 oocytes 60-100 µm. C) Protein bands were measured by Densitometry and are represented as percentage of maximum ± SEM (n= 5 replicates). Analysis by ANOVA and Chi-Square Test.

2.3.2. Expression of nPR during preantral and early antral follicle growth

The percentage of nPR-labelled cells per cell type and follicle stage is summarised in Table 2.1. Follicle cell nPR expression was observed in the nuclei and cytoplasm of granulosa cells of primordial, primary, secondary, and early antral follicles, theca cell of secondary and early antral follicles, cumulus cells from early antral follicles and in the oocyte nucleus and cytoplasm in all follicle stages (Figure 2.2).

The Aperio Nuclear v9 algorithm was employed to determine nuclear specific nPR labelling by cell type. There was no difference in mean granulosa cell nPR labelling ($p>0.07$) (Figure 2.3.A). However, the analysis of the homogeneity of variances reveal that variances were not equal across the groups ($p<0.004$) (Figure 2.3.B). Granulosa cells from primordial and primary follicles had a wider dispersion of the PR-stained cells than the following stages of follicle growth. Additionally, the percentage of nPR-labelled granulosa cells was negatively correlated with follicle diameter ($R=-0.31$, $p<0.05$) (Figure 2.4). Thus, the number of granulosa cells which expressed nPR remained stable and did not increase in line with follicle growth. The percentage of nPR-labelled theca cells was higher in secondary follicles group compared to early-antral follicles (11.4 ± 1.96 vs. 6.63 ± 1.24, $p\leq0.05$) (Figure 2.5.A). Similar to the granulosa cells, the proportion of nPR-positive theca cells decreased as follicle diameter

increased (R=-0.31, p<0.1) (Figure 2.5.B). Whereas 20% of cumulus cells were labelled in early antral follicles (19.9±3.61) (Figure 2.6).

Table 2.1. The percentage of PR-stained cells in all cell groups and follicular stages.

Follicular Size	Follicle number	Diameter μm	% PR Granulosa	% PR Theca	% PR Cumulus
Primordial Follicle	17	40.43 ± 1.54	21.28 ± 4.05	-	-
Primary Follicle	10	41.94 ± 4.28	29.13 ± 7.85	-	-
Secondary Follicle	18	296.3 ± 24.73	14.99 ± 3.07	11.40 ± 1.96[a]	-
Early-Antral Follicle	16	734.4 ± 47.02	9.85 ± 2.06	6.63 ± 1.24[b]	19.9 ± 3.61

Values are expressed as means ± SEM. Means with different superscripts differ significantly (p<0.05). Statistical analysis performed by ANOVA followed by a Kruskal-Wallis test. PR Granulosa: Progesterone receptor granulosa cell stained. PR Theca: Progesterone receptor theca cell stained. PR Cumulus: Progesterone receptor cumulus cell stained.

A total of 61 oocytes within the above-described follicles were assessed for nPR-positive staining. All oocytes (100%) in primordial and primary follicles oocytes and 94% of secondary and early-antral follicle oocytes presented positive nPR-labelling (Figure 2.7).

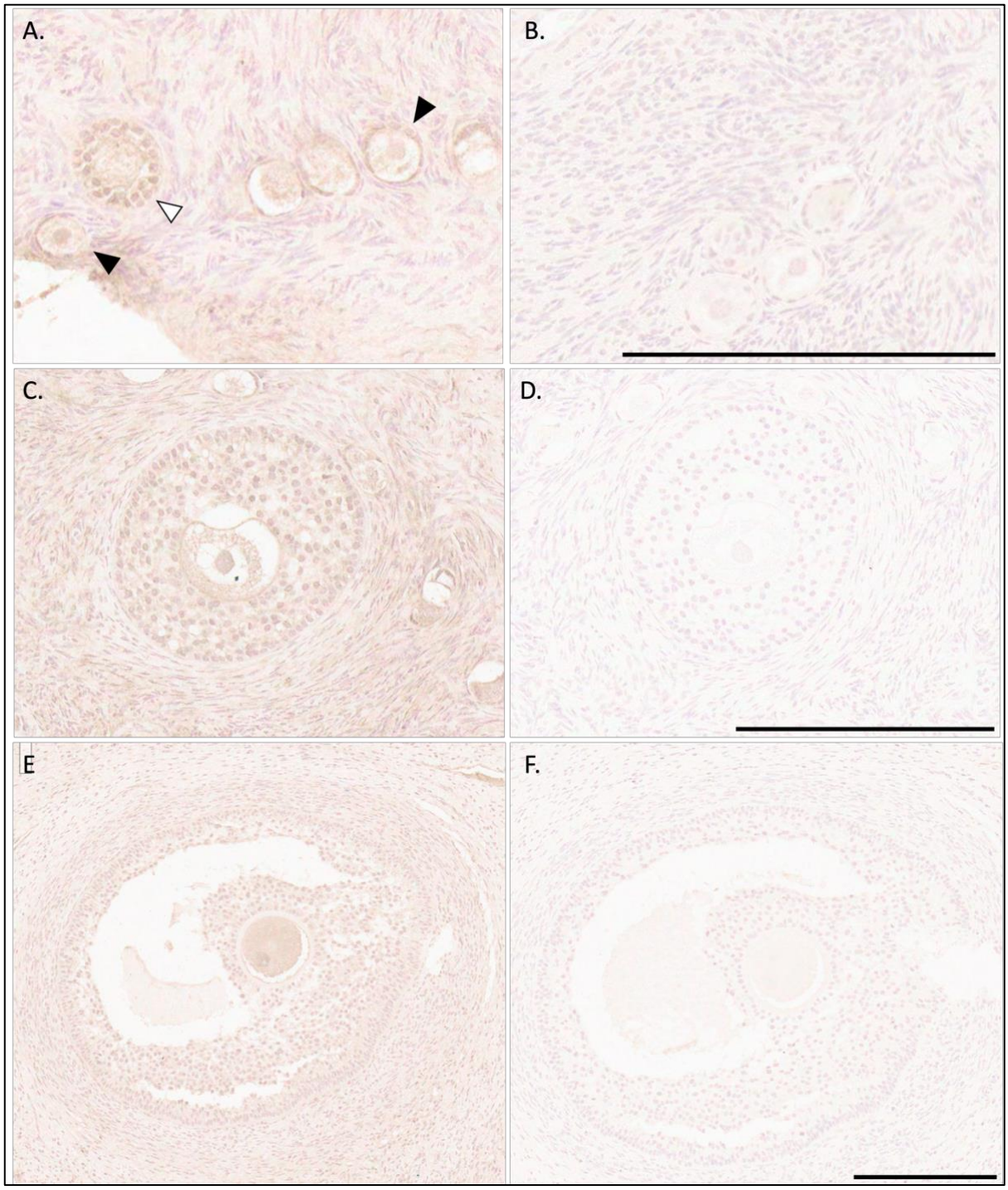

Figure 2.2. Scanning of immunohistochemical staining for bovine ovarian cell types showing nPR expression. A) Primordial (black arrowhead) and primary follicle (white arrowhead) labelling for nPR. **C)** Secondary follicle. **E)** Early-Antral Follicle. **B)** Primordial follicle Rabbit IgG control. **D)** Secondary follicle Rabbit IgG control. **F)** Early-Antral Rabbit IgG control. Scale bars = 200 μm.

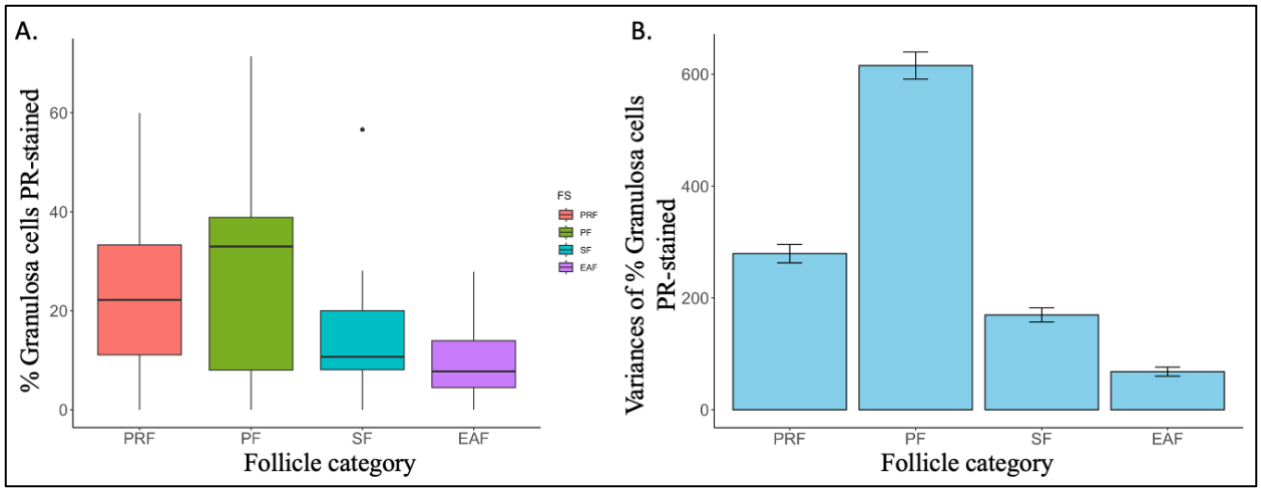

Figure 2.3. Variation of the nPR labelling in granulosa cells across bovine follicle sizes. A) Boxplots showing the variability of the percentage of granulosa cell nPR labelling according to follicle category. Statistical analysis performed by ANOVA followed by a Kruskal-Wallis test. **B)** Boxplots showing Flinger-Killeen test of the homogeneity of variances for each follicle category ($p<0.05$) (n=3 replicates). PRF: primordial follicle (red). PF: primary follicle (green). SF: secondary follicle (blue). EAF: early-antral follicle (purple).

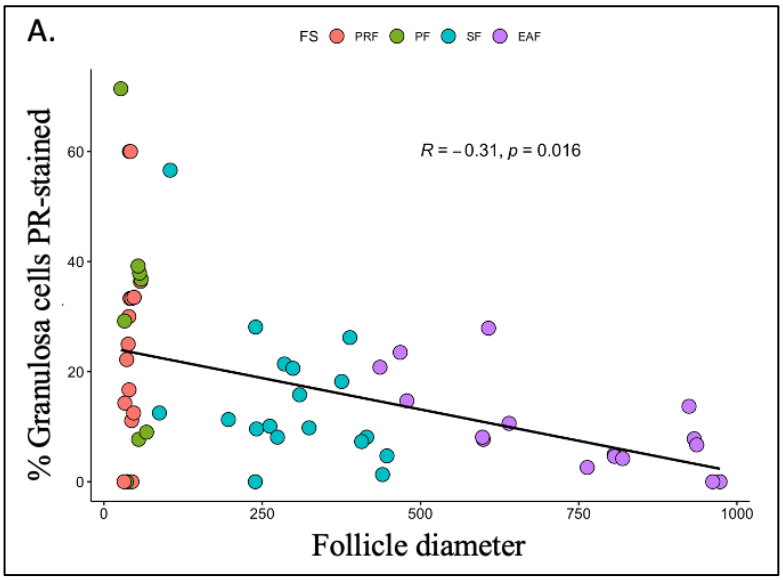

Figure 2.4. Correlation between the percentage of nPR labelling in granulosa cells and bovine follicle size. A) Scatter plot comparing the percentage of nPR labelling in granulosa cells versus the follicle diameter. Each dot represents the percentage of nPR labelling in granulosa cells and each colors represent different follicle categories (n=3 replicates). Analysis by Poisson linear regression. Spearman correlation coefficient (R). PRF: primordial follicle (red). PF: primary follicle (green). SF: secondary follicle (blue). EAF: early-antral follicle (purple).

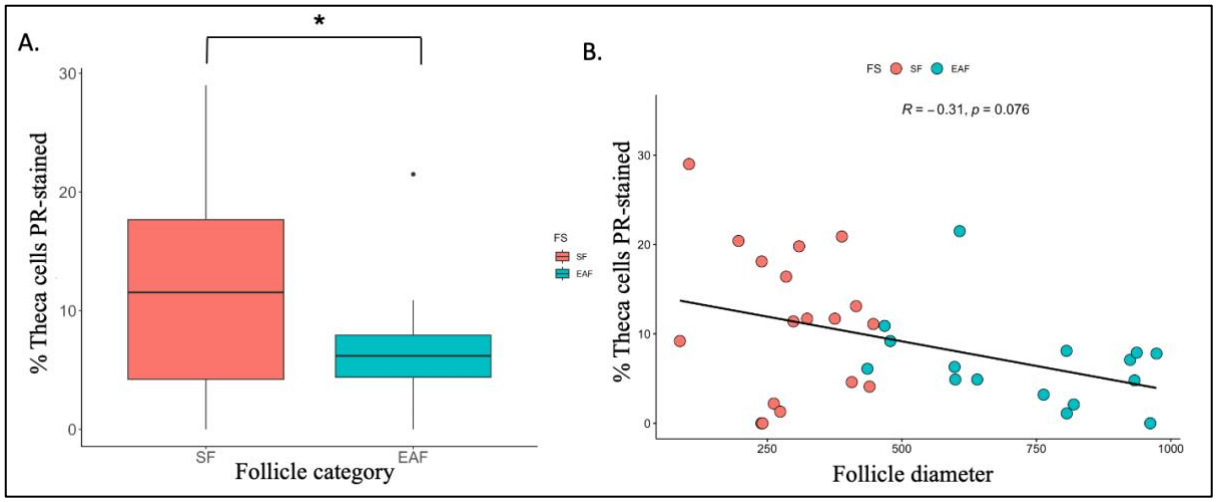

Figure 2.5. Variation and correlation of the nPR labelling in theca cells across bovine follicle sizes. A) Boxplots showing the variability of the percentage of theca cell nPR labelling according to follicle category. Statistical analysis performed by ANOVA followed by a Kruskal-Wallis test ($p<0.05$). **B)** Scatter plot comparing the percentage of nPR labelling in theca cells versus the follicle diameter. Each dot represents the percentage of nPR labelling in theca cells and each colours represent different follicle categories (n=3 replicates). Analysis by Poisson linear regression. Spearman correlation coefficient (R). SF: secondary follicle (red). EAF: early-antral follicle (blue).

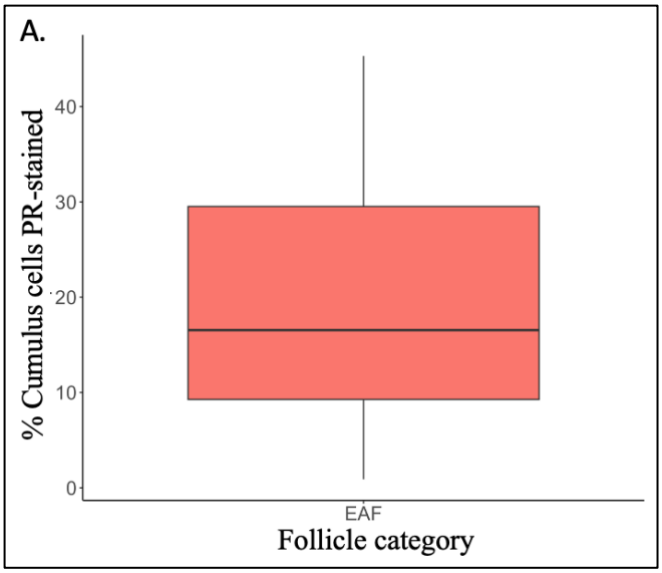

Figure 2.6. Variation of the nPR labelling in the cumulus cell in early antral follicles. A) Boxplot showing the variability of the percentage of cumulus nPR labelling in early antral follicles. Statistical analysis performed by ANOVA followed by a Kruskal-Wallis test (n=3 replicates).

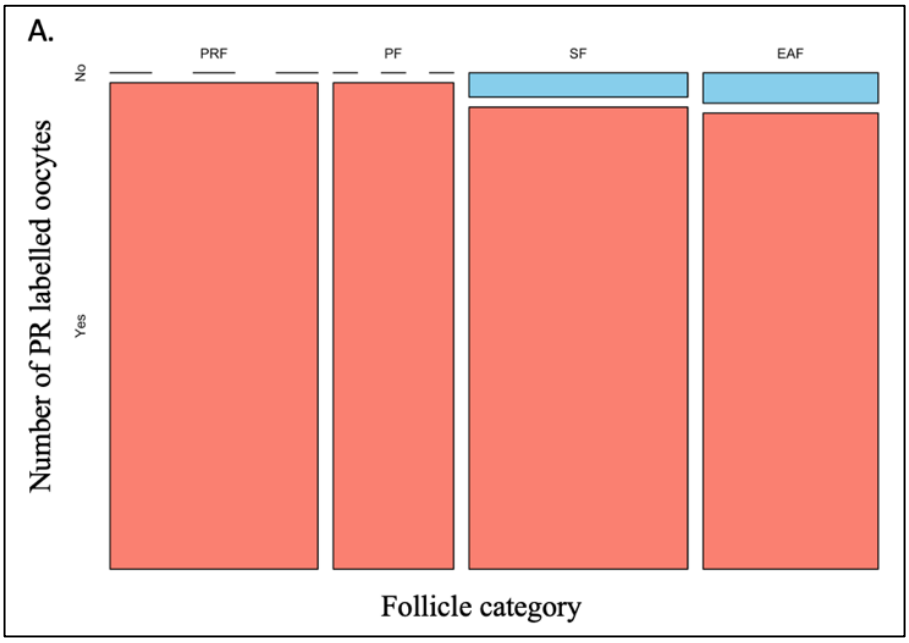

Figure 2.7. Oocyte labelling for nPR across follicle size. A) Mosaic plot showing the total number of oocytes stained for nPR in all follicle sizes. The red bars represent the labelled oocytes while the blue bars represent the oocytes with no labelling. PRF: primordial follicle. PF: primary follicle. SF: secondary follicle. EAF: early-antral follicle.

2.3.3. Localisation of nPR in growing bovine oocytes

A total of 263 oocytes were processed for wholemount immunofluorescent labelling and confocal microscopy. The resulting z-stacks were convoluted in 3D images and the number of nPR fluorescent foci, and the volume of each oocyte were quantified. Genomic nPR-A labelling was localised in the cytoplasm and the nucleus of all oocytes

The mean number of nPR-A localised in the cytoplasm and the nucleus increased as oocyte diameter increased, the results are summarised in Table 2.2.

Table 2.2. nPR-A expression in growing oocytes.

Oocyte size μm	**Oocyte number**	**Cytoplasmic nPR-A foci**	**Cytoplasmic volume** μm^3	**Nuclear nPR-A foci**	**Nuclear volume** μm^3
60 – 70	37	95 ± 14.13	18469 ± 2295	48 ± 7.63[a]	3525 ± 246
70 – 80	40	180 ± 19.08[a]	16368 ± 1706	59 ± 6.88	3190 ± 303
80 – 90	63	176 ± 13.03	35213 ± 3278	50 ± 9.07[c]	4044 ± 336
90 – 100	43	230 ± 20.60	47202 ± 4241	71 ± 6.98	4269 ± 350
100 – 110	40	998 ± 59.52	130531 ± 5427	159 ± 12.73[b,d]	6703 ± 354
120 – 130	40	1013 ± 84.71[b]	211331 ± 8673	129 ± 13.46[d]	5707 ± 482

Values are expressed as means ± SEM. Means with different superscripts differ significantly ($p<0.05$). Statistical analysis performed by ANOVA followed by a Kruskal-Wallis test.

Photomicrographs of oocytes displaying fluorescent labelling of nPR are presented in Figure 2.8. The pattern of labelling varied according to oocyte diameter; labelled foci were arranged in a clustered pattern in oocytes 60-80 μm in diameter, whereas larger oocytes (oocytes ≥90 μm in diameter), presented a more dispersed pattern of localisation. Additionally, the expression of nPR-A was localised in the cytoplasm of the cumulus cells from all oocyte group sizes but not in their nucleus.

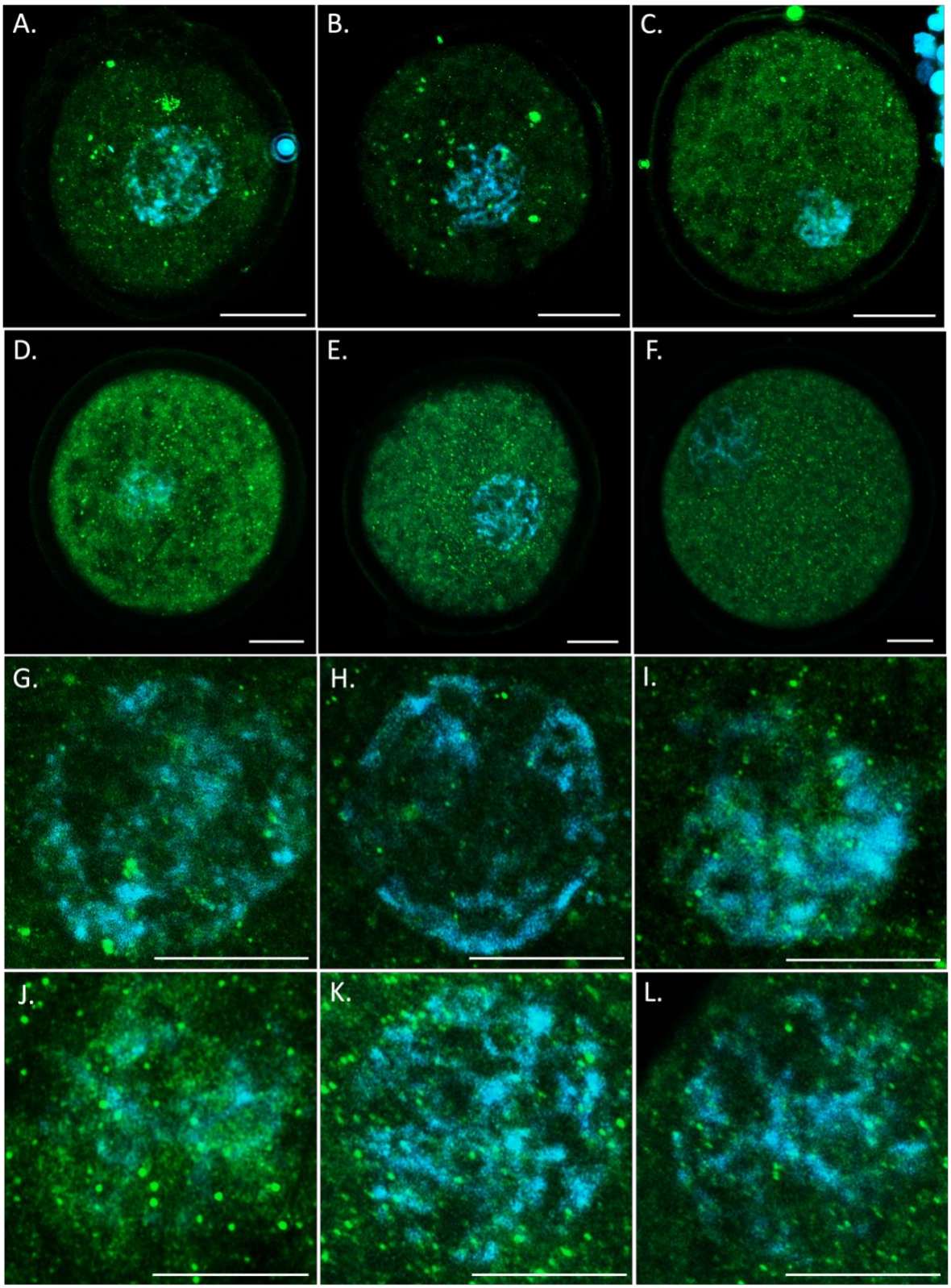

Figure 2.8. nPR expression and localisation in growing bovine oocytes. Confocal laser scanning photomicrographs show immunofluorescent detection of nPR in growing and fully grown bovine oocytes. Genomic PR was visualised in green, and DNA was visualised in blue (DAPI). Whole oocytes measuring. **A)** 60 - 70 µm; **B)** 70 – 80 µm; **C)** 80 – 90 µm; **D)** 90 – 100 µm; **E)** 100 - 110 µm and **F)** 120 – 130 µm in diameter. Scale bar = 20 µm. Zoomed in micrographs of nuclear nPR labelling in the same oocytes are shown: **G)** 60 - 70 µm; **H)** 70 – 80 µm; **I)** 80 – 90 µm; **J)** 90 – 100 µm; **K)** 100 - 110 µm and **L)** 120 – 130 µm oocytes. Note the presentation of nPR labelling as disperse foci. (n = 4 replicates).

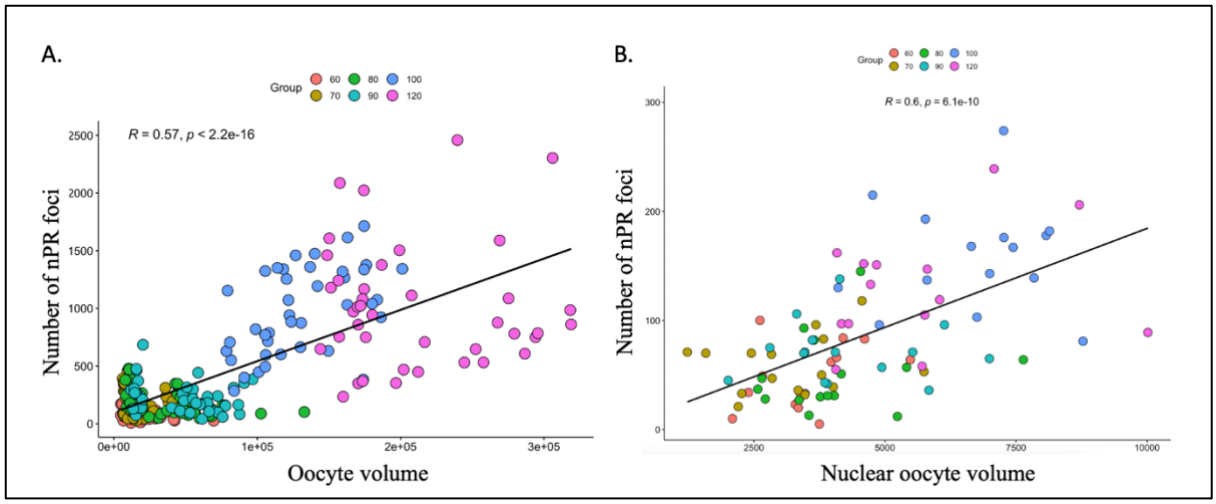

Figure 2.9. Correlation between nPR foci and bovine oocyte size. **A)** Scatter plot comparing oocyte volume versus the number of nPR foci per µm^3 and **B)** Scatter plot comparing oocyte nucleus volume and the number of nPR foci per µm^3. Each dot represents the number of nPR foci per µm^3 of oocytes and colors represent size groups (n=5 replicates). Analysis by Poisson linear regression. Pearson correlation coefficient (R).

The number of nPR-A foci was positively correlated with oocyte and nuclear volume (R= 0.57 and R= 0.6, (p<0.001), respectively) (Figure 2.9).

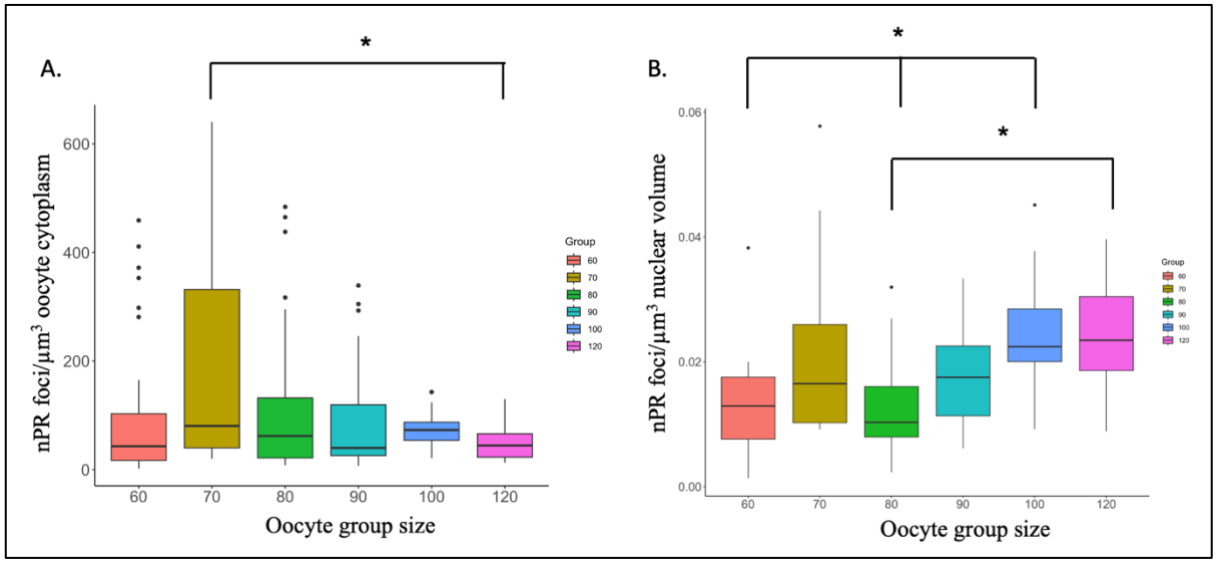

Figure 2.10. Variation of the nPR foci/µm3 across bovine oocyte sizes. **A)** Boxplots showing the variability of the number of nPR foci per µm^3 according to oocyte diameter. **B)** Boxplots showing the variability of the number of nPR foci per µm^3 according to oocyte nuclear volume. Each color represents a group size (n=5 replicates). Statistical analysis performed by ANOVA followed by a Kruskal-Wallis test.

Comparing the total number of nPR foci per µm^3 of oocyte volume, variability was greatest in oocytes within the 70 – 80 µm diameter group compared to oocytes within the 120-130 µm group (181±19.08 vs 49±84.70, p<0.05). Similarly, the number of nPR-A foci per

nuclear volume was significantly more variable in oocytes from 60 – 70 µm (48±7.6) and 80 – 90 µm (50±9.1) compared with oocytes from 100 – 110 µm (159±12.8) and 120 – 130 µm (129±13.5), diameter groups ($p<0.05$) (Figure 2.10).

2.4. DISCUSSION

This current study builds on our earlier work describing nPR expression in fully-grown immature and IVM bovine oocytes (Aparicio et al., 2011; O'Shea et al., 2013), by detailing nPR expression in growing bovine oocytes, COCs and follicle cells from the primordial follicle to early antral follicle stages. Our findings show continuous nPR expression during follicle growth by the oocyte and follicle cells, suggesting an important role for this receptor during folliculogenesis.

In an earlier study, Van den Broeck et al., 2002, applying immunohistochemical analysis, described the expression of nPR in the bovine follicles, but did not describe nPR expression in the oocytes within. The Authors reported higher nPR expression in primary follicle cells compared to all other follicle stages. In agreement with these findings, we detected maximum number of nPR expressing granulosa cells in primary follicles (29.13%). Followed by primordial follicles (21.3%), secondary follicles (15%), and early-antral follicles (~10%). Following activation of the primordial follicle, the follicle begins a unidirectional process in which follicles become integrated into the growing follicle pool as granulosa cells resume mitosis (see Fair, 2010, for review). Progesterone has been previously described as a survival factor in granulosa cells of rat and human follicles, as well as in bovine luteal cells (Svensson et al., 2000; Svensson et al., 2001; Rueda et al., 2000) and inhibition of nPR is associated with increased apoptotic activity (O'Shea et al., 2013). Therefore, the current findings suggest a pro-survival role for nPR during early folliculogenesis.

The number of oocytes in the mammalian ovary is controlled by atresia. A critical aspect of atresia is the susceptibility of the oocyte and granulosa cells to death, which varies throughout folliculogenesis (Clark et al., 2004; Rodgers & Irving-Rodgers et al., 2010). In antral follicles, programmed cell death is triggered by the granulosa cells (Ireland & Roche, 1983; Grimes et al., 1987), whereas preantral follicle death, appears to be trigged by the oocyte itself (Rajakoski, 1960; Marion et al., 1968, Yadav et al., 2018; Telfer at al., 2023). A key characteristic in these atretic follicles is the substantially elevated P4 levels in the follicular fluid (Irving-Rodgers et al., 2003). Van den Broeck et al., 2002 described the presence of nPR expression in follicle cells of atretic antral follicles, but no staining in apoptotic bodies.

Therefore, depending on the environment or specific stimulus, P4 and or nPR signalling may reflect the survival or atretic status of the cell.

As described above, the percentage of positively labelled granulosa cells decreased as follicular diameter increased, thus it appears that a sub-population of nPR expressing granulosa cells remains constant throughout follicle growth and granulosa cell proliferation. In antral follicles, granulosa cells play a major role in deciding the fate of follicles. While follicle-stimulating hormone (FSH) is crucial for granulosa cell survival, these cells also produce oestradiol, insulin-like growth factor I (IGF-I), and interleukin 6 (IL-6), which function as survival factors through paracrine/autocrine signalling and consequently suppressing apoptosis (for review, see Matsuda et al., 2012; Gaytan et al., 2018). Therefore, the continuous expression of nPR in granulosa cells could be involved in blocking cell death and promoting cell survival.

In rodents, the expression pattern is different, they express nPR specifically in the granulosa cells of the preovulatory follicles in response to LH surge before ovulation (Ismail et al., 2002; Teilmann et al., 2006; Robker et al., 2009). The prolonged expression of nPR in the granulosa cells could be understood by the fact that in contrast to rodents, the luteal phase in primates and humans is extended. Therefore, nPR may have species specific functions, for example, the nPR plays a role in follicle rupture and oocyte release in rodents, while in primates and humans nPR function is still under study (Robker et al., 2000; Smith et al., 2022).

The current findings also indicate a significant increase in the percentage theca cells expressing nPR in the secondary follicle compared with the theca cells from the early-antral follicle (11.4±1.96 vs. 6.63±1.24 $p<0.05$). Interestingly, Van den Broeck (2002) described the same expression profile in their bovine samples. Furthermore, similar findings were reported in pigs, dogs and sheep (Słomczyńska et al., 2000; Vermeirsch et al., 2000; Juengel et al., 2006). The involvement of nPR in the recruitment and deposition of the theca cells in secondary follicles could be interpreted from these observations. Although the origin of the theca cells remains unclear, current evidence suggest that the oocyte and granulosa cells secrete factors that induce thecal cell differentiation from stroma (Young & McNeilly, 2010; Telfer et al., 2023), adding further support for a possible role for nPR at the time of theca cell deposition.

The current study presents a continuous characterisation of nPR expression during oocyte growth and follicle development from primordial to early antral follicles. The data was obtained by a combination of immunohistochemistry analysis in bovine ovarian sections and whole-mount immunocytochemistry in fixed bovine oocytes (60 – 130 μm). This latter method allowed the quantification of the nPR foci in all oocyte diameter groups. Describing significant

variation in the number of nPR foci in oocytes from 70 to 80 μm in diameter compared to oocytes from 120-130 μm (181±19.08 vs 49±84.70, $p<0.05$). Intriguingly, the oocyte becomes transcriptionally active at this stage; some transcripts are immediately translated and others are stored for future maturation and fertilisation (Susor et al., 2016; Telfer at al., 2023; Fair & Lonergan, 2023). Thus, the variation in nPR expression within the 70 – 80 μm oocyte diameter group may reflect actual variation in molecular machinery as transcription and translation are ramped up (see reviews by Fair et al., 2003; Fair & Lonergan, 2024).

The number of nPR foci was positively correlated with oocyte and nuclear volume, suggesting that as the oocyte grows in diameter there is a translocation of the receptor into the nucleus for the activation or repression of target genes. The nPR isoforms act as transcription factors which directly bind to P4. In an inactive state, both receptor isoforms reside in the cytoplasm bound to chaperone proteins, upon P4 binding the nPRs dissociate and translocate into the nucleus to interact with PRE sequences at the promoter regions of target genes (Leonhardt et al., 2003). Gene activation via P4 stimulus involves two consecutive cycles of nucleosome remodelling (Vicent et al. 2009; Vicent et al. 2011; Wright et al. 2012). The first cycle takes place within the first 1-5 min after hormone exposure and consists of histone H1 (H1) phosphorylation of, resulting in its displacement from chromatin. The second cycle takes place between 5 and 30 min after exposure, leading to additional nucleosome remodelling and the displacement of histone H2A/H2B (Vicent et al., 2006; Yang et al., 2007). Hence, the actual activation of transcription takes place on a histone H3/H4 tetramer (Vicent et al., 2010). Nevertheless, recent studies demonstrated that P4 can also repress gene expression (Ballare et al., 2013). Repression requires binding of activated nPR to target sites in the gene promoter region, similar to those involved in gene activation (Natch et al., 2016). The activated nPR recruits a repressive complex composed of heterochromatin protein 1-γ (HP1γ), histone demethylases, histone deacetylases, the SRA RNA, and the ATPase Brahma-related gene-1 (BRG1) (Vicent et al., 2013; Natch et al., 2016). In this scenario, the BRG1 increases the linker histone H1.2 deposition and nucleosome occupancy, leading to chromatin compaction and loss of accessibility for the RNA pol II (Natch et al., 2016). Our data indicates increased nPR localisation in the nuclei of bovine oocytes >110 μm, which are transcriptionally quiescent (Fair 1996;1997). Thus, our findings suggest that nPR may enhance the expression of target genes during oocyte growth from 60 – 110 μm and act to repress transcription in oocytes >110 μm in diameter, implying an essential role for nPR during oocyte growth and acquisition of competence.

This study provides new knowledge on nPR expression in bovine oocytes, COCs, and follicle cells during folliculogenesis and oocyte growth. These findings open new avenues for further research to elucidate the precise functional roles of nPR in different stages of folliculogenesis and its potential implications for reproductive biology.

Chapter 3

Establishment of an *in-vitro* oocyte culture system to investigate the functional role of the nuclear Progesterone Receptor during bovine oocyte growth

3.1. INTRODUCTION

The development of *in-vitro* oocyte culture systems (IVOC) provides an environment that allows immature and developmentally incompetent oocytes to grow and acquire meiotic and developmental competence *ex-vivo*, offering a potential tool for both research and gamete salvage purposes (Luciano et al., 2021; Chelenga et al., 2023; Garcia Barros et al., 2023). There are two bovine IVOC systems recently described in the literature. The first described as *in-vitro* growth (IVG) system (Chelenga et al., 2023); and the second called long *in-vitro* oocyte culture (L-IVOC) system (Garcia Barros et al., 2023).

Both systems were developed for oocytes in the transition from the growing phase to the fully grown state. During this stage, the bovine oocyte undergoes significant changes, including chromatin compaction accompanied by transcriptional silencing, alterations in epigenetic signatures, and redistribution of cytoplasmic organelles. Together, these modifications confer full meiotic and developmental competence to the oocyte (Hyttel et al., 1997; Sun & Schatten, 2006; Lodde et al., 2008; Lodde et al., 2009; Luciano et al., 2014; Lodde et al., 2017; Fair & Lonergan, 2023).

There is evidence to support the contribution of progesterone (P4) and nuclear progesterone receptors (nPR) to bovine oocyte competence. The inhibition of P4 synthesis by Trilostane (blocking the 3 β-hydroxysteroid dehydrogenase which transforms pregnenolone into P4), or the nPR with RU486 (nPR antagonist) during *in-vitro* maturation (IVM) reduced significantly the blastocyst yield in the treated group compared to the control (Aparicio et al., 2011). These findings suggested a functional relevance of P4 and nPR activity during oocyte maturation to oocyte acquisition of developmental competence.

In the previous chapter, the expression of nPR was characterised in oocytes from primordial to early-antral follicles stages. Employing wholemount immunocytochemistry, the number of fluorescently labelled nPR-A positive foci was observed to increase in parallel with oocyte growth. Therefore, the hypothesis of the current study is that nPR plays a role in oocyte acquisition of competence during the growth phase. Building on the localisation and characterisation of the receptor in growing bovine oocytes, the objective was to implement an *in-vitro* growing bovine system to evaluate the function of the nPR in transcriptionally active

bovine oocytes at the latter stage of their growth phase, i.e., measuring 100 – 110 μm in diameter.

3.2. MATERIALS & METHODS

3.2.1. Bovine COC collection

Bovine ovaries collected at a local abattoir were washed, aspirated, and ovarian cortex slices of 1.2 – 2 mm thick were prepared using a surgical blade. The cortex slices were submerged in dissection medium [M199-D (TCM-199 with 0.4% BSA fraction V, 0.164 mM penicillin, 0.048 mM streptomycin and 1790 units/L heparin)] on a warm plate (37^{o}C). COCs were liberated from 0.5 – 2 mm follicles by follicle dissection. From the isolated COCs, the oocyte diameter were measured, and those within a range of 100 – 110 μm were placed in holding medium [M199-H (TCM199 supplemented with 2 mM glutamine, 0.4% fatty acid free BSA, 0.2 mM sodium pyruvate, 25 mM sodium bicarbonate, 0.1 mM cysteamine, 21.3 μg/mL of phenol red, 75 μg/mL of kanamycin, 4% Polyvinylpyrrolidone, and 5 μM cilostamide)] until the end of the isolation and selection procedure.

3.2.2. *In-vitro* growth (IVG) culture system

The IVG system was carried out according to the published protocols (Nagano et al., 2013; Chelenga et al., 2023). A total of 120 isolated COCs (across 6 replicates) were placed individually in the centre of a 96 well gas permeable plates with *in-vitro* oocyte culture medium (TCM199 supplemented with 0.91 mM sodium pyruvate, 10 ng/mL androstenedione, 5% foetal calf serum (FCS), 4 mM hypoxanthine, 4% polyvinylpyrrolidone, 10 mg/mL amphotericin B, 50 mg/mL gentamicin sulphate, and 10 μg astaxanthin).

The individual COCs were cultured for 8 days; during the first 4 days the COCs were incubated under 5% O_2, then the conditions were changed to 20% O_2 at 39°C for the remaining 4 days. The medium was refreshed on day 4. In order to assess oocyte growth, the diameter of the oocytes was measured (excluding the zona pellucida) on day 0 and on day 8 of IVG. After the completion of IVG, 3 replicates (60 COC) were submitted to pre-IVM and then placed into 24h of IVM; and the other 3 replicates (60 COC) were washed directly in IVM and submitted to 24h of maturation.

3.2.3. Pre *In-vitro* maturation (IVM) system

Once the 8 days of IVG were completed, 60 COC were washed in pre-IVM medium (TCM199 supplemented with 0.2 mM sodium pyruvate, 0.02 units/mL FSH, 1 mg/mL

oestradiol-17β, 10% FCS, 50 µg/mL gentamicin sulphate, and 0.5 mM IBMX (PDE inhibitor) and incubated for 5h in 5% CO_2 at 39°C. A graphical representation of this system is illustrated in the Figure 3.1.

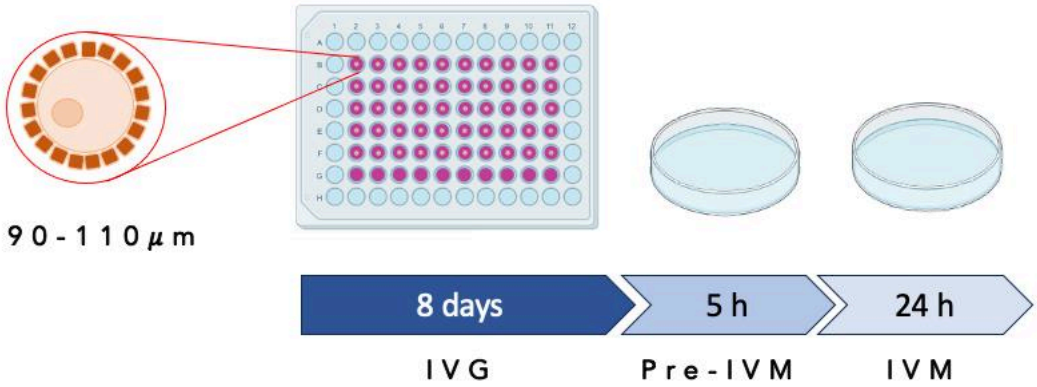

Figure 3.1. Graphical representation of the IVG system. Oocyte-cumulus-granulosa complexes were cultured for eight days in the gas-permeable culture device in the IVG culture medium. The oxygen environment was switched from low (5%) to high (20%) on Day 4 of IVG culture. After IVG, the COCs were exposed to pre-IVM for 5h and then to IVM for 24h.

3.2.4. IVG – IVM

On day 8 oocytes diameters were measured and afterwards 60 IVG COCs with pre-IVM, and 60 IVG COCs without pre-IVM were subjected to 24h of IVM culture using commercial Strobeck IVM culture medium. Briefly, COCs were washed 2 times in IVM medium, polled in groups of 10 COCs, and placed into 50 mL Strobeck-IVM droplets and then covered with paraffin oil at 39°C for 24h in 5% CO_2 in humidified air. Afterwards, COCs were denuded and processed for assessment.

3.2.5. Long in-vitro oocyte culture system (L-IVOC)

The L-IVOC system was carried out according to the published protocols (Luciano et al., 2021; Garcia-Barros et al., 2023). A total of 180 COCs (9 replicates) were placed individually in the centre of wells in a 96-well plate with long *in-vitro* oocyte culture medium [M199-L (TCM199 supplemented with 2 mM glutamine, 0.4% fatty acid free BSA, 0.2 mM sodium pyruvate, 25 mM sodium bicarbonate, 0.1 mM cysteamine, 21.3 µg/mL of phenol red, 75 µg/mL of kanamycin, 4% Polyvinylpyrrolidone, 0.15 µg/mL Zn sulphate, 10-4 IU/mL FSH, 10 ng/mL oestradiol, 50 ng/mL testosterone, 50 ng/mL progesterone, and 5 µM cilostamide)] for 5 days at 38.5 °C and 5% CO2 in air, maximum humidity. The medium in each treatment was refreshed on days 2 and 4.

On the first 3 replicates (1, 2, 3), oocyte diameter was measured on day 0, day 2, day 4 and day 5, and 5 COCs were collected, denuded and fixed to analyse chromatin stages on these days. For the following 3 replicates (4, 5, 6), oocyte diameter was measured on day 0 and day 5, and COCs were recovered after 5 days of L-IVOC, and processed for chromatin configuration analysis. In the remaining 3 replicates (7, 8, 9), COCs were submitted to 5 days of undisturbed L-IVOC, submitted to IVM, and finally processed for assessment.

3.2.6. L-IVOC - IVM

After L-IVOC, the COCs were washed in maturation medium (TCM199 supplemented with supplemented with 25 mM sodium bicarbonate, 2 mM Gluta-MAXTM, 0.4% BSA fatty acid free, 0.2 mM sodium pyruvate, 0.1 mM cysteamine, 50 µg/mL of kanamycin, and 0.1 IU/mL of r-hFSH), pooled into groups, submitted to 24h IVM and finally, processed for assessment. A graphical representation of this system is illustrated in the Figure 3.2.

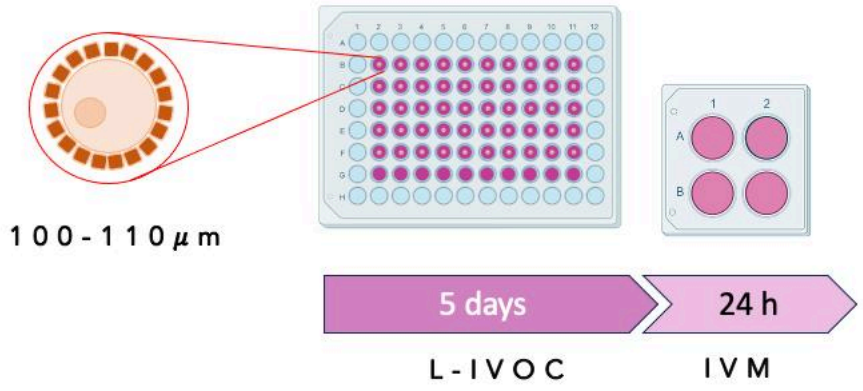

Figure 3.2. Graphical representation of the L-IVOC system. Growing oocytes were retrieved from early-antral follicles and cultured for 5 days in the L-IVOC culture medium. After L-IVOC, the COCs were matured for 24h in IVM culture medium.

3.2.7. L-IVOC and inhibition of nPR during oocyte growth

To assess the function of the nPR during oocyte growth a total of 259 (across 5 replicates) bovine COCs were submitted to L-IVOC under the presence or absence of P4 or nPR inhibitor (Aglepristone). The M199-L culture media, as described by Garcia Barros et al., 2023, was used as a control group. The three different growing media treatments were prepared: M199-L + Aglepristone (Treatment 1): M199-L culture medium with Aglepristone 1 µM (nPR antagonist); M199-L – P4 (Treatment 2): M199-L culture medium without 50 ng/mL

progesterone; and M199-L – P4 + Aglepristone (Treatment 3): M199-L without 50 ng/mL progesterone + Aglepristone 1 µM.

The selected COCs were randomly assigned to each treatment, they were cultured for 5 days at 38.5 °C and 5% CO2 in air, maximum humidity. The medium in each treatment was refreshed on days 2 and 4. On day 5 of L-IVOC, the COCs were removed from culture and their morphology was assessed, according Garcia Barros et al., 2023. Briefly, COCs with compact cumulus cells, showing no signs of expansion or cell degeneration were scored as Class 1. Class 2 COCs presented compact cumulus cells with no signs of expansion or cell degeneration but included antrum-like formation. Class 3 was characterised by cumulus cells with no signs of expansion and some disaggregation. Class 4 COCs exhibited abundant cumulus cell loss and cell degeneration. Classes 1, 2, and 3 were judged to be healthy, and selected to proceed into *in vitro* maturation. Whereas Class 4 was considered compromised due to evident signs of degeneration and were discarded.

Class 1, 2 and 3 cumulus-oocyte complex were submitted to in vitro maturation. The COCs were washed in maturation medium, pooled into groups and submitted to 24h IVM. Following IVM, oocytes were processed for chromatin configuration analysis.

Figure 3.3. Graphical representation of the experimental design. Growing oocytes were retrieved from early-antral follicles and cultured for 5 days in the L-IVOC culture medium (M199-L) as control, and also submitted to treatments. Treatment 1: M199-L with Aglepristone (nPR inhibitor). Treatment 2: M199-L without P4. Treatment 3: M199-L without P4 and with Aglepristone. After L-IVOC, the COCs were matured for 24h in IVM culture medium.

3.2.8. Germinal vesicle stage and chromatin configuration analysis

Following IVG, L-IVOC or IVM, COCs were denuded of their cumulus investment by gentle pipetting and fixed in 4% paraformaldehyde for 30 min at room temperature and washed repeatedly in PBS. Following which the denuded oocytes were mounted on clean glass slides

in MOLWIOL containing 1 µg/ml 4′,6-diamidino-2-phenylindole (DAPI) for nuclear and chromatin configuration assessment under a fluorescent microscope. Chromatin classification was performed according to Lodde et al., 2007, where four stages of germinal vesicle (GV) progression were described: GV0 stage characterised by the presence of diffuse filamentous chromatin in the entire nuclear area; GV1 stage similar to the GV0 configuration, but with some foci of condensed chromatin in the nucleus; GV2 stage characterised by further chromatin condensation, with chromatin arranged in clumps or strands, and GV3 stage, where chromatin is condensed into a single clump within the nuclear envelope.

3.2.9. Statistical analysis

Statistical analyses of the resulting data were carried out using R studio version 4.2.1 software package for MacOS 11. Differences between groups were considered significant at $p<0.05$. The oocyte diameter between day 0 and day 5 was assessed by T-test. Additionally, the variance of the mean between groups was analyzed by ANOVA followed by Tukey Test.

3.3. RESULTS

3.3.1. IVG system

A total of 120 bovine COCs were submitted to 8 days of IVG according to the published protocols. The diameter of the oocytes was measured on day 0 and day 8 of IVG, on average oocyte diameter was increased by 2 µm following culture (104 µm ± 1.52 vs 107 µm ± 2.20).

The protocol included a pre-IVM step, where the COCs were incubated for 5h in IVM media containing IBMX (PDE inhibitor), prior to submission to 24h of IVM (Chelenga et al., 2023). Three replicates, comprising 60 COCs were submitted to this protocol, however, as summarised in Table 3.1, the majority of the oocytes (67%), did not progress beyond their original GV0 stage, a small number of oocytes (20%) progressed to GV1 stage, and the remainder had degenerated.

Table 3.1. Bovine oocyte chromatin categorisation after 8 days of IVG and IVM conditions.

		Chromatin categorisation after IVM			
N Oocytes	**pre-IVM**	**%GV0**	**%GV2**	**%MII-like**	**%DEG**
60	+	67 ± 2	20 ± 1.4	0	13 ± 2.7
60	-	10 ± 7.1	48 ± 4.6	22 ± 3.5	20 ± 2.5

Values are presented as mean percentages ± SE. GV0: germinal vesicle. GV2: germinal vesicle 2. MII-like: metaphase II-like stage without GVBD. DEG: degrade oocytes.

As the oocytes appeared to be unable to resume meiosis, an additional 3 replicates (60 COCs) were submitted to 8 days of IVG and transferred directly into IVM without a pre-maturation step. Chromatin assessment revealed a higher proportion (48%) of oocytes had progressed to GV2, and ~22% of oocytes presented an aligned chromatin configuration within the nuclear envelop, referred to as MII-like, (Figure 3.1) and 20% of oocytes were degraded (Table 3.1).

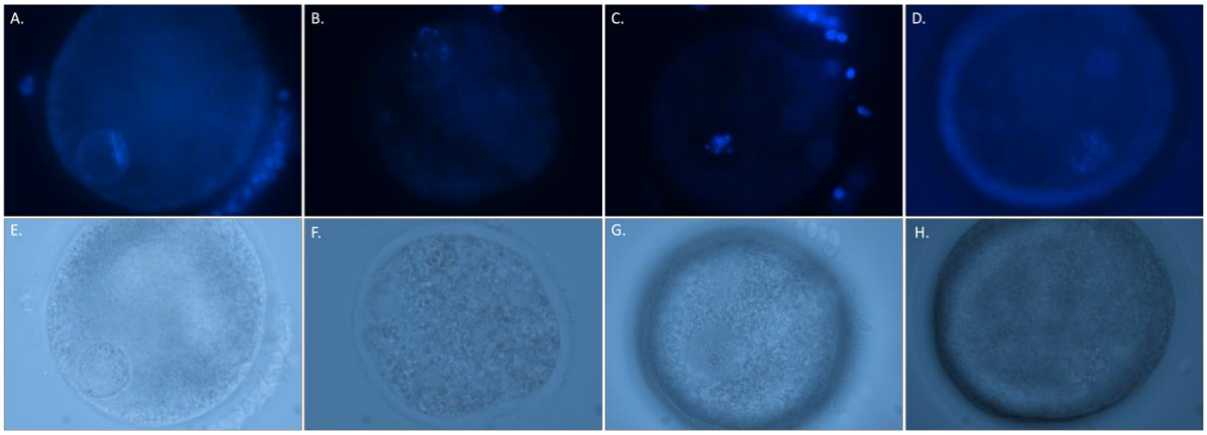

Figure 3.4. Bovine oocyte chromatine characterisation after IVG + IVM. Micrographs showing immunofluorescent labelling in the DNA showing different chromatin configurations after 8 days of IVG and posterior 24h IVM. DNA was visualised in blue (DAPI). **A)** Metaphase II-like **B)** and **C)** GV2 **D)** GV0. **E** – **H)** Brightfield correspondent to each oocyte (n = 6 replicates).

3.3.2. L-IVOC system

During the first 3 replicates (60 COCs) of the L-IVOC system, oocyte diameter was measured on day 0, 2, 4, and 5 of culture to corroborate oocyte growth. The results revealed an average increase in oocyte diameter of 2 µm (109 µm ± 1.66 vs 111 µm ± 1.60) during the 5 days of L-IVOC. Additionally, a progressive condensation of the chromatin was observed, from 100% of the oocytes at GV0 stage on day 0 to 60% at GV1 stage on day 2, 40% at GV2 and

33% at GV3 on day 4 and finally on day 5, 53% were at GV3 stage and 27% were at GV2 stage. The data is summarised in Table 3.2, and representative images are shown in Figure 3.2.

Table 3.2. Bovine COC GV stage on days 0, 2, 4 and 5 of L-IVOC.

Day of L-IVOC	N Oocytes	%GV0	%GV1	%GV2	%GV3	%DEG
0	**15**	100	0	0	0	0
2	**15**	7 ± 6.5	60 ± 20	0	7 ± 6.7	27 ± 17.6
4	**15**	0	13 ± 6.7	40	33 ± 13.3	13 ± 6.7
5	**15**	0	0	27 ± 6.7	53 ± 6.7	20

Values are presented as mean percentages ± SE. GV0: germinal vesicle. GV2: germinal vesicle 2. GV3: germinal vesicle 3. DEG: degrade oocytes.

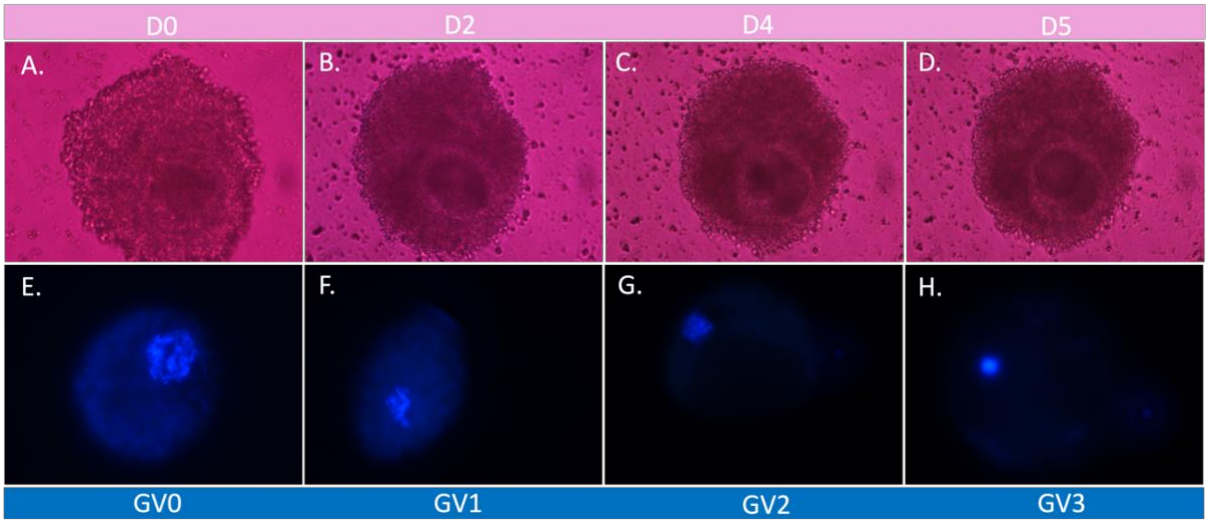

Figure 3.5. Bovine COCs morphology and chromatin condensation across L-IVOC days. Micrograph showing representative images of oocyte chromatin configurations on different days of L-IVOC. DNA was visualised in blue (DAPI). On the top panel COCs pictures in day 0, day 2, day 4 and day 5 of L-IVOC. **A)** COC at day 0 of L-IVOC. **B)** COC at day 2 of L-IVOC. **C)** COC at day 4 of L-IVOC. **D)** COC at day 5 of L-IVOC. On the bottom panel, chromatin condensation on their correspondent days of L-IVOC. **E)** GV0 stage. **F)** GV1 stage. **G)** GV2 stage. **H)** GV3 stage.

Once the oocyte growth and GV progression were confirmed during 5 days of L-IVOC, another 3 replicates (60 COCs) were submitted to culture without interruption. Samples were analysed on day 0, before culture, and on day 5, the final day of L-IVOC. At the end of the culture, oocyte diameter was significantly increased (106 µm ± 0.60 vs. 108 µm ± 0.61, $p<0.01$), illustrated in Figure 3.3. Chromatin assessment following 5 days of L-IVOC showed

that a high proportion of oocytes remained in meiotic arrest, but had progressed through the DNA condensation process. On day 0, 97% of analysed oocytes were at GV0 stage, and the 3% remaining were in GV1 stage. Whereas, on the last day of culture, 1% of oocytes had remained in GV0, 28% of oocytes had progressed to GV1 stage, 65% of oocytes had progressed to GV2 stage and 5% had degenerated. The data is summarised in Table 3.3.

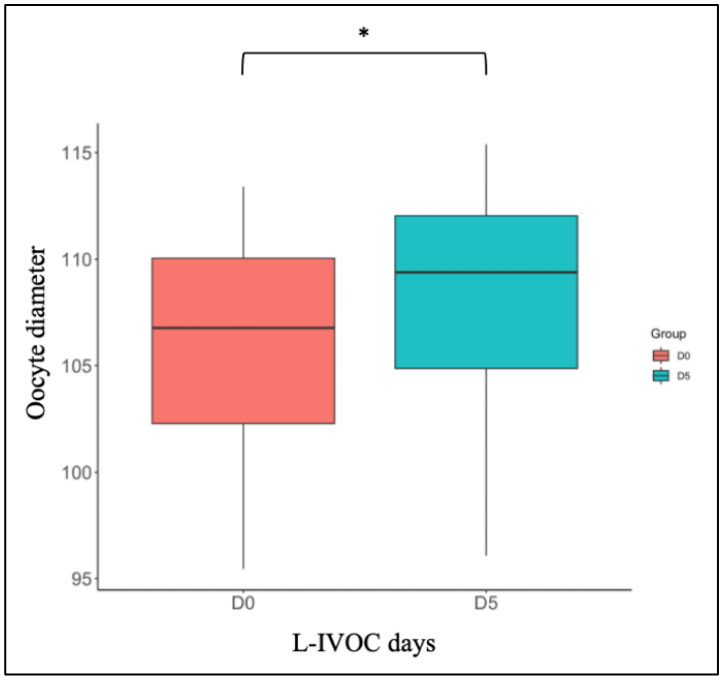

Figure 3.6. Bovine oocyte diameter growth during the 5 days of L-IVOC. Boxplot showing the oocyte diameter before L-IVOC and after 5 days of L-IVOC. Orange: L-IVOC day 0. Green: L-IVOC day 5. T-test analysis ($p<0.01$).

Table 3.3. Bovine COC chromatin condensation across day 0 and 5 of L-IVOC.

Day of L-IVOC	N Oocytes	%GV0	%GV1	%GV2	%GV3	%DEG
Day 0	60	97 ± 1.7	2 ± 1.7	0	2 ± 1.7	0
Day 5	60	0	1 ± 1.7	65 ± 2.9	28 ± 1.7	5 ± 1.7

Values are presented as mean percentages ± SE. GV0: germinal vesicle. GV2: germinal vesicle 2. GV3: germinal vesicle 3. DEG: degrade oocytes.

An additional 3 replicates of L-IVOC were carried out to assess the capability of COCs to develop to MII during IVM after 5 days of L-IVOC. A total of 120 COCs were submitted to the original protocol by Garcia-Barros et al., 2023. However, the chromatin assessment revealed that L-IVOC oocytes did not resume meiotic maturation, as all oocytes were arrested at GV3 stage following IVM (Figure 3.4).

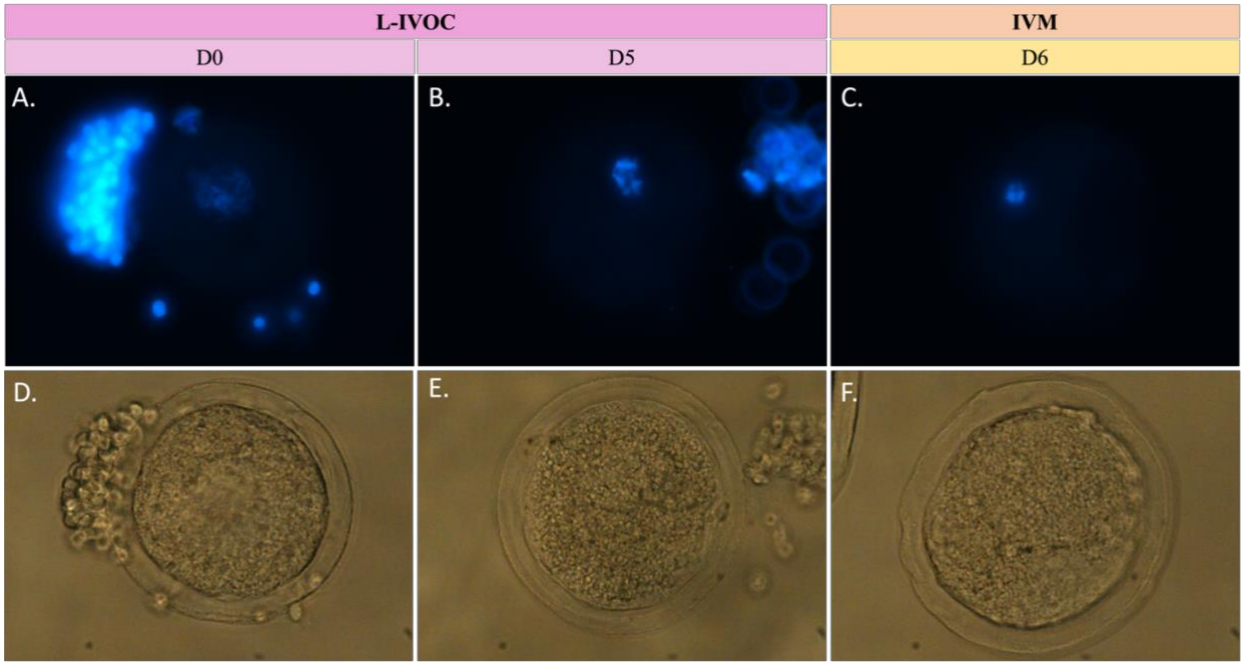

Figure 3.7. Bovine COCs morphology and chromatin condensation across L-IVOC + IVM. Micrographs showing immunofluorescent labelling in the DNA showing different chromatin configurations on day 0 and day 5 of L-IVOC, and IVM on day 6. DNA was visualised in blue (DAPI). On the top panel bovine chromatin status on day 0, day 2, day 6. **A)** Oocyte at day 0 of L-IVOC. **B)** Oocyte at day 5 of L-IVOC. **C)** Oocyte at day 6 after 24h IVM. On the bottom panel, brightfield on their correspondent days of L-IVOC and IVM. **D)** GV0 stage. **E)** GV2 stage. **F)** GV3 stage.

3.3.3. Nuclear PR inhibition during bovine oocyte growth and survival rate

The total number of COCs submitted to control and treatment groups for 5 days of L-IVOC are presented in Table 3.4.

Table 3.4. Total number of bovine COCs that were submitted before and after L-IVOC and the survival rate per treatment.

IVM Conditions	%Day 0	%Day 5	%Survival Rate
Control	13 ± 2.2 (65)	8.8 ± 1.7 (44)	68.06 ± 2.12[a]
Treatment 1 **M199-L + Aglepristone**	13.8 ± 2 (69)	4.8 ± 1.4 (24)	34.86 ± 2.01[b]
Treatment 2 **M199-L - P4**	14.6 ± 1.8 (57)	8 ± 1.2 (32)	56.31 ± 1.14
Treatment 3 **M199-L - P4 + Aglepristone**	13.6 ± 1.9 (68)	7 ± 1 (35)	53.25 ± 2.13

Values are presented as mean percentages ± SE. Data shown between () represent oocyte total number. Data with different letters within the same column indicate significant differences ($p<0.05$).

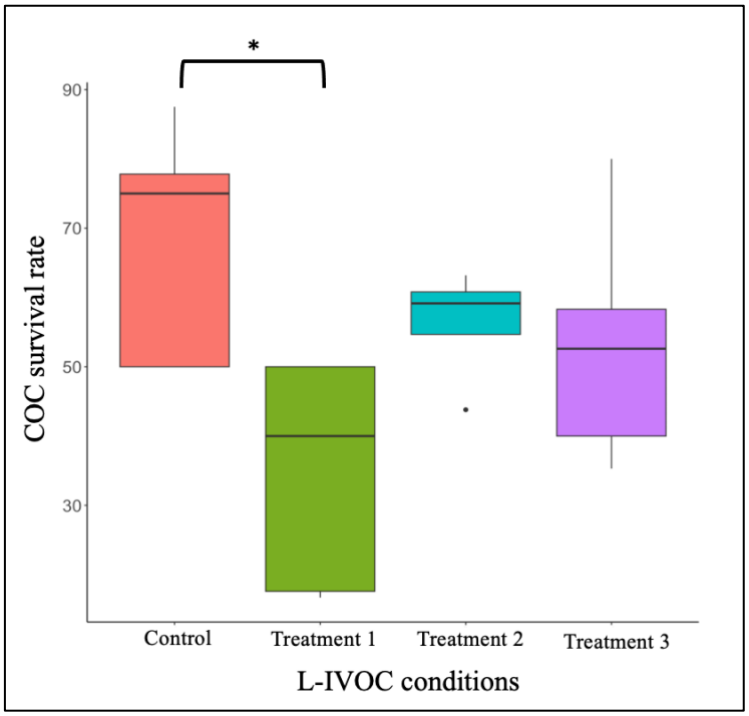

Figure 3.8. Variance of COC survival rate per treatment after 5 days of L-IVOC. Boxplots showing the variability number of COC that survived per L-IVOC treatment. There is a significant lower number of COCs in the treatment 1 (M199-L + Aglepristone) compared with the COCs that grew in the control group. Each color represents a treatment. Orange: Control; Green: Treatment 1 (M199-L + Aglepristone); Blue: Treatment 2 (M199-L – P4); Treatment 3: (M199-L - P4 + Aglepristone) (n=5 replicates). Statistical analysis performed by ANOVA followed by Tukey's test.

Analysis of the variance between groups revealed a significant decrease in the proportion of COCs that survived culture in M199-L + Aglepristone compared with untreated control COCs (68.06 ± 2.12 vs. 34.86 ± 2.01, $p<0.03$). However, survival rates for COCs cultured in L-IVOC without P4 or without P4 and Aglepristone did not significantly differ from the control (Figure 3.4).

3.3.4. *In-vitro* maturation after L-IVOC and meiosis progression

The meiotic competence of COCs that survived the L-IVOC, during which nPR activity was blocked, was tested by submitting them to IVM. Following which, their chromatin was labelled with DAPI and evaluated under a fluorescent microscope. Oocyte chromatin configurations were categorised as metaphase plate II (MII), metaphase plate I (MI), germinal vesicle (GV), misaligned or aberrant (AB) and degenerated oocytes (DEG) (Figure 3.5).

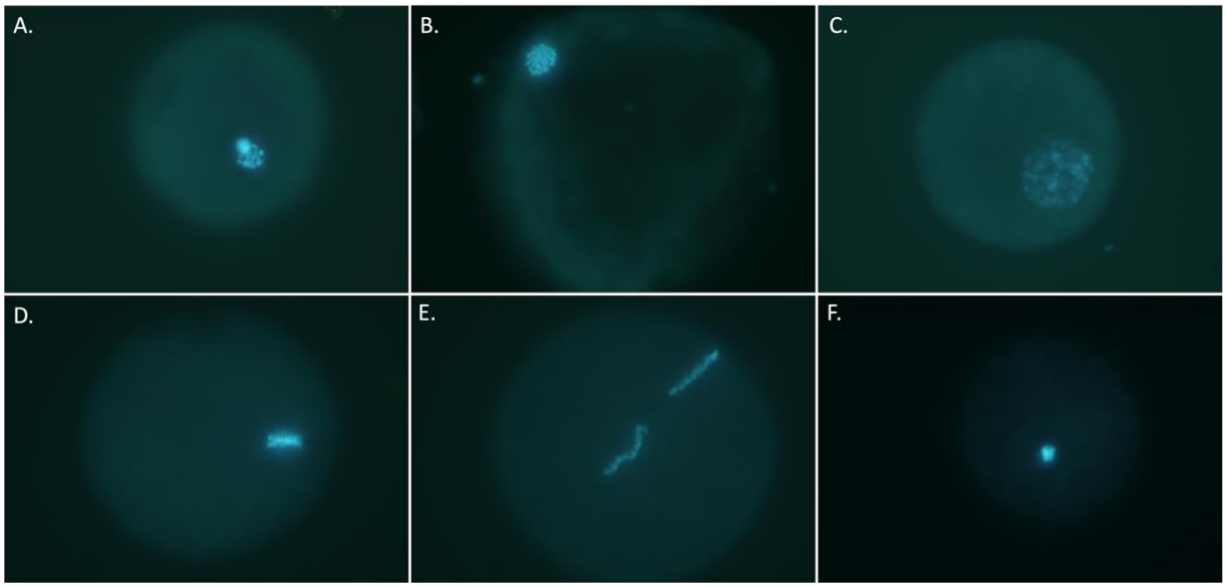

Figure 3.9. Bovine oocyte chromatine characterisation after L-IVOC + IVM. Micrographs showing immunofluorescent labelling in the DNA showing different chromatin configurations after 5 days of L-IVOC and posterior 24h IVM. DNA was visualised in blue (DAPI). **A)** Metaphase II plate. **B)** Metaphase I plate. **C)** Germinal Vesicle. **D)** Metaphase II plate aberration. **E)** Metaphase II plate aberration. **F)** Degenerated oocyte (n = 5 replicates). Scale bar = 20 μm.

Table 3.5. Total number of oocytes after L-IVOC + IVM categorised by chromatine configuration.

Conditions	%MII	%MI	%GV	%AB	%DEG
Control	43 ± 3.8 (20)	24 ± 2.8 (10)	16 ± 4.7 (6)	9 ± 6.7 (4)	9 ± 6.4 (4)
Treatment 1 M199-L + Aglepristone	25 ± 7.4 (6)	9 ± 7.2 (3)	15 ± 6.3 (5)	28 ± 19.6 (5)	23 ± 8 (5)
Treatment 2 M199-L - P4	28 ± 6.5 (10)	40 ± 6.5 (11)	8 ± 5.2 (3)	6 ± 5.6 (2)	18 ± 5.9 (6)
Treatment 3 M199-L - P4 + Aglepristone	41 ± 6.8 (15)	21 ± 6.8 (8)	0	10 ± 6.1 (3)	28 ± 5.1 (9)

Values are presented as mean percentages ± SE. Data shown between () represent oocyte total number. MII: metaphase II. MI: metaphase I. GV: germinal vesicle. AB: aberrancies. DEG: degrade oocytes.

The proportion of oocytes presenting chromatin configurations in each category are summarised in Table 3.5. The proportion of oocytes completing meiotic maturation *in-vitro* and presenting at MII, or remaining at GV, or showing signs of aberrant chromatin plates or degeneration did not differ significantly between groups ($p>0.1$). However, the proportion of

oocytes at MI was significantly lower in the treatment 1 (M199-L + Aglepristone) compared with the treatment 2 (M199-L - P4) (9 ± 7.2 vs 40 ± 6.5. $p<0.1$) (Figure 3.6).

The competence of the oocytes to resume meiosis and progress through germinal vesicle breakdown was assessed. To this end, the proportion of oocytes reaching MI or MII stages of meiosis were compared across treatment groups by analysis of variance. There was a significant decrease in the proportion of oocytes at MII/MI stages in treatment 1 (M199-L + Aglepristone) compared with the control group (34 ± 7.67 vs. 66 ± 3.65, $p<0.05$) (Figure 3.7).

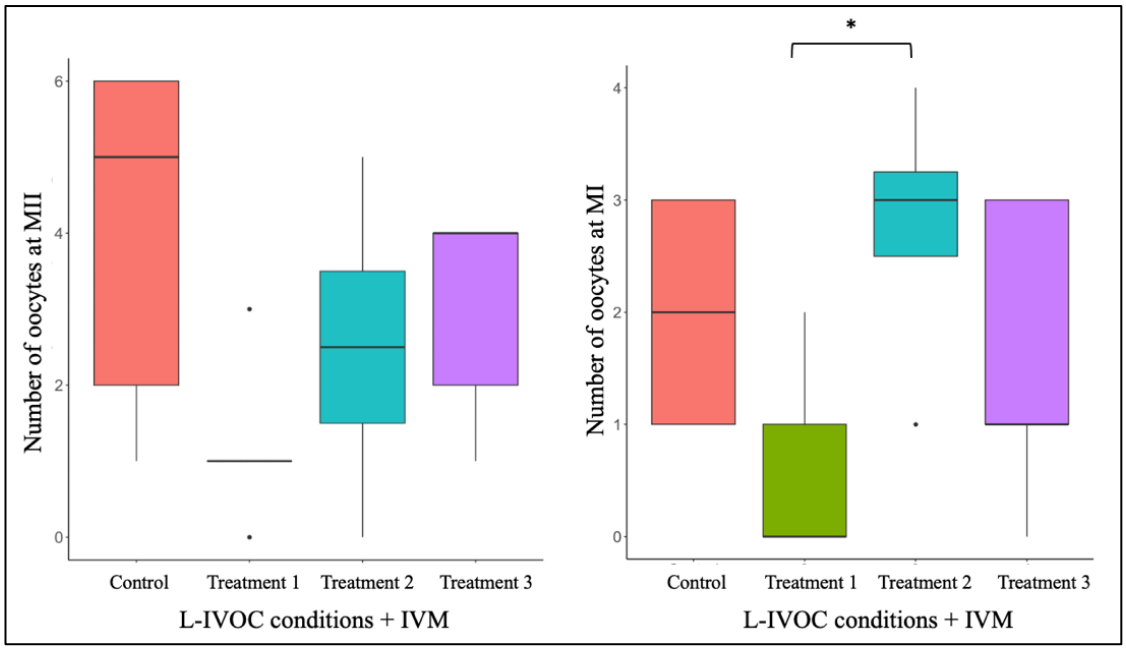

Figure 3.10. Variation in the number of different chromatin configuration after 5 days of L-IVOC and IVM in bovine oocytes. A) Boxplots showing the variability of the number at metaphase II stage in bovine oocytes. **B)** Boxplots showing the variability of the number at metaphase I stage in bovine oocytes (n=5 replicates). Orange: Control; Green: Treatment 1 (M199-L + Aglepristone); Blue: Treatment 2 (M199-L – P4); Purple: Treatment 3 (M199-L - P4 + Aglepristone) (n=5 replicates). Statistical analysis performed by ANOVA followed by Tukey test.

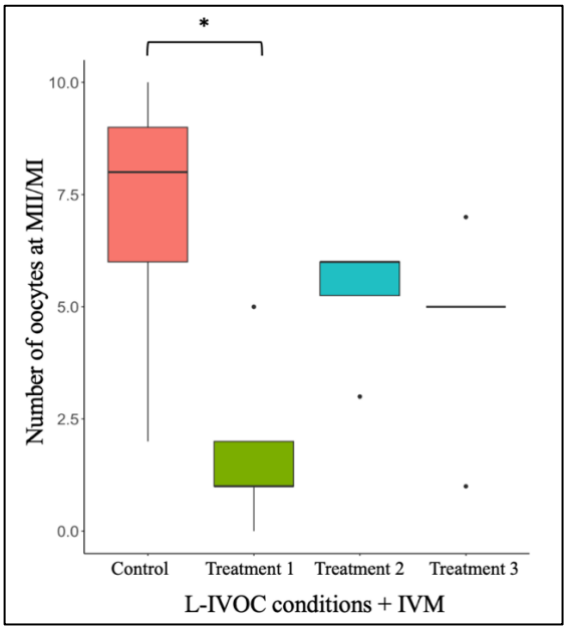

Figure 3.11. Variance of the number of oocytes reaching to MII/MI stages between L-IVOC treatments after IVM. Boxplots showing the variability number of oocytes reaching to MII/MI after 5 days of L-IVOC treatments and 24h IVM. There is a significant lower number of MII/MI oocytes in the treatment 2 (M199L with P4 + Aglepristone) compared with the MII/MI oocytes that grew in the control group. Each color represents a treatment. Orange: Control; Green: Treatment 1 (M199-L + Aglepristone); Blue: Treatment 2 (M199-L – P4); Purple: Treatment 3: (M199-L - P4 + Aglepristone) (n=5 replicates). Statistical analysis performed by ANOVA followed by Tukey test.

3.4. DISCUSSION

To understand the role of the nPR during bovine oocyte growth an *in vitro* growing bovine oocyte culture system was necessary to perform functional analyses. Therefore, the establishment of two systems was attempted, the IVG and the L-IVOC. Oocyte development appeared to be better following culture in the L-IVOC system as approximately 40% COC's successfully resumed and completed meiotic maturation, therefore, it was selected for the functional analysis. The inhibition of the nPR with Aglepristone, a pharmacological antagonist, during bovine oocyte growth affected COC survival and the ability of these oocytes to resume meiosis.

The IVG and the L-IVOC systems focus on the acquisition of meiotic and developmental competence of bovine growing oocytes during culture. Spontaneous resumption of meiosis is prevented by inhibiting phosphodiesterase (PDE) activity in the oocyte. Although both systems use different pharmacological inhibitors, PDE inhibitor 3-isobutyl-1-methylxanthine (IBMX) and phosphodiesterase-3 (PDE3) (cilostamide) respectively, they promote the accumulation of cAMP in oocytes, leading to the phosphorylation of cyclin-dependent kinase 1 and maturation-promoting factor, blocking the meiosis machinery.

There are several differences between the two systems; the IVG media contains FCS and the protocol uses two sequential oxygen conditions (4 days in 5% O_2 followed by 4 days in 20% O_2), during the 8 days of IVG, followed by a 5h pre-IVM step and 24h IVM. Whereas in the L-IVOC system, oocytes are cultured in defined media on collagen plates in 5% CO_2 for the 5 days of culture, this system does not include a pre-IVM step.

Another *in-vitro* bovine oocyte growth system reported in the literature (Fushii et al., 2021) appears to be a blended approach, in that similar to Garcia Barros et al. (2023) the Authors cultured the oocytes in defined culture medium, and in line with the protocol of Chelenga et al (2023), they employed a sequential atmosphere, 5% O_2 for the first 7 days of a 14 day culture period, followed by the remaining 7 days in 5% CO_2. The Authors cultured COCs and cumulus cell-mural granulosa cell in their system and reported that oocytes grew from 100 to 120 μm and acquired meiotic competence, with a more than 80% of maturation rate.

The reason for including the IVG system as a candidate was their reported *in-vitro* blastocyst rate at 22% when IVG COCs were submitted to pre-IVM prior to IVM. In this system, Chelenga et al., 2023 demonstrated a 70% maturation rate post-IVG, and this incredible success in maturation could be related in the presence of FCS in their culture media. However, after our attempts to establish the IVG system, there was no evidence of meiotic competence in our oocytes. The results from the first experiment corroborated oocyte growth by their increase in diameter by 2 μm at the end of the culture period, and chromatin progression from GV0 to GV2 stage on assessment after the pre-IVM step, but the oocytes did not successfully progress to MII during IVM. Thus, a second experiment was carried out which omitted the pre-IVM step and COCs were transferred directly to IVM following IVG. However, after 8 days of IVG and 24h of IVM, the oocytes presented a metaphase II like chromatin arrangement, but within an intact nuclear membrane and in the absence of polar body extrusion.

The L-IVOC system was established by confirming in several checks that the protocol was correctly performed. During the 5 days of L-IVOC the oocyte nucleus chromatin configuration progressed from GV0 to GV2/GV3, and oocyte diameter increased by 2 μm. Following repeated trials, during the nPR functional analysis 40% of oocytes in the control treatment completed meiosis maturation, in agreement with report of Garcia-Barros et al., 2023.

To assess the role of nPR during bovine growth, a functional analysis was performed using the L-IVOC system. Surprisingly, the COC survival rate for treatment 2 (M199-L – P4) and treatment 3 (M199-L – P4 + Aglepristone) were not affected by the absence of P4 and the

presence of nPR inhibitor, respectively. These treatments aimed to observe any additional detrimental effects on oocyte growth in the medium without P4 or with Aglepristone; however, this was not observed. Moreover, the COCs that survived and were subjected to IVM demonstrated an ability to resume meiosis.

In this study, the number of COCs that survived after five days nPR blocking in L-IVOC P4 + medium was significantly affected compared to control and the other treatments. Previous studies targeted the 24h maturation period *in-vitro*, indeed there was no effect of nPR blocking during this period on oocyte maturation rate, however blastocyst development was significantly impaired in the group treated with Aglepristone or RU 486 (mifepristone) (O'Shea et al., 2013; Aparicio et al., 2011). This evidence combined may suggest that nPR has a critical role in oocyte growth to achieve a correct cytoplasmic and nuclear maturation.

Contradictory studies suggest that nPR could have a species-specific role in acquisition of oocyte competence; Roh et al., 1988 conducted a study in mice to evaluate the potential role of P4 or the nPR in maturation, ovulation, fertilisation and embryo cleavage. They injected P4 or RU 486 for 2 days into the animals and found no differences in maturation or cleavage, however, the number of embryos was significantly reduced in the RU 486 treated group. Similarly, a recent study in canine oocytes also reveal that the addition of Aglepristone into the IVM media highly decrease the maturation rate compared with the control group (De los reyes et al., 2023).

Interestingly, treatment 2 (M199-L – P4) and 3 (M199-L – P4 + Aglepristone) did not significantly impact COC survival rate compared to treatment 1 (M199-L + Aglepristone) or control. In both treatments, P4 was not added into the culture media, thus there was some expectation that COC survival would be impacted. A preliminary analysis of P4 concentration in spent culture media revealed an increase in P4 levels in the L-IVOC medium from day 2 to day 5 in the treatment groups lacking P4 (unpublished data). Therefore, the recovery in the COC survival rate on these treatments could be related to the P4 synthesis by the cumulus cells during culture; many studies have confirmed that cumulus cells produce P4 during IVM, in a time dependent manner, achieving the highest concentration at 24h (40.12 ± 4.48 ng/ml) (Mingoti et al., 2002; Schoenfelder et al., 2003; Nuttinck et al., 2008; Aparicio et al., 2011; Tetsuka et al., 2019). However, this hypothesis does not address the conflicting survival rates of the two Aglepristone treatments.

There is an alternative mechanism whereby P4 binds with nongenomic receptors, activating rapid signaling events independent of transcriptional or genomic regulation

(Boonyaratanakornkit, 2004). This event involves the nongenomic membrane progesterone receptors (mPR) and its mediators P4 receptor membrane components 1 and 2 (PGRMC1 and PGRMC2) which belong to the membrane-associated P4 receptor (MAPR) protein family (Zhu et al., 2003; Cahill, 2007). Immature and matured bovine COCs express mPRα and mPRβ in both the oocyte and cumulus cells, whereas PGRMC1, and PGRMC2 expression was only detected in cumulus cells (Aparicio et al., 2011; O'Shea et al., 2013). These findings suggest that P4 may also act through non genomic receptors to enhance oocyte survival, reflecting that further studies are required for a deeper understanding of the PR activation and regulation.

The endpoint of this experiment was the evaluation of the MII stage after 5 days of growth and subsequent IVM, to analyze if the treatments impacted the acquisition of oocyte competence. Surprisingly, there was no significant difference in the number of oocytes at the metaphase II stage between the control and treatments. However, when comparing the capability of the oocytes to resume meiosis (pooling MII and MI oocytes together), we observed a significant reduction in the number of oocytes at MII and MI in treatment 1 (M199-L + Aglepristone) compared to the control.

Previous studies by our group evaluating the inhibition of the nPR (Aglepristone) or P4 (Trilostane) during IVM on the metaphase II stage in bovine oocytes revealed no difference between treatment and control (O'Shea et al., 2013). In this study, the inhibition of the nPR was performed at an earlier stage (during L-IVOC), and although the effect on the MII stage was not significant, there was a clear effect on the resumption of meiosis. This suggests that nPR inhibition prior to IVM might play a role in the resumption of meiosis. Nevertheless, future studies with adequate and established techniques for oocyte growth will improve this study and provide better clarification on this subject.

Although the L-IVOC system was successfully established, the oocyte maturation rate described by Garcia-Barros et al., 2023 provides a suitable strategy for fertility preservation programs in animals of high genetic merit, rather than for a functional analysis. Therefore, the variability observed between replicates in the nPR inhibitory experiment dot not allow us to conclude with certainty about the effect of the receptor during bovine oocyte growth.

In summary, this research confirmed that *in-vitro* bovine oocyte growth is a challenging process requiring ongoing refinement and optimisation to ensure replicability and the creation of a stable system that provides valuable insights into the factors regulating follicle and oocyte development. Further studies are necessary to elucidate the detailed mechanisms of nPR action

and its implications during oocyte growth. Understanding these processes will provide deeper insights into improving oocyte quality and embryo development in reproductive biotechnology.

Chapter 4

Effect of nuclear progesterone receptor in mitochondria profiling

4.1. INTRODUCTION

In Chapter 2, the expression profile of nuclear progesterone receptor (nPR) was detailed in oocytes and follicles from primordial to early-antral follicle stages, including the cytoplasmic distribution of the nPR-A isoform in bovine oocytes from 60-120 μm in diameter. Interestingly the nPR-A showed a size-dependent pattern of localisation, presenting a clustered pattern in oocytes 60-80 μm in diameter compared to a more dispersed arrangement in larger oocytes (oocytes ≥90 μm in diameter). Additionally, performing a functional analysis, the inhibition of the nPR-A during bovine oocyte growth *in-vitro* compromised oocyte competence, since very few oocytes survived and of those that did survive, their meiotic capability was reduced.

Nuclear progesterone receptors are important members of the steroid receptor family, an evolutionarily conserved group of transcription factors (Xin et al., 2016). In the absence of P4 in the extracellular space, nPR protein resides within the cytoplasm, forming a complex with chaperone proteins. These chaperones hold the receptor in an inactive state, primed to bind to ligands (Pratt & Toft, 1997). Upon ligand binding, nPR undergoes a conformational change which triggers release from the chaperone complex and favours receptor dimerisation (Pratt et al., 1999). Dimerised hormone-receptor complexes translocate to the nucleus, where they bind recognition sequences known as response elements. These sequences or progesterone response elements (PREs) are located in enhancer/promoter regions of the target genes. This domain is responsible for linking the receptors to the cellular transcriptional machinery and regulates transcription of target genes (Ham et al., 1988).

The acquisition of oocyte competence is a complex, well-orchestrated two-step process involving nuclear and cytoplasmic maturation (see review by Fair & Lonergan, 2023). Nuclear maturation mainly involves chromosomal segregation, whereas cytoplasmic maturation involves organelle reorganisation (Hyttel et al. 1989; Assey et al. 1994) and storage and processing of mRNAs, proteins and transcription factors that act in maturation, fertilisation and early embryogenesis (reviewed by Fair & Lonergan, 2023). Although they are distinct processes, both are interlinked events that occur simultaneously at determined times. Cytoplasmic maturation involves cytoskeleton dynamics, molecular maturation and the redistribution of various cell organelles (reviewed by Ferreira et al. 2009). Among them, the

mitochondria is the most abundant organelle in the mammalian oocyte, which undergoes a massive amplification in number (~40 fold-increase) from the primary to the mature-oocyte stage (Cao et al., 2007; Wai et al., 2008, Toranzo et al., 2018). Additionally, mitochondria play an extremely important role since they are a key component of the metabolic machinery responsible for the supply of energy that is consumed during the maturation process (Stojokovic et al., 2001).

Mitochondria are maternally inherited, semi-autonomous organelles with their own genomes (mtDNA), largely responsible for the generation of energy in the form of adenosine triphosphate (ATP). A series of large membrane protein complexes (I – V), in the inner mitochondrial membrane are responsible for this process, known as the electron transport chain. The electron transport chain takes electrons from metabolites and uses their energy to build a proton gradient across the inner mitochondrial membrane, which in turn powers production of ATP (Sousa et al., 2008; Hock et al., 2020). The majority of the correct functioning of mitochondria is based on the large electrochemical proton gradient, whose component, the inner mitochondrial membrane potential, is strictly controlled by ion transport through mitochondrial membranes (Szabo & Szewczyk, 2023).

Evidence demonstrates that oocyte competence is linked with oocyte mtDNA content (Reynier et al., 2001; Tamassia et al., 2004; Cummins, 2004; Shourbagy et al., 2006; Toranzo et al., 2018). Based on this concept, it has been proposed that the large amount of mtDNA and, by inference, the mitochondria present in the oocyte, may represent a genetic mechanism to ensure the distribution of these organelles and molecules to the gametes and somatic cells of future generations. Thus, mitochondria are not only crucial for oocyte metabolism, but their numbers also predict functional competence, as a reduced number of mitochondria may lead to abnormal distribution of the organelle during early embryogenesis (Shoubridge & Wai, 2007). Additionally, data published by Barbosa-Latorraca et al., 2024 showed that the expression of genes associated with the electron transport chain was negatively correlated with bovine oocyte size, suggesting a specific size-dependency for particular mitochondrial activity.

To date, the relationship between nPR and mitochondria in bovine oocyte growth, as well as their implications for oocyte competence, has not been assessed. Thus the mRNA expression data, the clustered distribution of the nPR-A in growing bovine oocytes, and the potential role for nPR during oocyte growth, led to the hypothesis of a possible relationship between mitochondria and this receptor. The aim of this study is to characterise mitochondrial distribution, activation and mitochondrial complex expression during bovine oocyte growth, as well as exploring the possibility of a functional relationship with nPR.

4.2. MATERIALS AND METHODS

4.2.1. Identification of genes containing PRE in bovine growing oocytes

Single cell RNAseq analysis of bovine oocytes, measuring 60 to 120 μm in diameter, identified a cluster of genes positively correlated with oocyte size, i.e., their expression increased during oocyte growth (Barbosa-Latorraca et al., 2024). These 1016 genes (Supplementary Table 1) were used as data base for the identification of genes containing the progesterone response element (PRE) core sequence "TGTTCT". Briefly, the 1000 upstream flank sequence of the promoter region of the 1016 genes were analysed by a Motif Fishing Script (below) in R Studio. Gene ontology (GO) analysis of the resulting genelist was performed in Database for Annotation, Visualisation and Integrated Discovery (DAVID) to identify enriched pathways. The gene pathways that GO analysis provided were considered enriched if the FDR<0.1.

PRE Script

```
library(Biostrings)
library(XVector)

# read the FASTA file as a DNAStringSet object
gene_seqs <- readDNAStringSet("data")

# extract the names of the genes
gene_names <- names(gene_seqs)

# create an empty vector to store the names of the genes that contain the sequence
genes_with_seq <- character()

# loop through each gene to check if it contains the sequence
for (i in 1:length(gene_names)) {
  # check if the sequence contains the desired pattern
  if (grepl("TGTTCT", gene_seqs[i])) {
    # if it does, add the gene name to the vector
    genes_with_seq <- c(genes_with_seq, gene_names[i])
  }
}

# print the number of genes and the list of genes that contain the sequence
cat("Number of genes:", length(gene_names), "\n")
cat("Genes with the sequence [TGTTCT]:", genes_with_seq, "\n")

# save the list of genes to a text file
writeLines(genes_with_seq, "genes_with_sequence.txt")
# print the number of genes and the list of genes that contain the sequence
cat("Number of genes:", length(gene_names), "\n")
cat("Genes with the sequence [TGTTCT]:", genes_with_seq, "\n")
```

4.2.2. Growing bovine oocyte collection

Immature cumulus-oocyte complexes (COCs) were obtained from ovaries collected at a local abattoir. The ovaries were submerged in dissection medium [TCM-199 with 0.4% BSA fraction V, 0.164 mM penicillin, 0.048 mM streptomycin, 1790 units/L heparin, and 5 μM cilostamide (Sigma, Ireland)] and oocytes were liberated from their follicles by slicing.

Good quality COCs were selected, denuded of their cumulus investment and the oocyte diameter was measured and subsequently, allocated to the following diameter groups 60-100 μm, 100-110 μm and 120-130 μm, snap-frozen in liquid N_2 for Western blotting, or incubated in MitoTracker Deep Red (Invitrogen #M22426) for mitochondria localisation or MitoTracker Orange CMTMRos (M7510 #ThermoScientific) to identify active mitochondria, followed by fixation in 4% paraformaldehyde for 20 minutes at room temperature. Fully-grown oocytes were recovered by follicle aspiration and were used as control samples.

4.2.3. nPR colocalisation with mitochondria

Immature COCs were incubated for 30 min in 500 μl IVM media (Stroebech Media, Denmark, Product. No. 1.03.020), containing 200 nM MitoTracker Deep Red (Invitrogen #M22426) and 5 μM cilostamide at 39°C in 5% CO_2. The oocytes were then denuded by repeated pipetting and fixed in 4% paraformaldehyde for 30 min at room temperature. The fixed samples were subsequently incubated in PBS containing 0.1% Triton X100 (PBSTx) for 1h under gentle rocking, followed by blocking in PBSTx containing 20% donkey serum at room temperature for 3h. To study the expression and localisation of the nPR in oocytes, the mouse anti-nPR antibody (Epredia #MS-298-P) antibody was used at 1:50 dilution in PBSTx containing 10% donkey serum overnight at 4°C. After incubation, samples were washed four times for 15 min each in PBSTx rocking at 300 rpm. Alexa flour 488 goat anti-mouse in a dilution of 1:500 (Invitrogen #A11029) was used as secondary antibody for 40 min at room temperature. After incubation, samples were washed for four times for 15 min each in PBSTx at 300 rpm and 1h in PBS at 300 rpm. Cellular DNA was stained with 4′,6-diamidino-2-phenylindole (DAPI, 1:1000 dilution) for 30 min. After several washes with PBS, cells were placed on a glass slide with mounting medium and covered with a glass coverslip. Immunolabeled oocytes were visualised using a Carl Zeiss LSM 800 Airy confocal microscopy system at 64X magnification (Carl Zeiss, Jena, Germany). The resulting z-stack images were converted into a orthogonal projection and analysed in ImageJ software to identify the

localisation of the nPR, the mitochondria and the colocalisation in each group size. A total of three replicates, each comprising 10 oocytes per group, were analysed.

4.2.4. Active mitochondria analysis during oocyte growth

Immature COCs grouped according to their diameter (60-100 μm, 100-110 μm and 120-130 μm) were incubated for 30 min in IVM media containing 200nM MitoTracker Orange CMTMRos (M7510 #ThermoScientific) and 5 μM cilostamide at 39°C in 5% CO_2. They were subsequently denuded, fixed in 4% paraformaldehyde, processed and visualised as described in the section above. described in the section above. A total of three replicates, each comprising 10 oocytes per group, were analysed.

4.2.5. Bovine oocyte collection for IVM

Immature COCs were obtained by aspirating follicles from the ovaries of cattle slaughtered at a local abattoir. Good quality COCs were selected and washed, and groups of up to 50 COCs were placed in 500 μl IVM media in a four-well dish and cultured at 39°C for 24 h in a humidified atmosphere containing 5% CO_2.

To study the effect nPR inhibition on oocyte meiotic resumption and developmental competence, IVM was performed in the presence or absence of 1μM Aglepristone for 24 h (n= 3 replicates). Matured COCs were washed four times in PBS, and snap-frozen in liquid N_2 for western blot analysis or incubated with MitoTracker Orange CMTMRos (M7510 #ThermoScientific) to assess the activity of oocyte mitochondria in both conditions.

4.2.6. Western Blotting

Five replicate pools of oocytes assigned to the three diameter groups 60-100 μm (100 oocytes); 100-110 μm (70 oocytes), and 120-130 μm (50 oocytes) were denuded by gentle pipetting and repeatedly washed in PBS containing 0.1% PVP. Oocyte samples were resuspended in lysis buffer (M-PER Mammalian Protein Extraction Reagent, Pierce #78503, Thermo Scientific, Rockford, IL), supplemented with Protease and Phosphatase Inhibitors Cocktail (Halt Protease Inhibitor Cocktail EDTA free and Halt Phosphatase Cocktail, Pierce #78415, #78420, respectively; Thermo Scientific) frozen and thawed three times and centrifuged for 15 min at 4°C. Protein was extracted from bovine kidney and liver tissue samples for use as positive controls. Proteins were denatured by boiling for 5 min at 95°C in loading buffer. The protein content of the cumulus cells, positive controls and oocyte pools

was calculated using the Bradford Assay. Twelve micrograms of protein were loaded and resolved by SDS-PAGE on a 4-12% Bis Tris gel (Invitrogen). Proteins were transferred onto a nitrocellulose membrane that was blocked with blocking buffer (5% BSA in Phosphatase buffered saline solution + Tween 20 (PBST) containing 10mM phosphate buffer, 137mM sodium chloride, 2.7mM potassium chloride, and 0.1% Tween 20) for 1h at room temperature. Immunoblotting was performed by incubating the membranes in blocking buffer overnight at 4°C with rabbit NDUFAB1 antibody (Cell Signalling #71814), SDHB antibody (Cell Signalling #92649), COX IV antibody (Cell Signalling #4850) at 1:000 dilution. Membranes were subsequently washed in PBST and incubated with secondary goat-rabbit antibody (Abcam #6271) at a 1:1000 dilution 1h at room temperature. Following which they were washed 3 times for 5 min each with PBST and the signal was visualised using SuperSignal West Pico Chemiluminescent Substrate Kit (Thermo Scientific #34077), according to the manufacturer's instructions. Bovine kidney and liver samples were used as positive controls. Anti-GAPDH antibody was used as loading control due to being a constitutively expressed housekeeping protein. Band intensity was quantified using the iBright analysis software (Invitrogen).

4.2.7. Statistical Analysis

All the statistical analyses were carried out using R studio, version 4.2.1, software package for MacOS 11. Differences between groups were considered significant when p-values were less <0.05. The densitometry data from the Western blots were analyzed using ANOVA and Kruskal-Wallis's rank sum test. Data from the immunolabelled oocytes were analysed by Poisson regression to determine the correlation between number of nPR foci, mitochondria, and oocyte diameter. The colocalisation of nPR and mitochondria/ μm^3 relative to oocyte diameter was evaluated by ANOVA followed by Tukey test or Kruskal-Wallis rank sum test followed by Dunn Post-Hoc test. The analysis of the intensity of active mitochondria labelling in growing oocytes was evaluated with ANOVA and Tukey test.

4.3. RESULTS

4.3.1. Identification of PRE genes in bovine growing oocytes

A subtotal of 230 genes containing the PRE core sequence "TGTTCT" were identified in the genelist by the Motif Fishing Script (Supplementary Table 2). Additionally, the core sequence was corroborated manually on the gene promoter regions. Gene ontology analysis performed in DAVID (FDR<0.1) revealed several enriched pathways, of which nucleus, stress

response and mitochondrial function are most noteworthy (Supplementary Table 3). The enriched pathways are presented in Figure 4.1.

A total of 43 genes were associated with nuclear process, most of which were involved in DNA repair, DNA binding, DNA or RNA transcription and gene expression. Regarding genes enriched in mitochondrial pathways, 13 genes were mainly associated with inner mitochondrial membrane organisation (Table 4.1).

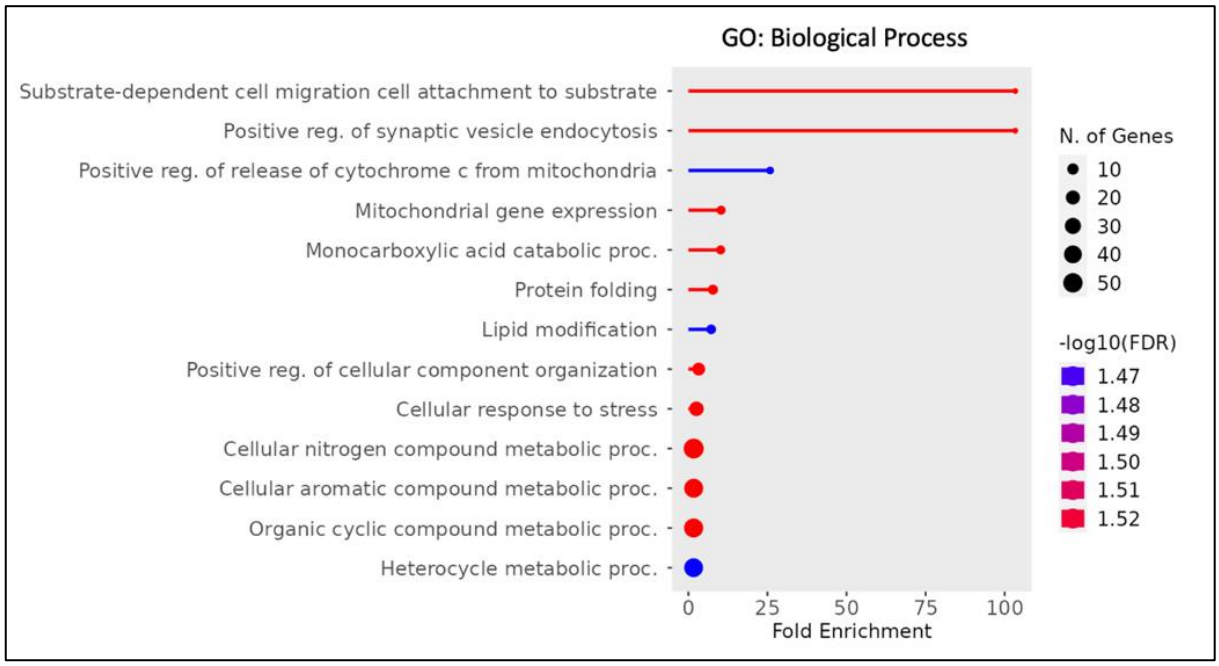

Figure 4.1. Gene Ontology (GO) enrichment analysis of genes increasing expression across bovine oocyte growth containing the progesterone response element (PRE) in their promoter region. Circle size refers to number of genes involved. The colors refer to the logarithmic scale of false rate discovery (FDR). The x-axis shows the fold enrichment.

Table 4.1. Gene list containing the "TGTTCT" PRE sequence in the promoter region.

Nuclear genes with "TGTTCT"	*DCLRE1A MIDEAS CSTF2 HJURP FAAP24 PMF1 H2BK1 PSMC3IP RNF113A PSMB4 FAM124B POLR2C SNRPD3 POLR2I CFAP20 TFAP2B H2AZ2 XRCC6 GPKOW POLM XRCC2 WDR74 DNTTIP1 MLH1 PARP12 DDB2 H2AL3 COPS4 MLLT11 MYCL PSMC5 NOPCHAP1 MRGBP POLR3C TBPL2 ID3 POLR1E ZSCAN26 SNRNP25 PFDN5 YPEL3*
Mitochondrial genes with "TGTTCT"	*UCP3 SLC25A33 SDHB TIMM10B LGALS3 ADCK1 MRPL46 TMBIM ATP5MC1 TIMM8B CPT2 TMEM11 MPV17L2*

Data published by Barbosa-Latorraca et al., 2024 from a cluster of genes positively correlated with bovine oocyte size.

4.3.2. Association between nPR and mitochondria localisation in growing bovine oocytes

A total of 30 oocytes per group were scanned using confocal microscopy and orthogonal projections images were quantified to calculate the total number of nPR foci and mitochondria. The mean foci nPR-A expression, mitochondria number, and colocalisation of nPR-A with mitochondria across oocyte groups are shown in Table 4.2.

Table 4.2. nPR and mitochondria expression in growing oocytes.

Oocyte group	Oocyte number	nPR foci	Mitochondria	Mitochondria and nPR colocalisation/μm^3
60-100 μm	30	423 ± 38	464 ± 45	55 ± 8[a]
100-110 μm	29	653 ± 58	436 ± 35	10 ± 2[b]
120-130 μm	30	701 ± 63	689 ± 73	15 ± 3[b]

Values are presented as mean percentages ± SE.

Oocytes from 60-100 μm were characterised by an even distribution of mitochondria throughout the cytoplasm, specifically surrounding the nucleus (Figure 4.2G). In contrast, oocytes >100-130 μm presented dispersed mitochondria in the oocyte cortex and small aggregations of mitochondria in the periphery of the oocyte (Figure 4.2H, 4.2I).

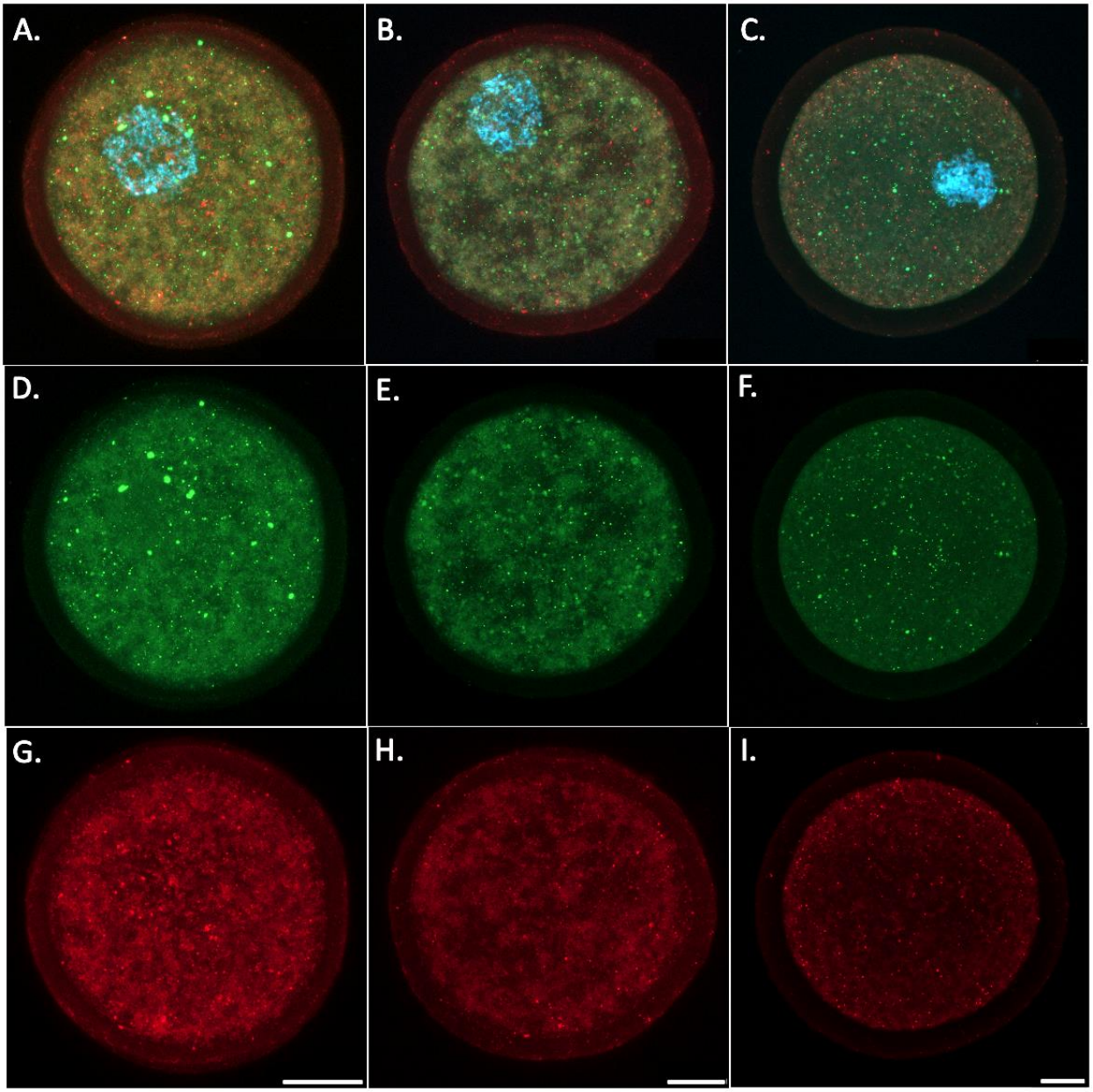

Figure 4.2. Mitochondria and nPR colocalisation in growing and fully grown bovine oocytes. Confocal laser scanning micrographs showing immunofluorescent labelling of mitochondria and nPR in growing and fully grown oocytes (60 – 130 µm). Mitochondria were visualised in red, genomic PR were visualised in green, and DNA was visualised in blue (DAPI). **A)** 60 - 100 µm; **B)** 100 – 110 µm; **C)** 120 – 130 µm showing colocalisation of mitochondria and nPR; **D)** 60 – 100 µm; **E)** 100 - 110 µm and **F)** 120 – 130 µm oocytes showing nPR foci localisation. **G)** 60 – 100 µm; **H)** 100 - 110 µm and **I)** 120 – 130 µm oocytes showing mitochondria localisation. Immunolocalisation of mitochondria and nPR is shown in denuded oocytes and appears disperse foci in the cytoplasm of growing and fully grown stage oocytes. (n=3 replicates). Scale bar = 20 µm.

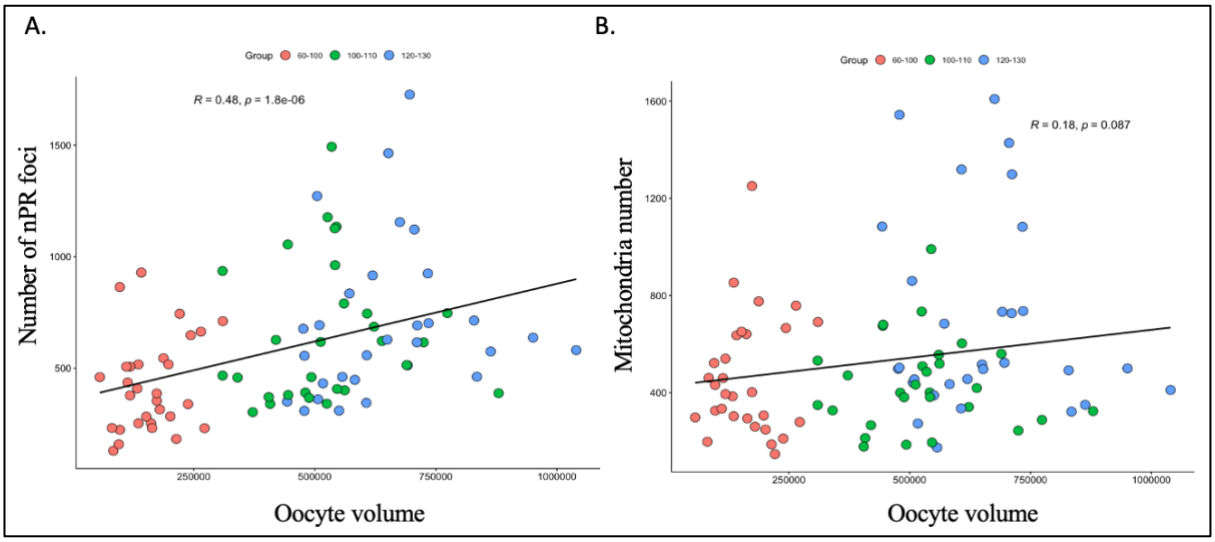

Figure 4.3. Correlation between nPR-A foci or mitochondria and oocyte size. A) Scatter plot comparing oocyte volume versus the number of nPR foci/ μm^3 and **B)** Scatter plot comparing oocyte volume versus the number of mitochondria/ μm^3. Each dot represents the number of nPR foci or mitochondria per μm^3 of oocytes and colors represent size groups (n=3 replicates). Analysis by Poisson linear regression. Pearson correlation coefficient (R).

The distribution of nPR-A foci was similar to the pattern described in the previous chapter (Chapter 2), i.e., the number of labelled foci increased gradually in line with oocyte growth in diameter. Regarding the mitochondria, there was a significantly greater number of this organelle in oocytes that were larger than 120 µm compared to the smaller diameter groups (689 ± 73 vs 438 ± 40) (Table 4.2).

Comparing the number of nPR-A foci or mitochondria per oocyte volume, there was a significant positive correlation between the number of receptor foci and oocyte diameter ($R=0.48$, $p<0.0001$), and a positive trend between the number of mitochondria and oocyte diameter ($R= 0.18$, $p<0.1$) (Figure 4.3).

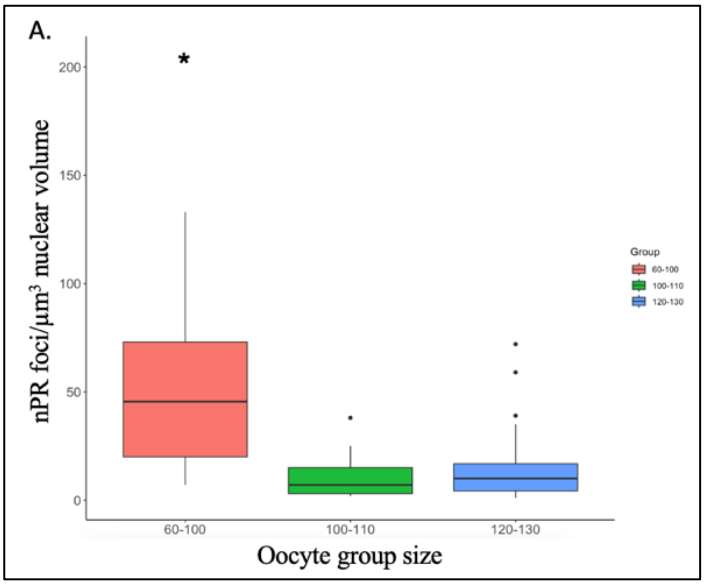

Figure 4.4. Mitochondria and nPR colocalisation in growing bovine oocytes. Boxplot comparing oocyte group size versus the colocalisation of mitochondria and nPR per µm^3. Each color represents a group size (n=3 replicates). Analysis by one-way ANOVA.

The colocalisation analysis showed that the number of nPR-A foci and mitochondria/ µm3 was significantly higher in the smaller oocytes (60-100 µm) compared to the oocytes 100-130 µm (517±75 vs 160±76, $p<0.01$) (Figures 4.4 and 4.5).

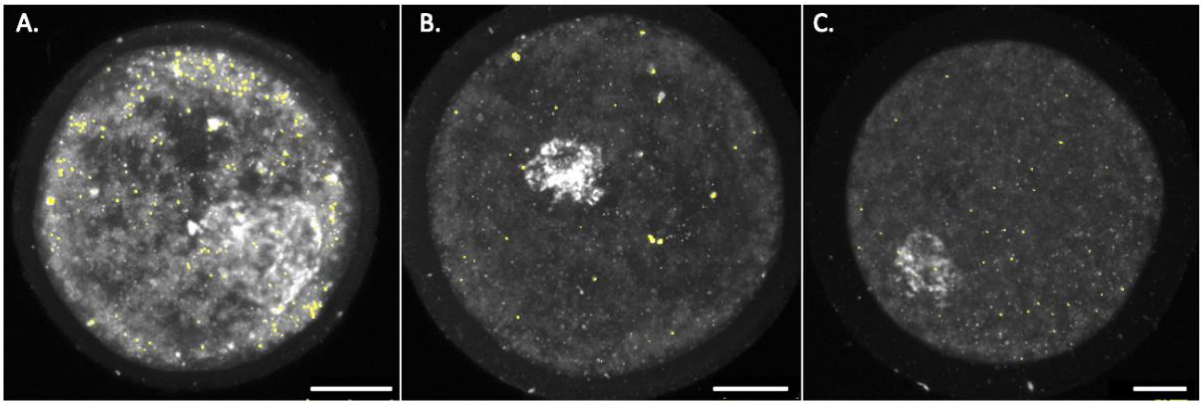

Figure 4.5. Colocalisation of nPR-A foci and mitochondria in bovine oocytes. ImageJ processed images showing the colocalisation labelling of mitochondria and nPR in growing and fully grown oocytes (60 – 130 µm). Colocalisation is shown in yellow. **A)** 60 - 100 µm; **B)** 100 – 110 µm; **C)** 120 – 130 µm. Scale bar = 20 µm.

4.3.3. Active mitochondria during bovine oocyte growth

To evaluate the presence of active mitochondria with intact membrane potential oocyte groups were co-incubated with Mitotracker Orange CMTMRos, which also provides

information on oxidative stress levels in these organelles. Following which, a total of 30 oocytes in each diameter category (60-100 μm, 100-110 μm, 120-130 μm and fully-grown oocytes from aspiration) were analyzed using ImageJ to measure mitochondrial intensity (Schneider et al., 2012). The active mitochondria were homogenously distributed in the cytoplasm of the smallest oocytes, whereas in the group of 100-110 μm diameter the mitochondria were dispersed in the oocyte cortex. The largest oocytes were characterised by a reduced localisation of active mitochondria in the periphery of the oocyte membrane (Figure 4.6).

Analysis of the variance revealed that the variability in the intensity of active mitochondria was significantly greater in the smaller oocytes (60-100 μm) compared to the larger oocytes (120-130 μm and fully-grown) (18.41 ± 1.90 vs 10.87 ± 1.45, $p<0.0001$). Furthermore, oocytes measuring 100-110 μm in diameter presented significantly more active mitochondria compared to those in the larger diameter groups (15.99 ± 1.65 vs 10.87 ± 1.45, $p<0.01$) (Table 4.3, Figure 4.7).

Table 4.3. Mitochondria Orange CMTMRos intensity across bovine oocyte growth.

Oocyte group	Mitochondria Orange Intensity
60-100 μm	18.41 ± 1.90^{a}
100-110 μm	15.99 ± 1.65^{c}
120-130 μm	$12.11 \pm 1.45^{b,d}$
FG	$9.63 \pm 1.46^{b,d}$

Data are represented as mean ± SEM. FG: Fully-grown oocytes.

4.3.4. Mitochondrial complexes during oocyte growth

To better understand the behavior of the mitochondrial complexes during bovine oocyte growth, the expression of a panel of mitochondrial complex proteins was evaluated; complex I (NDUFAB1), complex II (SDHB), and complex IV (COX IV). The selection of the latter two proteins was informed by the presence of the progesterone response element “TGTTCT” in their promoter regions. The inclusion of the mitochondrial complex I protein was restricted by antibody availability and reactivity with bovine samples.

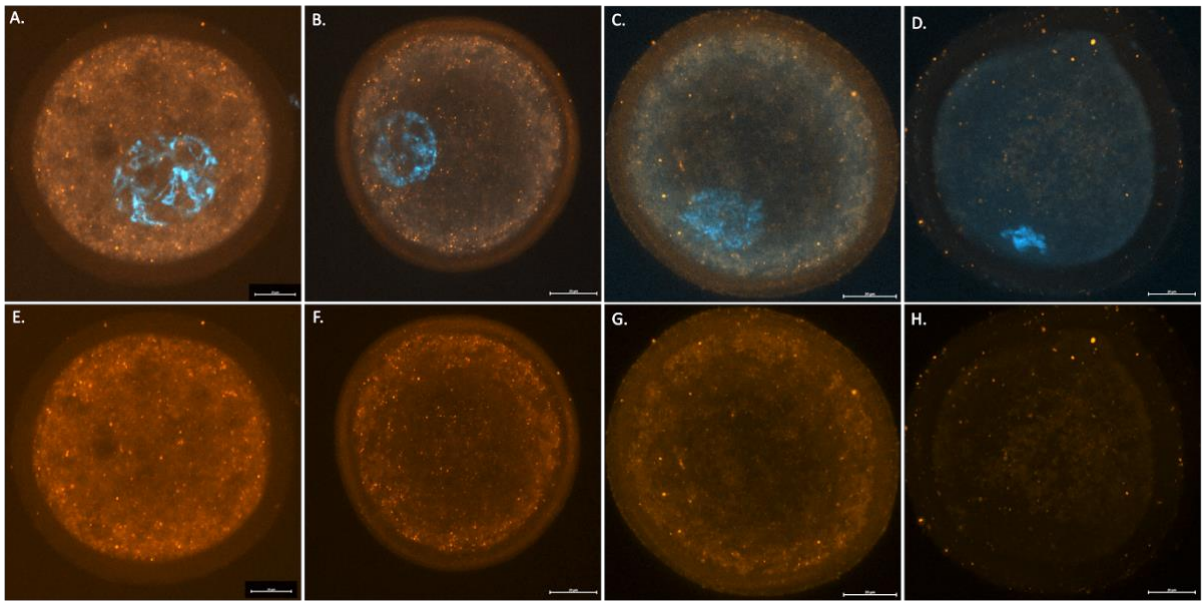

Figure 4.6. Active mitochondria in growing and fully grown bovine oocytes. Confocal laser scanning micrographs showing immunofluorescent labelling of Mitochondria Orange CMTMRos in growing and fully grown oocytes (60 – 130 µm). Mitochondria were visualised in orange and DNA was visualised in blue (DAPI). **A)** 40 - 100 µm; **B)** 100 – 110 µm; **C)** 120 – 130 µm; **D)** Aspirated fully-grown oocytes showing localisation of active mitochondria and DAPI staining; **E)** 40 – 100 µm; **F)** 100 - 110 µm and **G)** 120 – 130 µm; **H)** Aspirated fully-grown oocytes showing mitochondria Orange CMTMRos labelling. Immunolocalisation of active mitochondria shown in denuded bovine oocytes and the distribution of these organelle in the cytoplasm (n=3 replicates). Scale bar = 20 µm.

The expression of mitochondrial complexes I, II, and IV was individually assessed according to oocyte diameter. The expression of Mitochondrial Complex I was significantly lower in oocytes 120-130 µm in diameter compared to the smallest group (1.30 ± 0.09 vs. 2.11 ± 0.29, $p<0.1$). For Complex II, no statistical difference was observed between groups. However, a double band (referred to as SDHB2) was present in the samples, showing weaker expression in smaller oocytes that increased with oocyte size and was notably expressed in the fully grown group (0.01 ± 0.01 vs. 0.23 ± 0.19). SDHB has a molecular weight of 28 kDa, whereas the second band/SDHB2 was smaller an appeared below SDHB. In contrast, Mitochondrial Complex IV expression significantly increased in oocytes measuring 100-110 µm in diameter compared to the smallest oocyte group (0.55 ± 0.10 vs. 0.21 ± 0.06, $p<0.1$) (Figure 4.8).

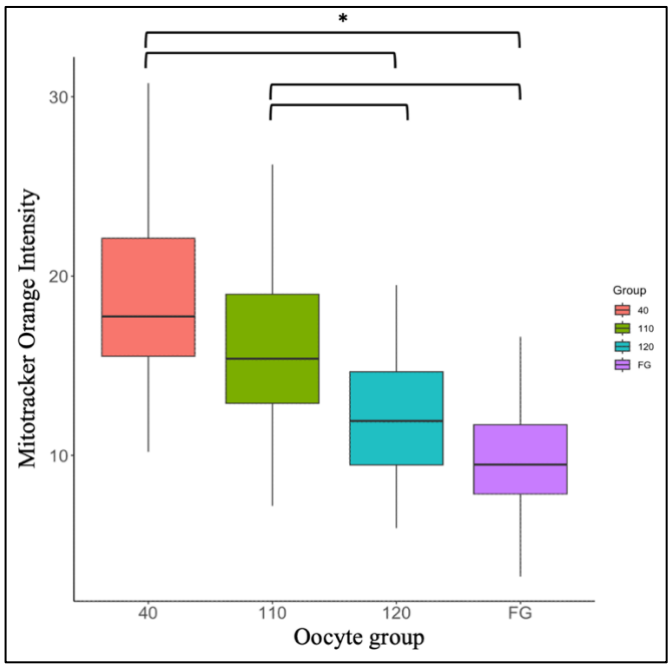

Figure 4.7. Mitotracker Orange CMTMRos intensity across bovine oocyte size. Boxplot comparing active mitochondria intensity versus oocyte group size. Each color represents a group size (n=3 replicates). Analysis by Kruskal-Wallis rank sum test followed by Dunn test. Orange= 40-100 µm; Green= 100-110 µm; Blue= 120-130 µm; Purple= Fully-grown aspirated oocytes.

4.3.5. nPR inhibition and effect on the mitochondria profiling and activation

A total number of 50 COCs were randomly submitted to IVM in control IVM or IVM media containing 1µM Aglepristone for 24h, to investigate the effect of nPR inhibition on mitochondrial function. Mitochondrial activity and mitochondrial complex expression were evaluated using Mitotracker labelling or Western blot analysis, respectively.

Active mitochondria were homogeneously distributed throughout the cytoplasm and in the extruded polar body in oocytes of the control IVM group. In contrast, oocytes in vitro matured in the presence of the nPR antagonist were characterised by a reduced number of active mitochondria or, in some cases none were detected (Figure 4.9). Nevertheless, the intensity of Mitotracker labelling was not significantly different on IVM + Aglepristone treated oocyte group compared to control IVM oocytes (11.41 ± 1.60 vs. 14.31 ± 1.77) (Figure 4.10).

The expression of Mitochondrial Complexes I and II did not differ between control IVM and IVM with 1µM Aglepristone oocyte groups ($p>0.05$); Mitochondrial Complex IV/COXIV while expressed in smaller oocytes (40-120 µm), was not detected in the IVM or IVM with 1µM Aglepristone oocyte group (Figure 4.11).

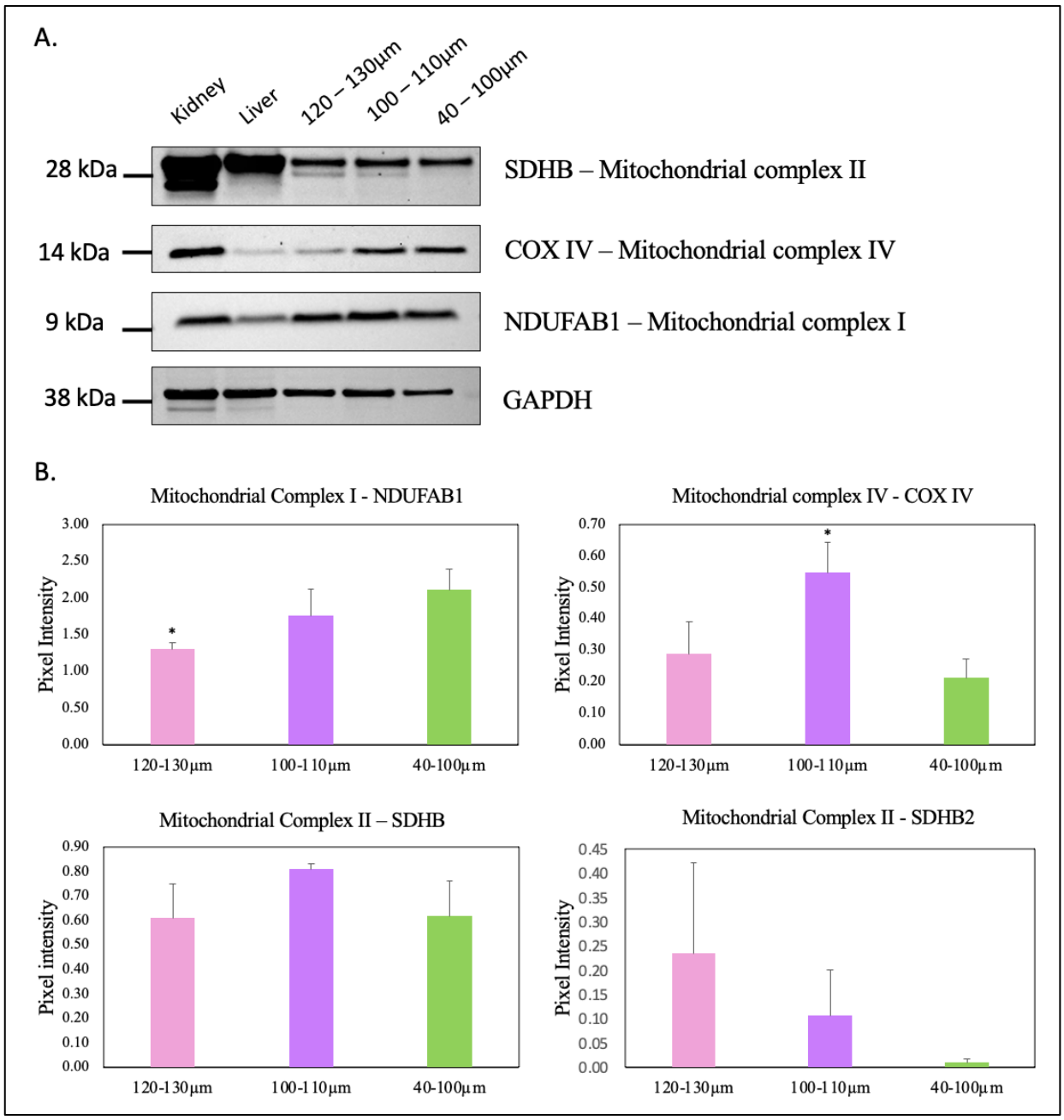

Figure 4.8. Mitochondria complexes behavior across bovine oocyte growth. A) Proteins were resolved by SDS-PAGE and immunoblotting was performed using a monoclonal antibody for mitochondrial complex I (9 kDa), mitochondrial complex II (28 kDa), mitochondrial complex IV (14 kDa), and GAPDH (38 kDa). Protein lysates from bovine kidney, liver and oocytes were resolved per lane. Lane 1. Kidney. Lane 2. Liver. Lane 3. Pool of 50 oocytes 120-130 µm. Lane 4. Pool of 70 oocytes 100-110 µm. Lane 5. Pool of 100 oocytes 40-100 µm. **B)** Protein bands were measured by densitometry and are represented pixel intensity ± SEM (n= 5 replicates). Analysis by ANOVA followed by Tukey test or Kruskal-Wallis test followed by Dunn test.

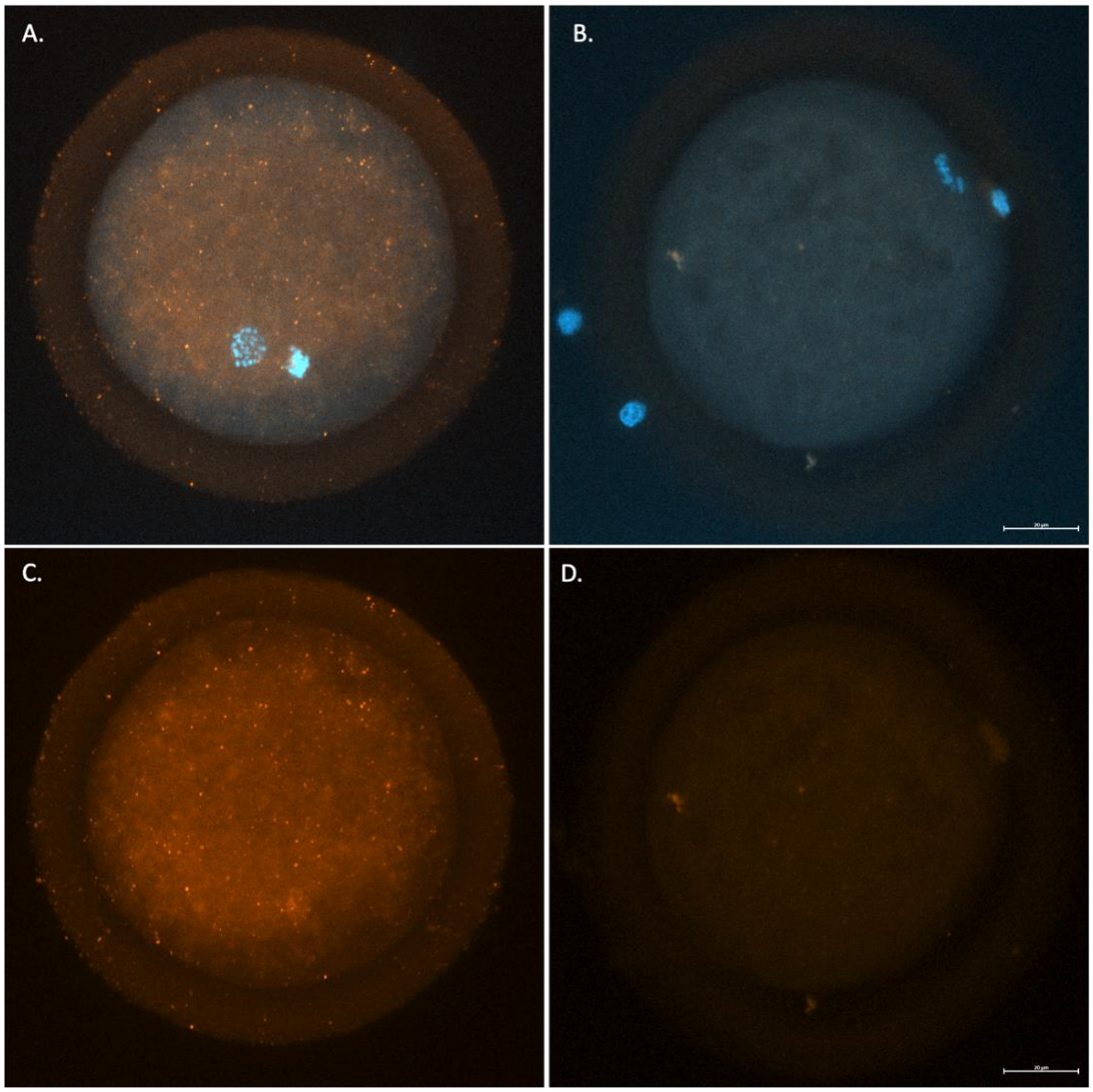

Figure 4.9. Active mitochondria distribution in bovine oocytes during IVM functional analysis. Confocal laser scanning micrographs showing immunofluorescent labelling of Mitochondria Orange CMTMRos in control *in-vitro* matured oocytes and oocytes matured in IVM media supplemented with nPR inhibitor (Aglepristone). Mitochondria were visualised in orange and DNA was visualised in blue (DAPI). **A)** Bovine oocyte from IVM control; **B)** Bovine oocyte from IVM with nPR inhibitor showing localisation of active mitochondria and DAPI staining; **C)** Bovine oocyte from IVM control; **D)** Bovine oocyte from IVM with nPR inhibitor showing localisation Mitochondria Orange CMTMRos labelling. Immunolocalisation of active mitochondria shown in denuded bovine oocytes and the distribution of these organelle in the cytoplasm (n=3 replicates). Scale bar = 20 µm.

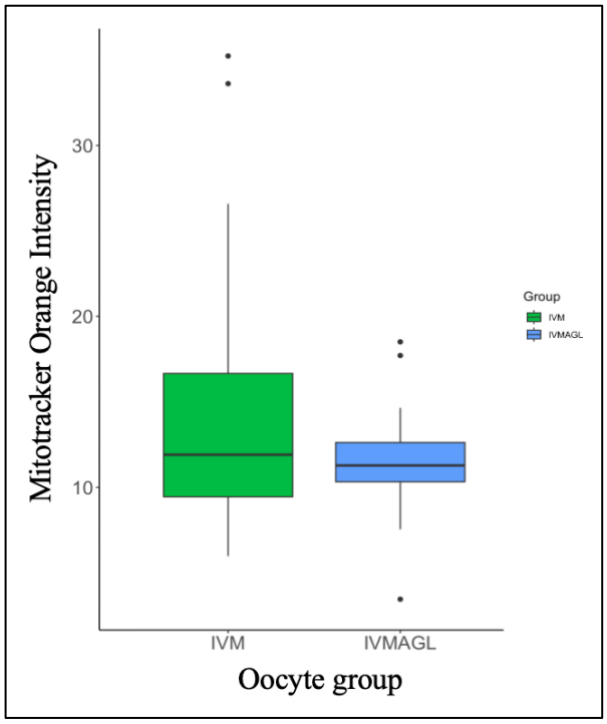

Figure 4.10. Mitotracker Orange CMTMRos intensity in bovine oocytes during IVM functional analysis. Boxplot comparing active mitochondria intensity versus IVM control oocytes and IVM with nPR inhibitor oocytes. Each color represents a oocyte group (n=3 replicates). Analysis by Kruskal-Wallis rank sum test followed by Dunn test. Green= IVM control; Blue= IVM with nPR inhibitor (Aglepristone).

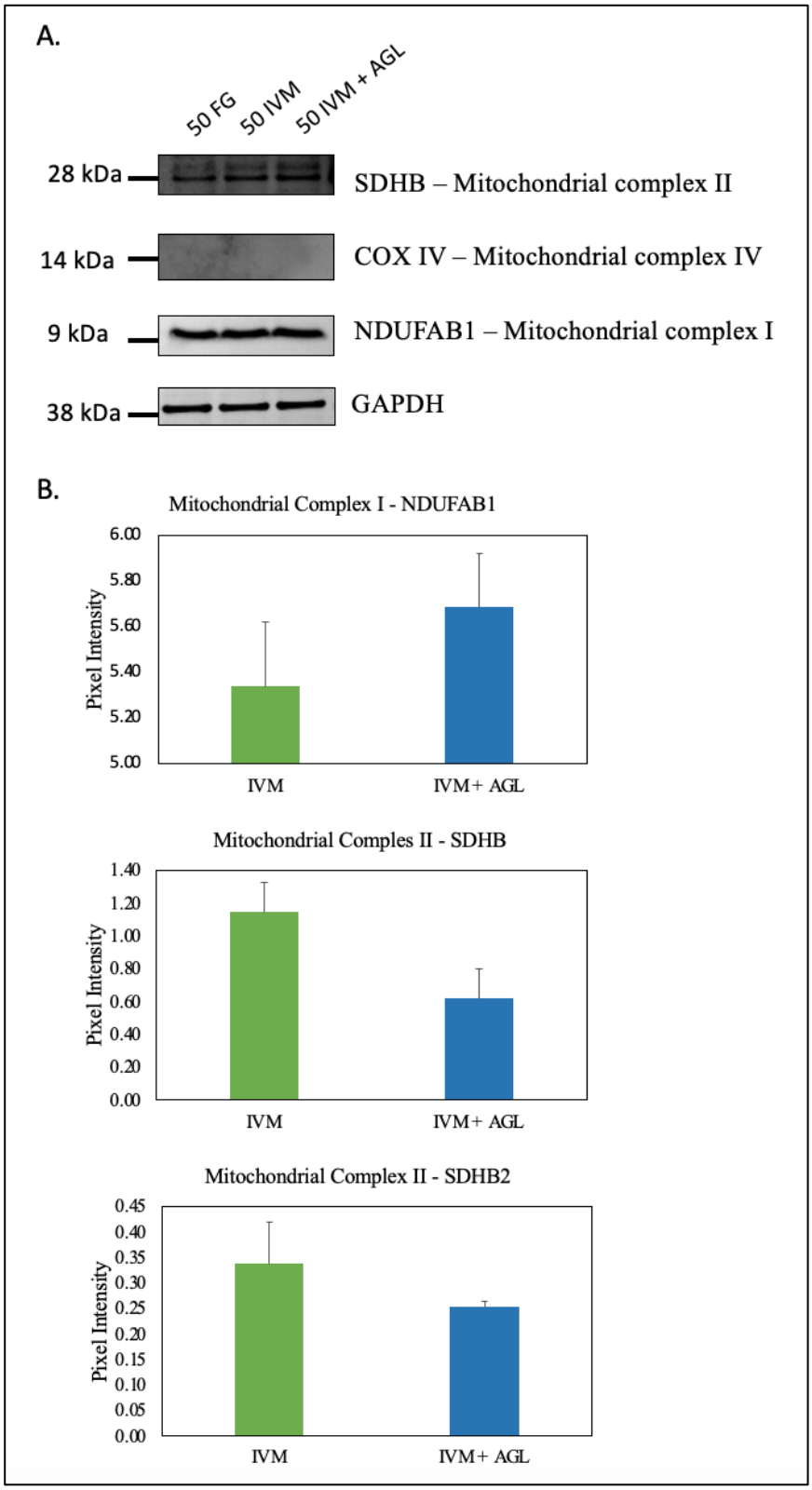

Figure 4.11. Mitochondria complexes behavior during IVM functional analysis. **A)** Proteins were resolved by SDS-PAGE and immunoblotting was performed using a monoclonal antibody for mitochondrial complex I (9 kDa), mitochondrial complex II (28 kDa), mitochondrial complex IV (14 kDa), and GAPDH (38 kDa). Protein lysates from oocytes were resolved per lane. Lane 1. Pool of 50 FG oocytes. Lane 2. Pool of 50 IVM oocytes. Lane 3. Pool of 50 oocytes IVM + Aglepristone oocytes. **B)** Protein bands were measured by densitometry and are represented pixel intensity ± SEM (n= 3 replicates). Analysis by ANOVA followed by Tukey test or Kruskal-Wallis test followed by Dunn test. FG= Fully-grown.

4.4. DISCUSSION

This study integrates our findings from the previous chapters regarding the expression of the nPR-A in bovine oocytes and a possible relationship with and organelle that is related to cell survival. In chapter 3, bovine COC survival was affected when nPR was inhibited during growth, this effect along with the clustered aggregations of the nPR-A in bovine oocytes from 40 - 80 μm hinted at a possible association with mitochondria at this stage of growth. To investigate this relationship, an in-silico analysis from single bovine oocytes transcriptomic data was performed to identify possible genes regulated by nPR.

The nPR is a transcription factor that can activate or suppress gene expression by binding to specific response elements in chromatin (Tsai & O'Malley, 1994; Xin et al., 2016). After binding to a ligand, dimerizing, and entering the nucleus, the nuclear receptor dimer attaches to recognition sequences called progesterone response elements (PRE) (Gronemeyer, 1991). These PREs typically consist of a palindromic hormone response element sequence, AGAACAnnnTGTTCT (Ham et al., 1988). However, in mice PR binding is not restricted to the complete PRE. It has been shown that PR can bind to the promoters of known progesterone target genes such as *Lifr*, *Gata2*, *Cyp26a1*, and *Ihh* with only half of the normal PRE sequence (Rubel et al., 2012).

In-silico analysis of a published cluster of genes (1016) shown to increase in expression during oocyte growth (Barbosa-Latorraca et al., 2024), identified a panel of 230 genes which contain the PRE core sequence “TGTTCT” in their promoter regions. Subsequent GO analysis revealed that enriched pathways were primarily associated with mitochondria and nuclear biological processes (FDR <0.1).

A total of 43 genes were associated with nuclear processes, most of which were involved in DNA repair, DNA binding, DNA or RNA transcription and gene expression. Among these genes, TATA-binding protein-like factor 2 (*TBPL2*) is a transcription factor expressed during oocyte growth and required to create RNA and protein reserves to achieve maternal competence (Müller & Tora, 2009; Yu et al., 2020). Deletion of *TBPL2* in female mice resulted in a reduce ovarian reserve, defective folliculogenesis, and infertility. Interestingly, *TBPL2* mutations were identified in woman with diminished ovarian reserve by whole-exome sequencing (He et al., 2020). Moreover, mutations of *TBPL2* in infertile patients were associated with oocyte maturation defects (Yang et al., 2019; Fei & Zhou, 2022). Another relevant gene related to oocyte maturation and quality was binding inhibitory factor 3 (*ID3*). Inhibition of *ID3* by siRNA during 20 hours of IVM in the COC disrupted mitochondrial dynamics and functionality. This led to a reduced first polar body extrusion rate, ATP

production, and antioxidation capacity, indicating that ID3 inhibition impairs bovine oocyte competence (Liu et al., 2023). Additionally, Poly (ADP-ribose) polymerase 12 (*PARP12*), was recently identified as a critical factor in oocyte maturation; *PARP12* depletion resulted in abnormal spindle organisation and chromosome misalignment in mouse oocytes, consequently increasing the frequency of chromosome aneuploidies (Cao et al., 2023). Taken together, these findings and others suggest that genes containing a PRE could be regulated by the nPR and may play a role in oocyte competence. Further studies are necessary to fully comprehend the functional relevance of these genes during oocyte growth.

Regarding genes enriched in mitochondrial pathways, 13 genes were mainly associated with inner mitochondrial membrane organisation. Within the oocyte, mitochondria are involved in ATP generation, calcium homeostasis, regulation of cytoplasmic reduction–oxidation, signal transduction, and apoptosis (Review by Roth, 2018). From the list of genes related to mitochondrial activities, none had been previously investigated in oocytes. Therefore, the findings relating nPR with mitochondrial genes, led us to further investigate this relationship regarding the localisation of both during bovine oocyte growth and mitochondrial activity.

Although the Seahorse is a valuable technique for assessing bioenergetic parameters such as oxygen consumption and extracellular acidification, is not ideal for growing oocytes due to its requirement for live cells or isolated mitochondria. The necessary sample preparation, including immobilisation, and oocyte sensitivity to experimental conditions further increase the risk of compromising the integrity of samples. In this study, the use of MitoTracker labelling and Western Blot protein expression analysis were appropriate alternatives, providing complementary insights into mitochondrial morphology and protein-level changes, aligning with the goals of this study. MitoTracker labelling allows visualisation of mitochondrial morphology and dynamics in both live and fixed cells, making it less invasive and more compatible with growing oocytes. Western Blot provides detailed insights into specific mitochondrial protein expression, such as those involved in oxidative phosphorylation, without requiring live samples. Together these methods collectively minimise manipulation-related damage while providing structural and molecular information relevant to the study of oocyte mitochondrial function.

Here, colocalisation of the nPR with mitochondria in bovine oocytes is described for the first time, moreover, colocalisation was highest in the smaller oocytes (40 - 100 μm). The total number and distribution pattern of mitochondria within the oocyte cytoplasm varied according to stage of bovine oocyte growth. Oocytes from 40 - 100 μm were characterised by

a homogeneous distribution in the cytoplasm surrounding the nucleus, whereas oocytes from 100 - 130 μm showed a heterogeneous distribution in the periphery of the oocyte. Earlier studies have described a 45-fold increase in mitochondria number from the primordial germ cell to the preovulatory follicular stage in bovine oocytes (Smith & Alicvar, 1993), with a mean mitochondrial copy number of 260,000 in mature oocytes (Michaels et al., 1982). Using electron microscopy, Fair et al., 1997 described similar changes in mitochondria number and distribution according to bovine oocyte diameter. Similarly, other groups reported the same pattern in immature fully-grown oocytes (Nagano et al., 2006; Terazona et al., 2006; Kątska-Książkiewicz et al., 2011; Dadarwal et al., 2017; Kere et al., 2020). These stage-dependent variations in the mitochondria distribution pattern were previously considered a determining factor for oocyte competence (Bavister and Squirrell, 2000). Oocytes with low maturational competence were reported to lack signs of mitochondrial organisation or, alternatively, present larger mitochondrial clumps throughout the cytoplasm. Whereas oocytes presenting large mitochondrial aggregations at the ooplasm periphery were associated with high maturation competence (Stojkovic et al., 2001).

Earlier ultrastructural studies described a spatial association of peripherally located mitochondria with vacuoles and lipid droplets in bovine oocytes (Hyttel et al., 1986; Hyttel et al., 1989; de Loos et al., 1989, Nagano et al., 2006). Such proximity of mitochondria to lipids may reflect a greater dependence of the oocytes on lipid-derived ATP generation for energy requirements (Dadarwal et al., 2015). Consequently, the relocation of mitochondria to regions with high energy demand is vital for the activation of specific metabolic pathways involved in protein synthesis and phosphorylation (Stojkovic et al., 2001). This evidence suggests that mitochondria play an extremely important role in the metabolic machinery responsible for the supply of energy that is consumed during oocyte growth.

The quantification of nPR expression revealed an increase in foci labelling as the oocyte grew in diameter, as previously described in Chapter 2. Moreover, the distribution pattern resembled that of the mitochondria in growing oocytes.

The colocalisation analysis of nPR and mitochondria in oocyte diameter groups revealed a significantly higher colocalisation in the smaller oocytes (40 - 100 μm). Furthermore, there was a higher number of active mitochondria in these oocytes compared to oocytes from the larger diameter groups (100 - 110 μm, 120 - 130 μm and fully-grown stage). These findings suggest that the nPR colocalises with active mitochondria with oxidative activity during oocyte growth.

The likely interpretation of these findings is related to P4 synthesis. Progesterone biosynthesis is a multistep process, converting cholesterol via a series of enzymatic reactions into P4 (Crivello & Jefcoate., 1980; Jefcoate et al., 1987; Wiltbank et al., 1993; Miller et al., 2017). Intracellular cholesterol is transported from the outer mitochondrial membrane to the inner membrane by the steroidogenic acute regulatory protein (STAR) (Clark et al., 1994; Niswender et al., 2002). Then the conversion of cholesterol to pregnenolone is catalyzed by the P450 side chain cleavage enzyme (CYP11A1) in the mitochondria. Finally, pregnenolone is converted to P4 by 3β-hydroxysteroid dehydrogenase (HSD3B) in the smooth endoplasmic reticulum (Rapoport et al., 1998; Manna et al., 2009; Hu et al., 2010). Endoplasmic reticulum (ER) and mitochondrial connections have been extensively described in the literature where it is proposed that ER-mitochondrial contact allows efficient local inter-organellar communication without altering the whole cell environment (Phillips et al., 2016; Fernández-Murray et al., 2016; Marchi et al., 2017; Kerkhofs et al., 2017; Csordás et al., 2018). Therefore, the increased number of nPR observed colocalised with mitochondria in smaller oocytes may reflect nPR bound to P4 produced by this organelle.

As electrons flow through the Complexes I- IV during oxidative phosphorylation, protons are released into the inter-membrane space forming the mitochondria's membrane potential. Reentry of protons into the mitochondrial matrix through the Complex V leads to ATP generation (Andersson et al., 2003). Due to their complexity, the assembly of each electron transport complex must be tightly regulated to minimise the production of toxic byproducts like reactive oxygen species (ROS) (Sousa et al., 2018; Pfanner et al., 2019; Barros & McStay, 2020).

In keeping with the findings of Barbosa-Latorraca et al., 2024, which described a negative correlation between electron transport chain gene mRNA expression and oocyte growth, Complex I expression was greatest in oocytes 40 - 100 μm in diameter compared to oocytes in the 120 - 130 μm diameter group. Complex I represents the entry point of electrons to the respiratory chain, oxidizing NADH to NAD+ in the mitochondrial matrix. Additionally, it is one of the main sources of ROS production (Sousa et al., 2018). Recent research in human primordial oocytes and early oocytes from *Xenopus laevis* showed an absence of Complex I expression, leading the Authors to propose this as a mechanism to avoid ROS production and extend oocyte lifespan (Rodriguez-Nuevo et al., 2022). In the current study, Complex I expression declined in larger oocytes (120-130 μm), and although primordial follicle oocytes were not evaluated, it is interesting to speculate that a similar protective mechanism exists at the opposite end of the growth phase when oocyte transcriptional activity is low and the oocyte

must be maintained in a quiescent state to avoid ROS-induced DNA fragmentation, protein oxidation, and lipid peroxidation prior to resumption of meiotic maturation.

Regarding Complex II, while the expression did not change during oocyte growth, it is noteworthy that a second protein band was detected in oocytes 100 - 110 μm in diameter. Moreover, the intensity of this second band was higher in the larger oocyte group (120 - 130 μm). Of all mitochondrial complexes, succinate dehydrogenase (SDH) is the only one whose 4 subunits are encoded by nuclear DNA (Bezawork-Geleta et al., 2017). Additionally, it is the only respiratory chain complex which does not pump protons across the inner mitochondrial membrane. It is part of the citric acid cycle, where it catalyzes the oxidation of succinate to fumarate, coupled to the reduction of ubiquinone to ubiquinol. Ubiquinol is a substrate for Complex III and thus Complex II provides a second direct link between the citric acid cycle and the respiratory chain (Sousa et al., 2018). In particular, the iron–sulfur SDH subunits B (SDHB) contains Fe–S clusters and the correct insertion of these clusters is required for the proper maturation of the complex (Sun et al., 2005; Ghezzi et al., 2009; Rutter et al., 2010). The second ~26 kDa band is unlikely to be related to a post-translational modification of SDHB, as the SDHA (~70 kDa) is the likely candidate for phosphorylation in the presence of ROS (Garaude et al., 2016). Further studies are required to understand the origin of this second band and the increase in its expression during oocyte growth.

The final and rate limiting step of the respiratory chain is cytochrome c oxidase (COX) which represents the regulatory center of oxidative phosphorylation. The subunit COX IV is encoded in the nuclear DNA, and fundamental in dimerisation with COX V for the initiation of the complex assembly (Glerum et al., 1997; Timón-Gómez et al., 2018; Kadenbach et al., 2021). Here, COX IV had a significantly higher expression in oocytes from 100 - 110 μm compared with the other oocyte sizes. While expression of mitochondrial complex proteins appears to be related to stage of oocyte growth, further studies are required to understand the functional relevance of the expression of specific complexes during oocyte growth. The current analysis was restricted by the limited availability of bovine specific and reactive antibodies against all complexes and their component subunits.

Although inhibition of nPR activity during IVM appeared to disrupt mitochondrial organisation within the ooplasm, the mitochondria intensity was not significantly different to the control. Mitochondria profiling of IVM oocytes has been widely described; the number of organelles is increased, and their distribution is more dispersed throughout the cytoplasm (Kruip et al., 1983; Hyttel et al., 1997; Stojkovic et al., 2001; Nagano et al., 2006; Terazona et al, 2006; Kątska-Książkiewicz et al., 2011). High mitochondrial activity levels are important

for maturation events which depend on ATP generation, such as nuclear and cytoplasmic maturation, cytoskeleton rearrangement, and the polyadenylation of mRNAs needed for early development before embryonic transcription begins (Reviewed by Van Blerkom, 2004). Following IVM, bovine oocytes presented a disperse distribution of the mitochondria in the cytoplasm, consistent with previous descriptive studies.

Previous studies from our group demonstrated that inhibiting P4 synthesis with Trilostane during IVM altered mitochondrial distribution within the cytoplasm compared to the control group (O'Shea et al., 2013). In this study, pharmacological inhibition of nPR activity tended to reduce the intensity of labelling for active mitochondria in the oocytes; however, this difference was not statistically significant between the treatment and control groups. Similarly, the expression of mitochondrial Complex proteins I-IV was not affected by pharmacological inhibition of nPR during IVM. These findings suggest that at this final stage of growth, nPR might not be critical for mitochondrial activity, although P4 present in the media does influence organelle activity in this moment. Functional analysis during earlier growth stages is required to clarify the relationship between nPR and mitochondria.

In conclusion, these findings emphasize the importance of mitochondria in oocyte growth and maturation, highlighting the need for further studies to explore the specific roles of different mitochondrial complexes and their regulation during oocyte development, as well as the possible association with nPR.

Chapter 5

General Discussion

In cattle, previous work supports the presence of progesterone receptors (PR) in fully grown oocytes and their crucial role during maturation. However, the timing of onset of expression and the associated signalling mechanisms remain unclear. Thus, this study aimed to investigate the kinetics, localisation, and function of nuclear PR (nPR) expression during bovine oocyte growth, as well as the identification of potential organelles involved in oocyte development.

The findings from this research revealed that nPR is consistently expressed by both oocytes and their surrounding follicle cells from the primordial follicle to the early-antral follicle -stage, potentially indicating a protective role during folliculogenesis (Figure 5.1). Notably, the number of nPR foci increased as the oocyte grew in diameter, plateauing at the oocyte's transition to a transcriptionally inactive state. Given that nPR is a transcription factor, it may promote or inhibit the transcription of specific genes in a follicle/oocyte -stage specific manner.

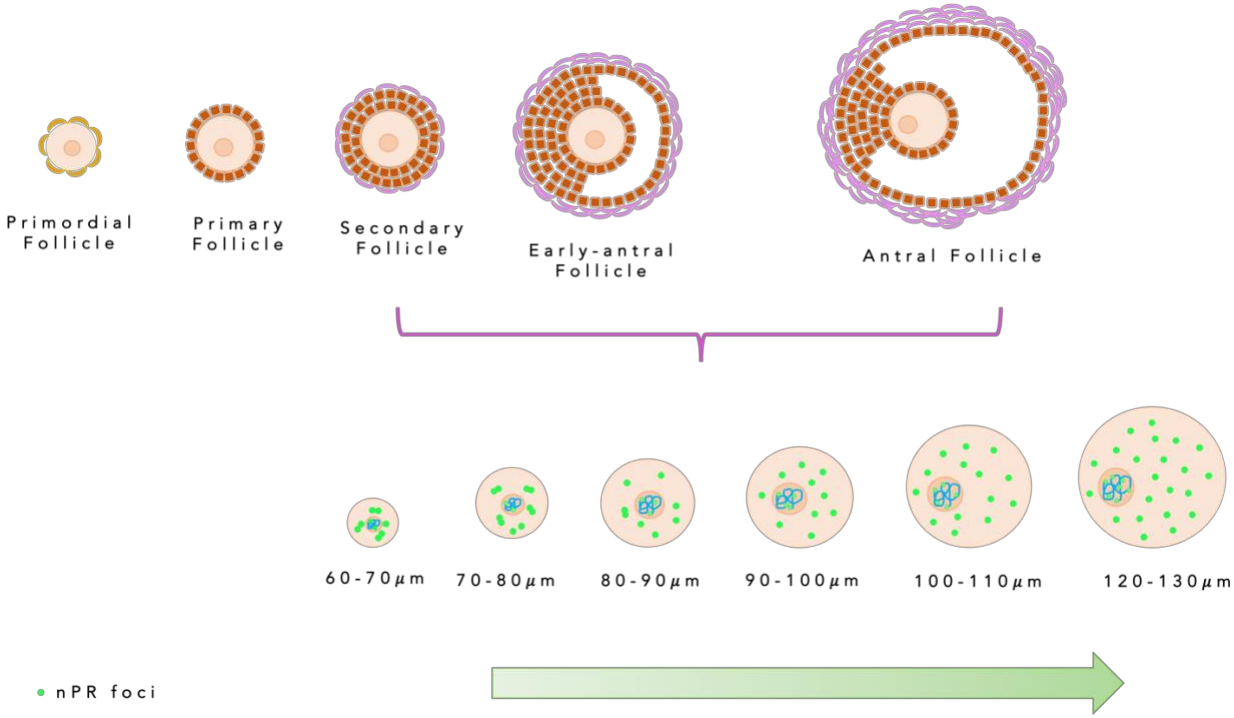

Figure 5.1. Nuclear progesterone expression representation in growing bovine oocytes. Top panel: Graphical representation of follicle stages of development. The expression of the nPR was detected in all follicle cells as well as the oocyte. Bottom panel: Graphical representation of oocyte growth from 60 – 130 µm. The distribution of nPR (green) in the oocyte was mainly cytoplasmic and nuclear; with a positive correlation of the nPR foci labelling and oocyte diameter.

The establishment of a culture system for growing bovine oocytes *in vitro* was essential for assessing nPR functionality during bovine oocyte growth. To achieve this, two *in-vitro* oocyte culture systems were tested; one of which was successfully established. Subsequently, inhibition of nPR was performed in the long *in-vitro* oocyte growth system, where the effect of pharmacological blocking of the nPR with Aglepristone caused a reduced oocyte survival during culture and impacted their capability to resume meiosis. While these findings support a crucial role for nPR during oocyte growth, the culture system was not without insurmountable limitations, therefore it's use was not continued.

In-silico analysis of a previously identified cohort of genes whose expression increased during oocyte growth, revealed an enrichment of mitochondrial genes with progesterone response element (PRE) in their promoter regions. These findings, together with the clustered localisation of nPR foci during oocyte growth resembling mitochondrial distribution, led to further investigation of this potential relationship. The results revealed an association between nPR and active mitochondria during the early stages of oocyte growth (Figure 5.2.). However, inhibition of the nPR during *in-vitro* maturation (IVM) did not affect mitochondrial activity or the expression of mitochondrial complexes. Previous results from our group, where P4 synthesis was inhibited during IVM, resulted in reduced mitochondrial activity. Therefore, further studies are required to better understand the relationship between mitochondrial activity, P4 synthesis and nPR function.

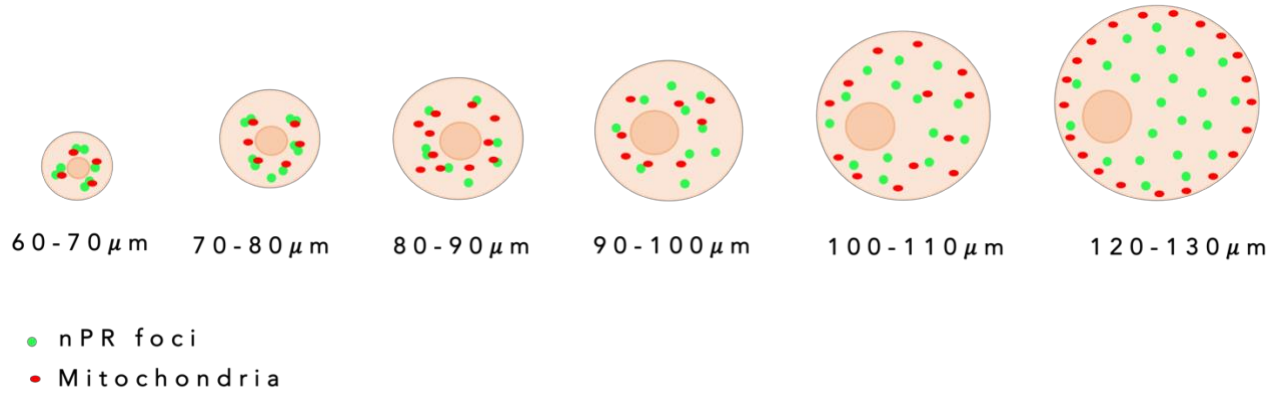

Figure 5.2. Mitochondria and nPR colocalisation across bovine oocyte growth. The number of nPR labelled foci (green) increased gradually, in line with oocyte growth in diameter. Mitochondria (red) were evenly distributed throughout the cytoplasm of oocytes measuring 60-100 µm in diameter, and around the nucleus. In contrast, oocytes >100-130 µm in diameter presented dispersed mitochondria in the oocyte cortex and small aggregations of mitochondria in the periphery of the oocyte. The colocalisation of the nPR and mitochondria was significantly higher in the smaller oocytes (60-100 µm) compared to their larger counterparts (oocytes 100-130 µm).

One of the unexpected findings of this research was the colocalisation of nPR with mitochondria. This correlation had not been previously described, suggesting a potential interaction between nPR and mitochondria during oocyte growth. Consequently, mitochondrial activity and the expression of mitochondrial complexes were thoroughly investigated. The intensity of mitochondrial labelling decreased as oocyte diameter increased, suggesting higher mitochondrial activity in smaller oocytes (Figure 5.3). While analysis of mitochondrial complex expression revealed no clear correlation with oocyte size (Figure 5.4), it is notable that COX IV expression was significantly higher in oocytes measuring 100–110 µm, a stage which coincides with greatest levels of oocyte transcription. Another intriguing finding was the decrease in NADUFAB1 expression in fully grown oocytes, which may indicate a protective mechanism against reactive oxygen species (ROS) production in the final stages of growth.

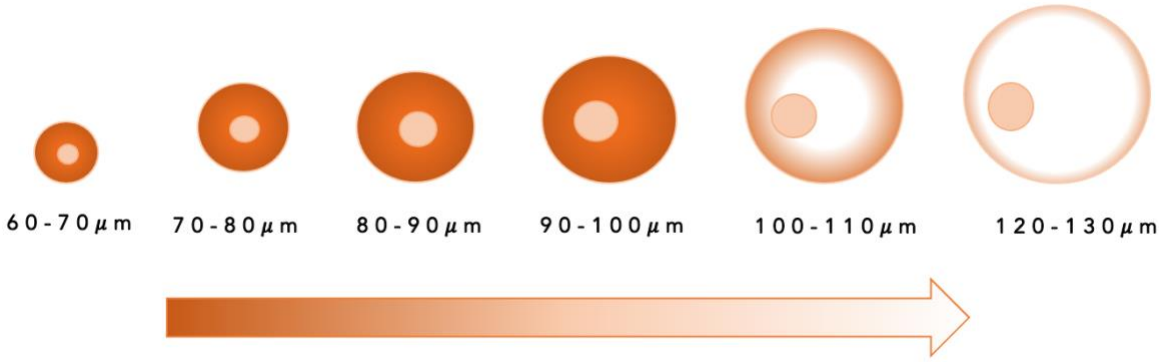

Figure 5.3. Mitochondria intensity across bovine oocyte growth. Mitochondria intensity (orange) decreased gradually in line with oocyte growth in diameter.

This research, the characterisation of nPR expression during bovine oocyte growth, contributes to our understanding of basic oocyte biology. The continuous expression of PR during folliculogenesis suggests a possible role for this receptor as "survival" factor. Additionally, for the first time an association between the nPR and mitochondria in mammalian oocytes is described. As mitochondria play a role in the "survival and death" of the cell, further studies are warranted to understand this association.

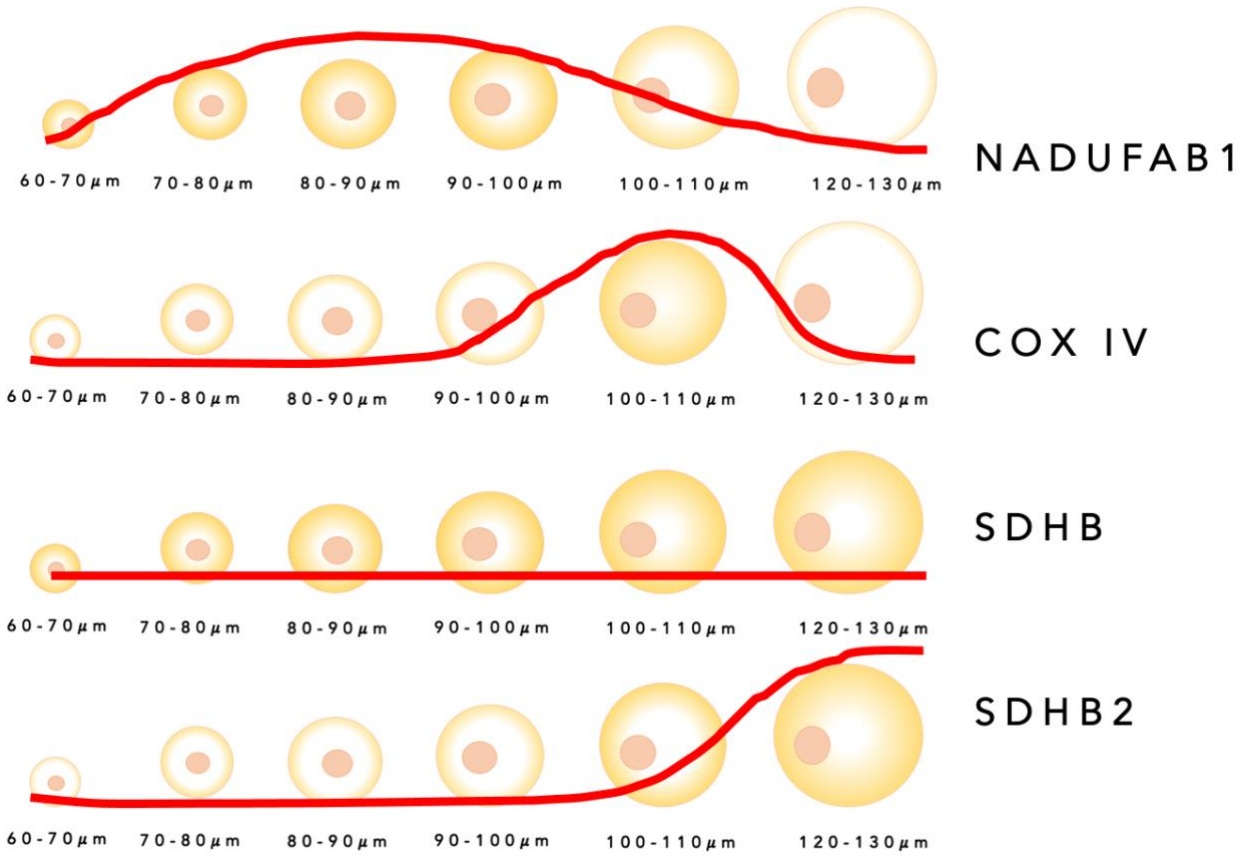

Figure 5.4. Mitochondria complexes expression across bovine oocyte growth. Mitochondrial complex expression (yellow) exhibits distinct behaviour throughout the bovine oocyte growing process. NADUFAB1 (Complex I) expression significantly decreased in fully grown oocytes (120–130 µm) compared to growing oocytes (60–110 µm). COX IV (Complex IV) expression was significantly higher in oocytes measuring 100–110 µm compared to both smaller and larger oocytes. In contrast, SDHB (Complex II) showed no significant changes in expression across oocyte growth, while SDHB2 (Complex II) exhibited a trend of increased expression in fully grown oocytes (120–130 µm).

The research faced several limitations, including issues with the specificity and reactivity of bovine antibodies, as well as inconsistency in antibodies from the same supplier. These challenges delayed further characterisation of mitochondrial complexes and prevented the study of genes possibly regulated by nPR. Additionally, the inability to establish a consistently reliable *in-vitro* bovine oocyte culture system restricted the exploration of nPR functionality during oocyte growth.

Future research should focus on the successful, replicable, and consistent establishment of an *in-vitro* bovine oocyte growth system. This will enable studies to gain a deeper understanding of the requirements for oocyte growth and facilitate further investigation into the role of nPR during oocyte development.

In addition, the relationship between nPR and mitochondria could be explored through various approaches, such as electron microscopy colocalisation studies, inhibition of P4 synthesis during oocyte *in vitro* maturation to determine whether P4 influences mitochondrial complex expression rather than nPR, wider analysis of the mitochondrial complexes, and/or utilisation of the Seahorse to measure multiple parameters of oocyte mitochondrial activity and function.

To further validate nPR-regulated genes, chromatin immunoprecipitation sequencing (ChIP-seq) could be performed on bovine oocytes to identify the precise sequence of the PRE in this species and determine genes regulated by nPR. Moreover, a recently developed technique, IHC sequencing, could enable transcriptomic analysis of smaller oocytes (30–50 μm). In combination with *in silico* analysis, such an approach could help complete the characterisation of PRE-regulated genes during bovine oocyte growth.

This study provides a descriptive foundation for future applied studies with more practical implications. For example, an *in-vivo* experiment where animals are categorised according to their circulating P4 levels during the luteal phase, their oocytes recovered for nPR expression and mitochondrial activity analysis. The resulting data may shed light on the importance of P4 anmd nPR activity to oocyte acquisition of developmental competence.

In conclusion, these findings create new opportunities for research to investigate the precise contribution of the nPR to oocyte and follicle development and the underlying mechanisms associated with progression to a developmentally competent stage. Additionally, the work highlights the urgent need for a replicable *in-vitro* oocyte culture system to allow a better understanding of the complex process of oocyte development.

References

Adhikari D, Liu K. The regulation of maturation promoting factor during prophase I arrest and meiotic entry in mammalian oocytes. Mol Cell Endocrinol. 2014 Jan 25;382(1):480-487. doi: 10.1016/j.mce.2013.07.027. Epub 2013 Aug 3. PMID: 23916417.

Aerts JM, Bols PE. Ovarian follicular dynamics: a review with emphasis on the bovine species. Part I: Folliculogenesis and pre-antral follicle development. Reprod Domest Anim. 2010 Feb;45(1):171-9.

Albertini DF. Cytoplasmic microtubular dynamics and chromatin organization during mammalian oogenesis and oocyte maturation. Mutat Res. 1992 Dec;296(1-2):57-68. doi: 10.1016/0165-1110(92)90032-5. PMID: 1279408.

Aparicio IM, Garcia-Herreros M, O'Shea LC, Hensey C, Lonergan P, Fair T. Expression, regulation, and function of progesterone receptors in bovine cumulus oocyte complexes during in vitro maturation. Biol Reprod. 2011 May;84(5):910-21. doi: 10.1095/biolreprod.110.087411. Epub 2011 Jan 12. PMID: 21228216.

Araújo VR, Gastal MO, Figueiredo JR, Gastal EL. In vitro culture of bovine preantral follicles: a review. Reprod Biol Endocrinol. 2014 Aug 13;12:78. doi: 10.1186/1477-7827-12-78. PMID: 25117631; PMCID: PMC4148547.

Assey RJ, Hyttel P, Greve T, Purwantara B. Oocyte morphology in dominant and subordinate follicles. Mol Reprod Dev. 1994 Mar;37(3):335-44. doi: 10.1002/mrd.1080370313. PMID: 8185939.

Azeez JM, Susmi TR, Remadevi V, Ravindran V, Sasikumar Sujatha A, Ayswarya RNS, Sreeja S. New insights into the functions of progesterone receptor (PR) isoforms and progesterone signaling. Am J Cancer Res. 2021 Nov 15;11(11):5214-5232. PMID: 34873457; PMCID: PMC8640821.

Baker TG, Franchi LL. The fine structure of chromosomes in bovine primordial oocytes. J Reprod Fertil. 1967 Dec;14(3):511-3. doi: 10.1530/jrf.0.0140511. PMID: 6071015.

Baker TG, Hunter RHF (1978) Oogenesis and follicular growth in the cow: implications for superovulation. In ‘Control of reproduction in the cow’. (Ed. JM Sreenan) pp. 34–49. (CEC Publications: Luxembourg).

Barros MH, McStay GP. Modular biogenesis of mitochondrial respiratory complexes. Mitochondrion. 2020 Jan;50:94-114. doi: 10.1016/j.mito.2019.10.008. Epub 2019 Oct 25. PMID: 31669617.

Bavister BD, Squirrell JM. Mitochondrial distribution and function in oocytes and early embryos. Hum Reprod. 2000 Jul;15 Suppl 2:189-98. doi: 10.1093/humrep/15.suppl_2.189. PMID: 11041524.

Bebbere D, Albertini DF, Coticchio G, Borini A, Ledda S. The subcortical maternal complex: emerging roles and novel perspectives. Mol Hum Reprod. 2021 Jul 1;27(7):gaab043. doi: 10.1093/molehr/gaab043. PMID: 34191027.
Bezawork-Geleta A, Rohlena J, Dong L, Pacak K, Neuzil J. Mitochondrial Complex II: At the Crossroads. Trends Biochem Sci. 2017 Apr;42(4):312-325. doi: 10.1016/j.tibs.2017.01.003. Epub 2017 Feb 7. PMID: 28185716; PMCID: PMC7441821.

Bisinotto RS, Chebel RC, Santos JE. Follicular wave of the ovulatory follicle and not cyclic status influences fertility of dairy cows. J Dairy Sci. 2010 Aug;93(8):3578-87. doi: 10.3168/jds.2010-3047. PMID: 20655426.

Bolcun-Filas E, Handel MA. Meiosis: the chromosomal foundation of reproduction. Biol Reprod. 2018 Jul 1;99(1):112-126. doi: 10.1093/biolre/ioy021. PMID: 29385397.

Boonyaratanakornkit V, Edwards DP. Receptor mechanisms of rapid extranuclear signalling initiated by steroid hormones. Essays Biochem. 2004;40:105-20. doi: 10.1042/bse0400105. PMID: 15242342.

Bramley T. Non-genomic progesterone receptors in the mammalian ovary: some unresolved issues. Reproduction. 2003 Jan;125(1):3-15. doi: 10.1530/rep.0.1250003. PMID: 12622691.

Braw-Tal R, Yossefi S. Studies in vivo and in vitro on the initiation of follicle growth in the bovine ovary. J Reprod Fertil. 1997 Jan;109(1):165-71. doi: 10.1530/jrf.0.1090165. PMID: 9068428.

Brevini TA, Vassena R, Francisci C, Gandolfi F. Role of adenosine triphosphate, active mitochondria, and microtubules in the acquisition of developmental competence of parthenogenetically activated pig oocytes. Biol Reprod. 2005 May;72(5):1218-23. doi: 10.1095/biolreprod.104.038141. Epub 2005 Jan 19. PMID: 15659704.

Brower PT, Schultz RM. Intercellular communication between granulosa cells and mouse oocytes: existence and possible nutritional role during oocyte growth. Dev Biol. 1982 Mar;90(1):144-53. doi: 10.1016/0012-1606(82)90219-6. PMID: 7199496.

Butler WR. Review: effect of protein nutrition on ovarian and uterine physiology in dairy cattle. J Dairy Sci. 1998 Sep;81(9):2533-9. doi: 10.3168/jds.S0022-0302(98)70146-8. PMID: 9785246.

Butler, W. Energy balance relationships with follicular development, ovulation and fertility in postpartum dairy cows. Livestock Production Science. 2003 83. 211-218.

Byskov AG, Skakkebaek NE, Stafanger G, Peters H. Influence of ovarian surface epithelium and rete ovarii on follicle formation. J Anat. 1977 Feb;123(Pt 1):77-86. PMID: 838624; PMCID: PMC1234254.

Cahill MA. Progesterone receptor membrane component 1: an integrative review. J Steroid Biochem Mol Biol. 2007 Jun-Jul;105(1-5):16-36. doi: 10.1016/j.jsbmb.2007.02.002. Epub 2007 May 16. PMID: 17583495.

Cao L, Shitara H, Horii T, Nagao Y, Imai H, Abe K, Hara T, Hayashi J, Yonekawa H. The mitochondrial bottleneck occurs without reduction of mtDNA content in female mouse germ cells. Nat Genet. 2007 Mar;39(3):386-90. doi: 10.1038/ng1970. Epub 2007 Feb 11. PMID: 17293866.

Chappell PE, Lydon JP, Conneely OM, O'Malley BW, Levine JE. Endocrine defects in mice carrying a null mutation for the progesterone receptor gene. Endocrinology. 1997 Oct;138(10):4147-52. doi: 10.1210/endo.138.10.5456. PMID: 9322923.

Chebel RC, Al-Hassan MJ, Fricke PM, Santos JE, Lima JR, Martel CA, Stevenson JS, Garcia R, Ax RL. Supplementation of progesterone via controlled internal drug release inserts during ovulation synchronization protocols in lactating dairy cows. J Dairy Sci. 2010 Mar;93(3):922-31. doi: 10.3168/jds.2009-2301. PMID: 20172212.

Chelenga M, Sakaguchi K, Kawano K, Furukawa E, Yanagawa Y, Katagiri S, Nagano M. Low oxygen environment and astaxanthin supplementation promote the developmental competence of bovine oocytes derived from early antral follicles during 8 days of in vitro growth in a gas-permeable culture device. Theriogenology. 2022 Jan 1;177:116-126. doi: 10.1016/j.theriogenology.2021.10.014. Epub 2021 Oct 18. PMID: 34695665.

Chelenga M, Yanagawa Y, Katagiri S, Nagano M. Pre-maturational culture promotes the developmental competence of bovine oocytes derived from an 8-day in vitro growth culture system. J Reprod Dev. 2023 Aug 11;69(4):214-217. doi: 10.1262/jrd.2023-022. Epub 2023 May 18. PMID: 37197977; PMCID: PMC10435529.

Cheng S, Altmeppen G, So C, Welp LM, Penir S, Ruhwedel T, Menelaou K, Harasimov K, Stützer A, Blayney M, Elder K, Möbius W, Urlaub H, Schuh M. Mammalian oocytes store mRNAs in a mitochondria-associated membraneless compartment. Science. 2022 Oct 21;378(6617):eabq4835. doi: 10.1126/science.abq4835. Epub 2022 Oct 21. PMID: 36264786.

Chenault JR, Thatcher WW, Kalra PS, Abrams RM, Wilcox CJ. Transitory changes in plasma progestins, estradiol, and luteinizing hormone approaching ovulation in the bovine. J Dairy Sci. 1975 May;58(5):709-17. doi: 10.3168/jds.S0022-0302(75)84632-7. PMID: 1170219.

Choi Y, Ballow DJ, Xin Y, Rajkovic A. Lim homeobox gene, lhx8, is essential for mouse oocyte differentiation and survival. Biol Reprod. 2008 Sep;79(3):442-9. doi: 10.1095/biolreprod.108.069393. Epub 2008 May 28. PMID: 18509161; PMCID: PMC2710541.

Clark BJ, Wells J, King SR, Stocco DM. The purification, cloning, and expression of a novel luteinizing hormone-induced mitochondrial protein in MA-10 mouse Leydig tumor cells. Characterization of the steroidogenic acute regulatory protein (StAR). J Biol Chem. 1994 Nov 11;269(45):28314-22. PMID: 7961770.

Clark LJ, Irving-Rodgers HF, Dharmarajan AM, Rodgers RJ. Theca interna: the other side of bovine follicular atresia. Biol Reprod. 2004 Oct;71(4):1071-8. doi: 10.1095/biolreprod.104.029652. Epub 2004 Jun 2. PMID: 15175236.

Clarke HJ. Transzonal projections: Essential structures mediating intercellular communication in the mammalian ovarian follicle. Mol Reprod Dev. 2022 Nov;89(11):509-525. doi: 10.1002/mrd.23645. Epub 2022 Sep 16. PMID: 36112806.

Conneely OM, Mulac-Jericevic B, Lydon JP, De Mayo FJ. Reproductive functions of the progesterone receptor isoforms: lessons from knock-out mice. Mol Cell Endocrinol. 2001 Jun 20;179(1-2):97-103. doi: 10.1016/s0303-7207(01)00465-8. PMID: 11420134.

Conti M, Andersen CB, Richard F, Mehats C, Chun SY, Horner K, Jin C, Tsafriri A. Role of cyclic nucleotide signaling in oocyte maturation. Mol Cell Endocrinol. 2002 Feb 22;187(1-2):153-9. doi: 10.1016/s0303-7207(01)00686-4. PMID: 11988323.

Crivello JF, Jefcoate CR. Intracellular movement of cholesterol in rat adrenal cells. Kinetics and effects of inhibitors. J Biol Chem. 1980 Sep 10;255(17):8144-51. PMID: 6251046.

Csordás G, Weaver D, Hajnóczky G. Endoplasmic Reticulum-Mitochondrial Contactology: Structure and Signaling Functions. Trends Cell Biol. 2018 Jul;28(7):523-540. doi: 10.1016/j.tcb.2018.02.009. Epub 2018 Mar 24. PMID: 29588129; PMCID: PMC6005738.

Cummins JM. The role of mitochondria in the establishment of oocyte functional competence. Eur J Obstet Gynecol Reprod Biol. 2004 Jul 1;115 Suppl 1:S23-9. doi: 10.1016/j.ejogrb.2004.01.011. PMID: 15196712.

Cunha, A. P., Guenther, J. N., Maroney, M. J., Giordano, J. O., Nascimento, A. B., Bas, S., Ayres, H., and Wiltbank, M. C. Effects of high vs. low progesterone concentrations during Ovsynch on double ovulation rate and pregnancies per AI in high producing dairy cows. J. Dairy Sci. 2008. 91(Suppl. 1), 246.

Dadarwal D, Adams GP, Hyttel P, Brogliatti GM, Caldwell S, Singh J. Organelle reorganization in bovine oocytes during dominant follicle growth and regression. Reprod Biol Endocrinol.

2015 Nov 14;13:124. doi: 10.1186/s12958-015-0122-0. PMID: 26577904; PMCID: PMC4650271.

Dadarwal D, Dias FCF, Adams GP, Singh J. Effect of follicular aging on ATP content and mitochondria distribution in bovine oocytes. Theriogenology. 2017 Feb;89:348-358. doi: 10.1016/j.theriogenology.2016.09.039. Epub 2016 Oct 3. PMID: 27793457.

Dai Q, Shah AA, Garde RV, Yonish BA, Zhang L, Medvitz NA, Miller SE, Hansen EL, Dunn CN, Price TM. A truncated progesterone receptor (PR-M) localizes to the mitochondrion and controls cellular respiration. Mol Endocrinol. 2013 May;27(5):741-53. doi: 10.1210/me.2012-1292. Epub 2013 Mar 21. PMID: 23518922; PMCID: PMC3634113.
Davies TH, Ning YM, Sánchez ER. A new first step in activation of steroid receptors: hormone-induced switching of FKBP51 and FKBP52 immunophilins. J Biol Chem. 2002 Feb 15;277(7):4597-600. doi: 10.1074/jbc.C100531200. Epub 2001 Dec 20. PMID: 11751894.

de Loos F, van Vliet C, van Maurik P, Kruip TA. Morphology of immature bovine oocytes. Gamete Res. 1989 Oct;24(2):197-204. doi: 10.1002/mrd.1120240207. PMID: 2793058.

De Los Reyes M, Palomino J, Villagra A, Ramirez G, Peralta OA, Parraguez VH, Aspee K. Effect of progesterone on in vitro meiotic maturation of canine oocytes associated with Cx37 and Cx43 gene expression. Theriogenology. 2023 Jul 1;204:50-57. doi: 10.1016/j.theriogenology.2023.04.005. Epub 2023 Apr 10. PMID: 37068395.

de Vant'ery C, Gavin AC, Vassalli JD, Schorderet-Slatkine S. An accumulation of p34cdc2 at the end of mouse oocyte growth correlates with the acquisition of meiotic competence. Dev Biol. 1996 Mar 15;174(2):335-44. doi: 10.1006/dbio.1996.0078. PMID: 8631505.

de Vantéry C, Stutz A, Vassalli JD, Schorderet-Slatkine S. Acquisition of meiotic competence in growing mouse oocytes is controlled at both translational and posttranslational levels. Dev Biol. 1997 Jul 1;187(1):43-54. doi: 10.1006/dbio.1997.8599. PMID: 9224673.

Dekel N, Beers WH. Rat oocyte maturation in vitro: relief of cyclic AMP inhibition by gonadotropins. Proc Natl Acad Sci U S A. 1978 Sep;75(9):4369-73. doi: 10.1073/pnas.75.9.4369. PMID: 212746; PMCID: PMC336116.

Denicol AC, Lopes G Jr, Mendonça LG, Rivera FA, Guagnini F, Perez RV, Lima JR, Bruno RG, Santos JE, Chebel RC. Low progesterone concentration during the development of the first follicular wave reduces pregnancy per insemination of lactating dairy cows. J Dairy Sci. 2012 Apr;95(4):1794-806. doi: 10.3168/jds.2011-4650. PMID: 22459828.

Dieleman SJ, Bevers MM, Poortman J, van Tol HT. Steroid and pituitary hormone concentrations in the fluid of preovulatory bovine follicles relative to the peak of LH in the peripheral blood. J Reprod Fertil. 1983 Nov;69(2):641-9. doi: 10.1530/jrf.0.0690641. PMID: 6226779.

Diskin MG, Sreenan JM. Fertilization and embryonic mortality rates in beef heifers after artificial insemination. J Reprod Fertil. 1980 Jul;59(2):463-8. doi: 10.1530/jrf.0.0590463. PMID: 7431304.

Edwards RG. Maturation in vitro of mouse, sheep, cow, pig, rhesus monkey and human ovarian oocytes. Nature. 1965 Oct 23;208(5008):349-51. doi: 10.1038/208349a0. PMID: 4957259.

El Shourbagy SH, Spikings EC, Freitas M, St John JC. Mitochondria directly influence fertilisation outcome in the pig. Reproduction. 2006 Feb;131(2):233-45. doi: 10.1530/rep.1.00551. PMID: 16452717.

Eppig JJ. Intercommunication between mammalian oocytes and companion somatic cells. Bioessays. 1991 Nov;13(11):569-74. doi: 10.1002/bies.950131105. PMID: 1772412.

Erickson BH. Development and senescence of the postnatal bovine ovary. J Anim Sci. 1966 Aug;25(3):800-5. doi: 10.2527/jas1966.253800x. PMID: 6007918.

Fair T, Hulshof SC, Hyttel P, Greve T, Boland M. Oocyte ultrastructure in bovine primordial to early tertiary follicles. Anat Embryol (Berl). 1997 Apr;195(4):327-36. doi: 10.1007/s004290050052. PMID: 9108198.

Fair T, Hyttel P, Greve T, Boland M. Nucleus structure and transcriptional activity in relation to oocyte diameter in cattle. Mol Reprod Dev. 1996 Apr;43(4):503-12. doi: 10.1002/(SICI)1098-2795(199604)43:4<503::AID-MRD13>3.0.CO;2-#. PMID: 9052942.

Fair T, Hyttel P, Greve T. Bovine oocyte diameter in relation to maturational competence and transcriptional activity. Mol Reprod Dev. 1995 Dec;42(4):437-42. doi: 10.1002/mrd.1080420410. PMID: 8607973.

Fair T, Hyttel P, Oocyte growth in cattle—ultrastructure, transcription and developmental competence. 1997. In: Motta P.M. (Ed.), Microscopy of Reproduction and Development: A Dynamic Approach. Antonio Delfino, Rome, pp. 109–118.

Fair T, Lonergan P. The oocyte: the key player in the success of assisted reproduction technologies. Reprod Fertil Dev. 2023 Dec;36(2):133-148. doi: 10.1071/RD23164. PMID: 38064189.

Fair T, Lonergan P. The role of progesterone in oocyte acquisition of developmental competence. Reprod Domest Anim. 2012 Aug;47 Suppl 4:142-7. doi: 10.1111/j.1439-0531.2012.02068.x. PMID: 22827363.

Fair T. Follicular oocyte growth and acquisition of developmental competence. Anim Reprod Sci. 2003 Oct 15;78(3-4):203-16. doi: 10.1016/s0378-4320(03)00091-5. PMID: 12818645.

Fair T. Mammalian oocyte development: checkpoints for competence. Reprod Fertil Dev. 2010;22(1):13-20. doi: 10.1071/RD09216. PMID: 20003841.

Fernandes R, Tsuda C, Perumalsamy AL, Naranian T, Chong J, Acton BM, Tong ZB, Nelson LM, Jurisicova A. NLRP5 mediates mitochondrial function in mouse oocytes and embryos. Biol Reprod. 2012 May 3;86(5):138, 1-10. doi: 10.1095/biolreprod.111.093583. PMID: 22357545; PMCID: PMC3364921.

Fernández-Murray JP, McMaster CR. Lipid synthesis and membrane contact sites: a crossroads for cellular physiology. J Lipid Res. 2016 Oct;57(10):1789-1805. doi: 10.1194/jlr.R070920. Epub 2016 Aug 12. PMID: 27521373; PMCID: PMC5036376.

Ferreira EM, Vireque AA, Adona PR, Meirelles FV, Ferriani RA, Navarro PA. Cytoplasmic maturation of bovine oocytes: structural and biochemical modifications and acquisition of developmental competence. Theriogenology. 2009 Mar 15;71(5):836-48. doi: 10.1016/j.theriogenology.2008.10.023. Epub 2009 Jan 3. Erratum in: Theriogenology. 2010 May;73(8):1164. PMID: 19121865.

Findlay JK, Hutt KJ, Hickey M, Anderson RA. How Is the Number of Primordial Follicles in the Ovarian Reserve Established? Biol Reprod. 2015 Nov;93(5):111. doi: 10.1095/biolreprod.115.133652. Epub 2015 Sep 30. PMID: 26423124.

Fonseca FA, Britt JH, McDaniel BT, Wilk JC, Rakes AH. Reproductive traits of Holsteins and Jerseys. Effects of age, milk yield, and clinical abnormalities on involution of cervix and uterus, ovulation, estrous cycles, detection of estrus, conception rate, and days open. J Dairy Sci. 1983 May;66(5):1128-47. doi: 10.3168/jds.S0022-0302(83)81910-9. PMID: 6683729.

Forde N, Beltman ME, Lonergan P, Diskin M, Roche JF, Crowe MA. Oestrous cycles in Bos taurus cattle. Anim Reprod Sci. 2011 Apr;124(3-4):163-9. doi: 10.1016/j.anireprosci.2010.08.025. Epub 2010 Sep 27. PMID: 20875708.

Fortune JE. Ovarian follicular growth and development in mammals. Biol Reprod. 1994 Feb;50(2):225-32. doi: 10.1095/biolreprod50.2.225. PMID: 8142540.

Frandson, R., Wilke, W.L., Fails, A.D. Anatomy and physiology of farm animals. 2003. Lippincott Williams and Wilkins, Baltimore.

Fulka J Jr, First NL, Moor RM. Nuclear and cytoplasmic determinants involved in the regulation of mammalian oocyte maturation. Mol Hum Reprod. 1998 Jan;4(1):41-9. doi: 10.1093/molehr/4.1.41. PMID: 9510010.

Fushii M, Yamada R, Miyano T. In vitro growth of bovine oocytes in oocyte-cumulus cell complexes and the effect of follicle stimulating hormone on the growth of oocytes. J Reprod

Dev. 2021 Feb 15;67(1):5-13. doi: 10.1262/jrd.2020-102. Epub 2020 Oct 30. PMID: 33132227; PMCID: PMC7902213.

Gallardo TD, John GB, Shirley L, Contreras CM, Akbay EA, Haynie JM, Ward SE, Shidler MJ, Castrillon DH. Genomewide discovery and classification of candidate ovarian fertility genes in the mouse. Genetics. 2007 Sep;177(1):179-94. doi: 10.1534/genetics.107.074823. Epub 2007 Jul 29. PMID: 17660561; PMCID: PMC2013718.

Garaude J, Acín-Pérez R, Martínez-Cano S, Enamorado M, Ugolini M, Nistal-Villán E, Hervás-Stubbs S, Pelegrín P, Sander LE, Enríquez JA, Sancho D. Mitochondrial respiratory-chain adaptations in macrophages contribute to antibacterial host defense. Nat Immunol. 2016 Sep;17(9):1037-1045. doi: 10.1038/ni.3509. Epub 2016 Jun 27. PMID: 27348412; PMCID: PMC4994870.

Garcia Barros R, Lodde V, Franciosi F, Luciano AM. A refined culture system of oocytes from early antral follicles promotes oocyte maturation and embryo development in cattle. Reproduction. 2023 Jan 6;165(2):221-233. doi: 10.1530/REP-22-0277. PMID: 36473031.

Garg D, Ng SSM, Baig KM, Driggers P, Segars J. Progesterone-Mediated Non-Classical Signaling. Trends Endocrinol Metab. 2017 Sep;28(9):656-668. doi: 10.1016/j.tem.2017.05.006. Epub 2017 Jun 23. PMID: 28651856.

Gaytan F, Morales C, Roa J, Tena-Sempere M. Changes in keratin 8/18 expression in human granulosa cell lineage are associated to cell death/survival events: potential implications for the maintenance of the ovarian reserve. Hum Reprod. 2018 Apr 1;33(4):680-689. doi: 10.1093/humrep/dey010. PMID: 29401296.

Ghezzi D, Goffrini P, Uziel G, Horvath R, Klopstock T, Lochmüller H, D'Adamo P, Gasparini P, Strom TM, Prokisch H, Invernizzi F, Ferrero I, Zeviani M. SDHAF1, encoding a LYR complex-II specific assembly factor, is mutated in SDH-defective infantile leukoencephalopathy. Nat Genet. 2009 Jun;41(6):654-6. doi: 10.1038/ng.378. Epub 2009 May 24. PMID: 19465911.

Glerum DM, Tzagoloff A. Submitochondrial distributions and stabilities of subunits 4, 5, and 6 of yeast cytochrome oxidase in assembly defective mutants. FEBS Lett. 1997 Aug 4;412(3):410-4. doi: 10.1016/s0014-5793(97)00799-0. PMID: 9276437.

Grealy M, Diskin MG, Sreenan JM. Protein content of cattle oocytes and embryos from the two-cell to the elongated blastocyst stage at day 16. J Reprod Fertil. 1996 Jul;107(2):229-33. doi: 10.1530/jrf.0.1070229. PMID: 8882289.

Grimes RW, Matton P, Ireland JJ. A comparison of histological and non-histological indices of atresia and follicular function. Biol Reprod. 1987 Aug;37(1):82-8. doi: 10.1095/biolreprod37.1.82. PMID: 3651553.

Hadley, M. E. Endocrinology. Hormones and female reproductive physiology. 2000 5th ed. Prentice Hall, Inc. Upper Saddle River, NJ.

Ham J, Thomson A, Needham M, Webb P, Parker M. Characterization of response elements for androgens, glucocorticoids and progestins in mouse mammary tumour virus. Nucleic Acids Res. 1988 Jun 24;16(12):5263-76. doi: 10.1093/nar/16.12.5263. PMID: 2838812; PMCID: PMC336766.

Hamazaki N, Kyogoku H, Araki H, Miura F, Horikawa C, Hamada N, Shimamoto S, Hikabe O, Nakashima K, Kitajima TS, Ito T, Leitch HG, Hayashi K. Reconstitution of the oocyte transcriptional network with transcription factors. Nature. 2021 Jan;589(7841):264-269. doi: 10.1038/s41586-020-3027-9. Epub 2020 Dec 16. PMID: 33328630.

Hansel W, Convey EM. Physiology of the estrous cycle. J Anim Sci. 1983 Jul;57 Suppl 2:404-24. PMID: 6413474.

Harasimov K, Uraji J, Mönnich EU, Holubcová Z, Elder K, Blayney M, Schuh M. Actin-driven chromosome clustering facilitates fast and complete chromosome capture in mammalian oocytes. Nat Cell Biol. 2023 Mar;25(3):439-452. doi: 10.1038/s41556-022-01082-9. Epub 2023 Feb 2. Erratum in: Nat Cell Biol. 2023 Jun;25(6):917. doi: 10.1038/s41556-023-01156-2. PMID: 36732633; PMCID: PMC10014578.

Hasegawa J, Yanaihara A, Iwasaki S, Otsuka Y, Negishi M, Akahane T, Okai T. Reduction of progesterone receptor expression in human cumulus cells at the time of oocyte collection during IVF is associated with good embryo quality. Hum Reprod. 2005 Aug;20(8):2194-200. doi: 10.1093/humrep/dei005. Epub 2005 Mar 31. PMID: 15802315.

Hild-Petito S, Stouffer RL, Brenner RM. Immunocytochemical localization of estradiol and progesterone receptors in the monkey ovary throughout the menstrual cycle. Endocrinology. 1988 Dec;123(6):2896-905. doi: 10.1210/endo-123-6-2896. PMID: 3197647.

Hock DH, Reljic B, Ang CS, Muellner-Wong L, Mountford HS, Compton AG, Ryan MT, Thorburn DR, Stroud DA. HIGD2A is Required for Assembly of the COX3 Module of Human Mitochondrial Complex IV. Mol Cell Proteomics. 2020 Jul;19(7):1145-1160. doi: 10.1074/mcp.RA120.002076. Epub 2020 Apr 21. PMID: 32317297; PMCID: PMC7338084.

Hosoe M, Shioya Y. Distribution of cortical granules in bovine oocytes classified by cumulus complex. Zygote. 1997 Nov;5(4):371-6. doi: 10.1017/s0967199400003956. PMID: 9563685.

Hu J, Zhang Z, Shen WJ, Azhar S. Cellular cholesterol delivery, intracellular processing and utilization for biosynthesis of steroid hormones. Nutr Metab (Lond). 2010 Jun 1;7:47. doi: 10.1186/1743-7075-7-47. PMID: 20515451; PMCID: PMC2890697.

Hu W, Zeng H, Shi Y, Zhou C, Huang J, Jia L, Xu S, Feng X, Zeng Y, Xiong T, Huang W, Sun P, Chang Y, Li T, Fang C, Wu K, Cai L, Ni W, Li Y, Yang Z, Zhang QC, Chian R, Chen Z, Liang X, Kee K. Single-cell transcriptome and translatome dual-omics reveals potential mechanisms of human oocyte maturation. Nat Commun. 2022 Aug 30;13(1):5114. doi: 10.1038/s41467-022-32791-2. PMID: 36042231; PMCID: PMC9427852.

Hulshof SC, Figueiredo JR, Beckers JF, Bevers MM, van den Hurk R. Isolation and characterization of preantral follicles from foetal bovine ovaries. Vet Q. 1994 Jul;16(2):78-80. doi: 10.1080/01652176.1994.9694423. PMID: 7985360.

Hyttel P, Fair T, Callensen H, Greve T. Oocyte growth, capacitation and final maturation in cattle. Theriogenology 1997;47:23– 32.
Hyttel P, Greve T, Callesen H. Ultrastructural aspects of oocyte maturation and fertilization in cattle. J Reprod Fertil Suppl. 1989;38:35-47. PMID: 2677348.

Hyttel P, Xu KP, Smith S, Greve T. Ultrastructure of in-vitro oocyte maturation in cattle. J Reprod Fertil. 1986 Nov;78(2):615-25. doi: 10.1530/jrf.0.0780615. PMID: 3806520.

Inskeep EK. Preovulatory, postovulatory, and postmaternal recognition effects of concentrations of progesterone on embryonic survival in the cow. J Anim Sci. 2004;82 E-Suppl:E24-39. doi: 10.2527/2004.8213_supplE24x. PMID: 15471804.

Ireland JJ, Mihm M, Austin E, Diskin MG, Roche JF. Historical perspective of turnover of dominant follicles during the bovine estrous cycle: key concepts, studies, advancements, and terms. J Dairy Sci. 2000 Jul;83(7):1648-58. doi: 10.3168/jds.S0022-0302(00)75033-8. PMID: 10908068.

Ireland JJ, Roche JF. Growth and differentiation of large antral follicles after spontaneous luteolysis in heifers: changes in concentration of hormones in follicular fluid and specific binding of gonadotropins to follicles. J Anim Sci. 1983 Jul;57(1):157-67. doi: 10.2527/jas1983.571157x. PMID: 6309727.

Irving-Rodgers HF, Krupa M, Rodgers RJ. Cholesterol side-chain cleavage cytochrome P450 and 3beta-hydroxysteroid dehydrogenase expression and the concentrations of steroid hormones in the follicular fluids of different phenotypes of healthy and atretic bovine ovarian follicles. Biol Reprod. 2003 Dec;69(6):2022-8. doi: 10.1095/biolreprod.103.017442. Epub 2003 Aug 20. PMID: 12930727.

Ismail PM, Li J, DeMayo FJ, O'Malley BW, Lydon JP. A novel LacZ reporter mouse reveals complex regulation of the progesterone receptor promoter during mammary gland development. Mol Endocrinol. 2002 Nov;16(11):2475-89. doi: 10.1210/me.2002-0169. PMID: 12403837.

Iwai T, Nanbu Y, Iwai M, Taii S, Fujii S, Mori T. Immunohistochemical localization of oestrogen receptors and progesterone receptors in the human ovary throughout the menstrual cycle. Virchows Arch A Pathol Anat Histopathol. 1990;417(5):369-75. doi: 10.1007/BF01606025. PMID: 2122584.

Jefcoate CR, DiBartolomeis MJ, Williams CA, McNamara BC. ACTH regulation of cholesterol movement in isolated adrenal cells. J Steroid Biochem. 1987;27(4-6):721-9. doi: 10.1016/0022-4731(87)90142-7. PMID: 2826904.

Jentoft IMA, Bäuerlein FJB, Welp LM, Cooper BH, Petrovic A, So C, Penir SM, Politi AZ, Horokhovskyi Y, Takala I, Eckel H, Moltrecht R, Lénárt P, Cavazza T, Liepe J, Brose N, Urlaub H, Fernández-Busnadiego R, Schuh M. Mammalian oocytes store proteins for the early embryo on cytoplasmic lattices. Cell. 2023 Nov 22;186(24):5308-5327.e25. doi: 10.1016/j.cell.2023.10.003. Epub 2023 Nov 2. PMID: 37922900.

Jo M, Komar CM, Fortune JE. Gonadotropin surge induces two separate increases in messenger RNA for progesterone receptor in bovine preovulatory follicles. Biol Reprod. 2002 Dec;67(6):1981-8. doi: 10.1095/biolreprod.102.004366. PMID: 12444077.

Jolly PD, Tisdall DJ, Heath DA, Lun S, McNatty KP. Apoptosis in bovine granulosa cells in relation to steroid synthesis, cyclic adenosine 3',5'-monophosphate response to follicle-stimulating hormone and luteinizing hormone, and follicular atresia. Biol Reprod. 1994 Nov;51(5):934-44. doi: 10.1095/biolreprod51.5.934. PMID: 7849196.

Joshi S, Davies H, Sims LP, Levy SE, Dean J. Ovarian gene expression in the absence of FIGLA, an oocyte-specific transcription factor. BMC Dev Biol. 2007 Jun 13;7:67. doi: 10.1186/1471-213X-7-67. PMID: 17567914; PMCID: PMC1906760.

Juengel JL, Heath DA, Quirke LD, McNatty KP. Oestrogen receptor alpha and beta, androgen receptor and progesterone receptor mRNA and protein localisation within the developing ovary and in small growing follicles of sheep. Reproduction. 2006 Jan;131(1):81-92. doi: 10.1530/rep.1.00704. PMID: 16388012.

Kadenbach B. Complex IV - The regulatory center of mitochondrial oxidative phosphorylation. Mitochondrion. 2021 May;58:296-302. doi: 10.1016/j.mito.2020.10.004. Epub 2020 Oct 15. PMID: 33069909.

Kastner P, Krust A, Turcotte B, Stropp U, Tora L, Gronemeyer H, Chambon P. Two distinct estrogen-regulated promoters generate transcripts encoding the two functionally different human progesterone receptor forms A and B. EMBO J. 1990 May;9(5):1603-14. doi: 10.1002/j.1460-2075.1990.tb08280.x. PMID: 2328727; PMCID: PMC551856.

Kątska-Książkiewicz L, Alm H, Torner H, Heleil B, Tuchscherer A, Ryńska B. Mitochondrial aggregation patterns and activity in in vitro cultured bovine oocytes recovered from early antral

ovarian follicles. Theriogenology. 2011 Mar 1;75(4):662-70. doi: 10.1016/j.theriogenology.2010.10.006. Epub 2010 Nov 26. PMID: 21111463.

Kere M, Liu PC, Chen YK, Chao PC, Tsai LK, Yeh TY, Siriboon C, Intawicha P, Lo NW, Chiang HI, Fan YK, Ju JC. Ultrastructural Characterization of Porcine Growing and In Vitro Matured Oocytes. Animals (Basel). 2020 Apr 11;10(4):664. doi: 10.3390/ani10040664. PMID: 32290459; PMCID: PMC7222836.

Kerkhofs M, Giorgi C, Marchi S, Seitaj B, Parys JB, Pinton P, Bultynck G, Bittremieux M. Alterations in Ca2+ Signalling via ER-Mitochondria Contact Site Remodelling in Cancer. Adv Exp Med Biol. 2017;997:225-254. doi: 10.1007/978-981-10-4567-7_17. PMID: 28815534.

Kim NH, Cho SK, Choi SH, Kim EY, Park SP, Lim JH. The distribution and requirements of microtubules and microfilaments in bovine oocytes during in vitro maturation. Zygote. 2000 Feb;8(1):25-32. doi: 10.1017/s0967199400000794. PMID: 10840871.

Kline D. Attributes and dynamics of the endoplasmic reticulum in mammalian eggs. Curr Top Dev Biol. 2000;50:125-54. doi: 10.1016/s0070-2153(00)50007-6. PMID: 10948453.

Korte JM, Isola JJ. An immunocytochemical study of the progesterone receptor in rabbit ovary. Mol Cell Endocrinol. 1988 Jul;58(1):93-101. doi: 10.1016/0303-7207(88)90057-3. PMID: 3208991.

Kruip TAM, Cran DG, Van Beneden TH, Dieleman SJ. Structural changes in bovine oocytes during final maturation in vivo. Gamete Res 1983;8:29–47.

Labrecque R, Lodde V, Dieci C, Tessaro I, Luciano AM, Sirard MA. Chromatin remodelling and histone m RNA accumulation in bovine germinal vesicle oocytes. Mol Reprod Dev. 2015 Jun;82(6):450-62. doi: 10.1002/mrd.22494. Epub 2015 May 4. PMID: 25940597.

Lamas-Toranzo I, Pericuesta E, Bermejo-Álvarez P. Mitochondrial and metabolic adjustments during the final phase of follicular development prior to IVM of bovine oocytes. Theriogenology. 2018 Oct 1;119:156-162. doi: 10.1016/j.theriogenology.2018.07.007. Epub 2018 Jul 7. PMID: 30015144.

Latorraca LB, Galvão A, Rabaglino MB, D'Augero JM, Kelsey G, Fair T. Single-cell profiling reveals transcriptome dynamics during bovine oocyte growth. BMC Genomics. 2024 Apr 6;25(1):335. doi: 10.1186/s12864-024-10234-0. PMID: 38580918; PMCID: PMC10998374.

Leonhardt SA, Boonyaratanakornkit V, Edwards DP. Progesterone receptor transcription and non-transcription signaling mechanisms. Steroids. 2003 Nov;68(10-13):761-70. doi: 10.1016/s0039-128x(03)00129-6. PMID: 14667966.

Li GP, Liu Y, Bunch TD, White KL, Aston KI. Asymmetric division of spindle microtubules and microfilaments during bovine meiosis from metaphase I to metaphase III. Mol Reprod Dev. 2005 Jun;71(2):220-6. doi: 10.1002/mrd.20255. PMID: 15791589.

Li Q, Jimenez-Krassel F, Bettegowda A, Ireland JJ, Smith GW. Evidence that the preovulatory rise in intrafollicular progesterone may not be required for ovulation in cattle. J Endocrinol. 2007 Mar;192(3):473-83. doi: 10.1677/JOE-06-0020. PMID: 17332517.

Liu X, Morency E, Li T, Qin H, Zhang X, Zhang X, Coonrod S. Role for PADI6 in securing the mRNA-MSY2 complex to the oocyte cytoplasmic lattices. Cell Cycle. 2017 Feb 16;16(4):360-366. doi: 10.1080/15384101.2016.1261225. Epub 2016 Dec 8. PMID: 27929740; PMCID: PMC5324759.

Liu YJ, Nakamura T, Nakano T. Essential role of DPPA3 for chromatin condensation in mouse oocytogenesis. Biol Reprod. 2012 Feb 14;86(2):40. doi: 10.1095/biolreprod.111.095018. PMID: 22034526.

Lodde V, Franciosi F, Tessaro I, Modina SC, Luciano AM. Role of gap junction-mediated communications in regulating large-scale chromatin configuration remodeling and embryonic developmental competence acquisition in fully grown bovine oocyte. J Assist Reprod Genet. 2013 Sep;30(9):1219-26. doi: 10.1007/s10815-013-0061-7. Epub 2013 Jul 24. PMID: 23881161; PMCID: PMC3800535.

Lodde V, Luciano AM, Franciosi F, Labrecque R, Sirard MA. Accumulation of Chromatin Remodelling Enzyme and Histone Transcripts in Bovine Oocytes. Results Probl Cell Differ. 2017;63:223-255. doi: 10.1007/978-3-319-60855-6_11. PMID: 28779321.

Lodde V, Modina S, Galbusera C, Franciosi F, Luciano AM. Large-scale chromatin remodeling in germinal vesicle bovine oocytes: interplay with gap junction functionality and developmental competence. Mol Reprod Dev. 2007 Jun;74(6):740-9. doi: 10.1002/mrd.20639. PMID: 17075796.

Lodde V, Modina S, Maddox-Hyttel P, Franciosi F, Lauria A, Luciano AM. Oocyte morphology and transcriptional silencing in relation to chromatin remodeling during the final phases of bovine oocyte growth. Mol Reprod Dev. 2008 May;75(5):915-24. doi: 10.1002/mrd.20824. PMID: 17948251.

Lodde V, Modina SC, Franciosi F, Zuccari E, Tessaro I, Luciano AM. Localization of DNA methyltransferase-1 during oocyte differentiation, in vitro maturation and early embryonic development in cow. Eur J Histochem. 2009 Dec 29;53(4):e24. doi: 10.4081/ejh.2009.e24. PMID: 22073356; PMCID: PMC3167337.

Lonergan P, Fair T, Corcoran D, Evans AC. Effect of culture environment on gene expression and developmental characteristics in IVF-derived embryos. Theriogenology. 2006 Jan

7;65(1):137-52. doi: 10.1016/j.theriogenology.2005.09.028. Epub 2005 Nov 9. PMID: 16289260.

Lonergan P, Fair T, Forde N, Rizos D. Embryo development in dairy cattle. Theriogenology. 2016 Jul 1;86(1):270-7. doi: 10.1016/j.theriogenology.2016.04.040. Epub 2016 Apr 21. PMID: 27158131.

Lonergan P, Fair T. Maturation of Oocytes in Vitro. Annu Rev Anim Biosci. 2016;4:255-68. doi: 10.1146/annurev-animal-022114-110822. Epub 2015 Nov 9. PMID: 26566159.

Lonergan P, Forde N, Spencer T. Role of progesterone in embryo development in cattle. Reprod Fertil Dev. 2016;28(1-2):66-74. doi: 10.1071/RD15326. PMID: 27062875.

Lonergan P, Rizos D, Gutierrez-Adan A, Fair T, Boland MP. Oocyte and embryo quality: effect of origin, culture conditions and gene expression patterns. Reprod Domest Anim. 2003 Aug;38(4):259-67. doi: 10.1046/j.1439-0531.2003.00437.x. PMID: 12887565.

Lonergan P, Rizos D, Ward F, Boland MP. Factors influencing oocyte and embryo quality in cattle. Reprod Nutr Dev. 2001 Sep-Oct;41(5):427-37. doi: 10.1051/rnd:2001142. PMID: 11993800.

Lonergan P, Sánchez JM. Symposium review: Progesterone effects on early embryo development in cattle. J Dairy Sci. 2020 Sep;103(9):8698-8707. doi: 10.3168/jds.2020-18583. Epub 2020 Jul 1. PMID: 32622590.

Lonergan P. Influence of progesterone on oocyte quality and embryo development in cows. Theriogenology. 2011 Dec;76(9):1594-601. doi: 10.1016/j.theriogenology.2011.06.012. PMID: 21855985.

Luciano AM, Barros RG, Soares ACS, Buratini J, Lodde V, Franciosi F. Recreating the Follicular Environment: A Customized Approach for In Vitro Culture of Bovine Oocytes Based on the Origin and Differentiation State. Methods Mol Biol. 2021;2273:1-15. doi: 10.1007/978-1-0716-1246-0_1. PMID: 33604842.

Luciano AM, Franciosi F, Dieci C, Lodde V. Changes in large-scale chromatin structure and function during oogenesis: a journey in company with follicular cells. Anim Reprod Sci. 2014 Sep;149(1-2):3-10. doi: 10.1016/j.anireprosci.2014.06.026. Epub 2014 Jun 30. PMID: 25028181.

Luciano AM, Lodde V, Franciosi F, Ceciliani F, Peluso JJ. Progesterone receptor membrane component 1 expression and putative function in bovine oocyte maturation, fertilization, and early embryonic development. Reproduction. 2010 Nov;140(5):663-72. doi: 10.1530/REP-10-0218. Epub 2010 Aug 25. PMID: 20739377.

Lucy MC. Reproductive loss in high-producing dairy cattle: where will it end? J Dairy Sci. 2001 Jun;84(6):1277-93. doi: 10.3168/jds.S0022-0302(01)70158-0. PMID: 11417685.

Lussier JG, Matton P, Dufour JJ. Growth rates of follicles in the ovary of the cow. J Reprod Fertil. 1987 Nov;81(2):301-7. doi: 10.1530/jrf.0.0810301. PMID: 3430454.

Lydon JP, DeMayo FJ, Funk CR, Mani SK, Hughes AR, Montgomery CA Jr, Shyamala G, Conneely OM, O'Malley BW. Mice lacking progesterone receptor exhibit pleiotropic reproductive abnormalities. Genes Dev. 1995 Sep 15;9(18):2266-78. doi: 10.1101/gad.9.18.2266. PMID: 7557380.

Machatkova M, Krausova K, Jokesova E, Tomanek M. Developmental competence of bovine oocytes: effects of follicle size and the phase of follicular wave on in vitro embryo production. Theriogenology. 2004 Jan 15;61(2-3):329-35. doi: 10.1016/s0093-691x(03)00216-4. PMID: 14662132.

Maller JL, Krebs EG. Regulation of oocyte maturation. Curr Top Cell Regul. 1980;16:271-311. doi: 10.1016/b978-0-12-152816-4.50012-1. PMID: 6249544.

Manna PR, Dyson MT, Stocco DM. Regulation of the steroidogenic acute regulatory protein gene expression: present and future perspectives. Mol Hum Reprod. 2009 Jun;15(6):321-33. doi: 10.1093/molehr/gap025. Epub 2009 Mar 25. PMID: 19321517; PMCID: PMC2676994.

Marchi S, Bittremieux M, Missiroli S, Morganti C, Patergnani S, Sbano L, Rimessi A, Kerkhofs M, Parys JB, Bultynck G, Giorgi C, Pinton P. Endoplasmic Reticulum-Mitochondria Communication Through Ca2+ Signaling: The Importance of Mitochondria-Associated Membranes (MAMs). Adv Exp Med Biol. 2017;997:49-67. doi: 10.1007/978-981-10-4567-7_4. PMID: 28815521.

Marion GB, Gier HT, Choudary JB. Micromorphology of the bovine ovarian follicular system. J Anim Sci. 1968 Mar;27(2):451-65. doi: 10.2527/jas1968.272451x. PMID: 5646345.

Masui Y, Markert CL. Cytoplasmic control of nuclear behavior during meiotic maturation of frog oocytes. J Exp Zool. 1971 Jun;177(2):129-45. doi: 10.1002/jez.1401770202. PMID: 5106340.

Matsuda F, Inoue N, Manabe N, Ohkura S. Follicular growth and atresia in mammalian ovaries: regulation by survival and death of granulosa cells. J Reprod Dev. 2012;58(1):44-50. doi: 10.1262/jrd.2011-012. PMID: 22450284.

McGeady TA, Quinn PJ, FitzPatrick, ES, Ryan MT, Kilroy D, Lonergan P; Illustrations by S. Cahalan and S. Kilroy. Assisted reproductive technologies used in domestic species. Veterinary Embryology. Second edition. Chichester, West Sussex ;: John Wiley & Sons Inc. 2017.

McLaren A. Sex determination. The making of male mice. Nature. 1991 May 9;351(6322):96. doi: 10.1038/351096a0. PMID: 2030741.

Medina-Laver Y, Rodríguez-Varela C, Salsano S, Labarta E, Domínguez F. What Do We Know about Classical and Non-Classical Progesterone Receptors in the Human Female Reproductive Tract? A Review. Int J Mol Sci. 2021 Oct 19;22(20):11278. doi: 10.3390/ijms222011278. PMID: 34681937; PMCID: PMC8538361.

Medvedev S, Pan H, Schultz RM. Absence of MSY2 in mouse oocytes perturbs oocyte growth and maturation, RNA stability, and the transcriptome. Biol Reprod. 2011 Sep;85(3):575-83. doi: 10.1095/biolreprod.111.091710. Epub 2011 May 25. PMID: 21613634; PMCID: PMC3159539.

Mehlmann LM, Saeki Y, Tanaka S, Brennan TJ, Evsikov AV, Pendola FL, Knowles BB, Eppig JJ, Jaffe LA. The Gs-linked receptor GPR3 maintains meiotic arrest in mammalian oocytes. Science. 2004 Dec 10;306(5703):1947-50. doi: 10.1126/science.1103974. PMID: 15591206.

Meirelles FV, Caetano AR, Watanabe YF, Ripamonte P, Carambula SF, Merighe GK, Garcia SM. Genome activation and developmental block in bovine embryos. Anim Reprod Sci. 2004 Jul;82-83:13-20. doi: 10.1016/j.anireprosci.2004.05.012. PMID: 15271440.

Michaels GS, Hauswirth WW, Laipis PJ. Mitochondrial DNA copy number in bovine oocytes and somatic cells. Dev Biol. 1982 Nov;94(1):246-51. doi: 10.1016/0012-1606(82)90088-4. PMID: 6295849.

Mihm M, Curran N, Hyttel P, Knight PG, Boland MP, Roche JF. Effect of dominant follicle persistence on follicular fluid oestradiol and inhibin and on oocyte maturation in heifers. J Reprod Fertil. 1999 Jul;116(2):293-304. doi: 10.1530/jrf.0.1160293. PMID: 10615254.

Miller WL. Disorders in the initial steps of steroid hormone synthesis. J Steroid Biochem Mol Biol. 2017 Jan;165(Pt A):18-37. doi: 10.1016/j.jsbmb.2016.03.009. Epub 2016 Mar 6. PMID: 26960203.

Mingoti GZ, Garcia JM, Rosa-e-Silva AA. Steroidogenesis in cumulus cells of bovine cumulus-oocyte-complexes matured in vitro with BSA and different concentrations of steroids. Anim Reprod Sci. 2002 Feb 15;69(3-4):175-86. doi: 10.1016/s0378-4320(01)00187-7. PMID: 11812628.

Mogessie B, Schuh M. Actin protects mammalian eggs against chromosome segregation errors. Science. 2017 Aug 25;357(6353):eaal1647. doi: 10.1126/science.aal1647. PMID: 28839045.

Moreno RD, Schatten G, Ramalho-Santos J. Golgi apparatus dynamics during mouse oocyte in vitro maturation: effect of the membrane trafficking inhibitor brefeldin A. Biol Reprod. 2002 May;66(5):1259-66. doi: 10.1095/biolreprod66.5.1259. PMID: 11967185.

Mueck AO, Ruan X, Seeger H, Fehm T, Neubauer H. Genomic and non-genomic actions of progestogens in the breast. J Steroid Biochem Mol Biol. 2014 Jul;142:62-7.

Mulac-Jericevic B, Lydon JP, DeMayo FJ, Conneely OM. Defective mammary gland morphogenesis in mice lacking the progesterone receptor B isoform. Proc Natl Acad Sci U S A. 2003 Aug 19;100(17):9744-9. doi: 10.1073/pnas.1732707100. Epub 2003 Aug 1. PMID: 12897242; PMCID: PMC187836.

Mulac-Jericevic B, Mullinax RA, DeMayo FJ, Lydon JP, Conneely OM. Subgroup of reproductive functions of progesterone mediated by progesterone receptor-B isoform. Science. 2000 Sep 8;289(5485):1751-4. doi: 10.1126/science.289.5485.1751. PMID: 10976068.

Nacht AS, Pohl A, Zaurin R, Soronellas D, Quilez J, Sharma P, Wright RH, Beato M, Vicent GP. Hormone-induced repression of genes requires BRG1-mediated H1.2 deposition at target promoters. EMBO J. 2016 Aug 15;35(16):1822-43. doi: 10.15252/embj.201593260. Epub 2016 Jul 7. PMID: 27390128; PMCID: PMC5010049.

Nagano M, Kang SS, Koyama K, Huang W, Yanagawa Y, Takahashi Y. In vitro maturation system for individual culture of bovine oocytes using micro-volume multi-well plate. Jpn J Vet Res. 2013 Nov;61(4):149-54. PMID: 24404749.

Nagano M, Katagiri S, Takahashi Y. ATP content and maturational/developmental ability of bovine oocytes with various cytoplasmic morphologies. Zygote. 2006 Nov;14(4):299-304. doi: 10.1017/S0967199406003807. PMID: 17266788.
Nagano M, Katagiri S, Takahashi Y. Relationship between bovine oocyte morphology and in vitro developmental potential. Zygote. 2006 Feb;14(1):53-61. doi: 10.1017/S0967199406003510. PMID: 16700976.

Nasser LF, Sá Filho MF, Reis EL, Rezende CR, Mapletoft RJ, Bó GA, Baruselli PS. Exogenous progesterone enhances ova and embryo quality following superstimulation of the first follicular wave in Nelore (Bos indicus) donors. Theriogenology. 2011 Jul 15;76(2):320-7. doi: 10.1016/j.theriogenology.2011.02.009. Epub 2011 Apr 14. PMID: 21496903.

Niswender GD. Molecular control of luteal secretion of progesterone. Reproduction. 2002 Mar;123(3):333-9. doi: 10.1530/rep.0.1230333. PMID: 11882010.

Niswender GD. Response of the corpus luteum to luteinizing hormone. Environ Health Perspect. 1981 Apr;38:47-50. doi: 10.1289/ehp.813847. PMID: 6263609; PMCID: PMC1568440.

Nolfi-Donegan D, Braganza A, Shiva S. Mitochondrial electron transport chain: Oxidative phosphorylation, oxidant production, and methods of measurement. Redox Biol. 2020 Oct;37:101674. doi: 10.1016/j.redox.2020.101674. Epub 2020 Aug 6. PMID: 32811789; PMCID: PMC7767752.

Nuttinck F, Marquant-Le Guienne B, Clément L, Reinaud P, Charpigny G, Grimard B. Expression of genes involved in prostaglandin E2 and progesterone production in bovine cumulus-oocyte complexes during in vitro maturation and fertilization. Reproduction. 2008 May;135(5):593-603. doi: 10.1530/REP-07-0453. PMID: 18411408.

O'Shea LC, Hensey C, Fair T. Progesterone regulation of AVEN protects bovine oocytes from apoptosis during meiotic maturation. Biol Reprod. 2013 Dec 26;89(6):146. doi: 10.1095/biolreprod.113.111880. PMID: 24174577.

Oktay K, Briggs D, Gosden RG. Ontogeny of follicle-stimulating hormone receptor gene expression in isolated human ovarian follicles. J Clin Endocrinol Metab. 1997 Nov;82(11):3748-51. doi: 10.1210/jcem.82.11.4346. PMID: 9360535.

Paulini F, Melo EO. The role of oocyte-secreted factors GDF9 and BMP15 in follicular development and oogenesis. Reprod Domest Anim. 2011 Apr;46(2):354-61. doi: 10.1111/j.1439-0531.2010.01739.x. Epub 2010 Dec 30. PMID: 21198974.

Payne C, Schatten G. Golgi dynamics during meiosis are distinct from mitosis and are coupled to endoplasmic reticulum dynamics until fertilization. Dev Biol. 2003 Dec 1;264(1):50-63. doi: 10.1016/j.ydbio.2003.08.004. PMID: 14623231.

Peavey MC, Wu SP, Li R, Liu J, Emery OM, Wang T, Zhou L, Wetendorf M, Yallampalli C, Gibbons WE, Lydon JP, DeMayo FJ. Progesterone receptor isoform B regulates the Oxtr-Plcl2-Trpc3 pathway to suppress uterine contractility. Proc Natl Acad Sci U S A. 2021 Mar 16;118(11):e2011643118. doi: 10.1073/pnas.2011643118. PMID: 33707208; PMCID: PMC7980420.

Pfanner N, Warscheid B, Wiedemann N. Mitochondrial proteins: from biogenesis to functional networks. Nat Rev Mol Cell Biol. 2019 May;20(5):267-284. doi: 10.1038/s41580-018-0092-0. Erratum in: Nat Rev Mol Cell Biol. 2021 May;22(5):367. doi: 10.1038/s41580-021-00361-x. PMID: 30626975; PMCID: PMC6684368.

Phillips MJ, Voeltz GK. Structure and function of ER membrane contact sites with other organelles. Nat Rev Mol Cell Biol. 2016 Feb;17(2):69-82. doi: 10.1038/nrm.2015.8. Epub 2015 Dec 2. PMID: 26627931; PMCID: PMC5117888.

Picton H, Briggs D, Gosden R. The molecular basis of oocyte growth and development. Mol Cell Endocrinol. 1998 Oct 25;145(1-2):27-37. doi: 10.1016/s0303-7207(98)00166-x. PMID: 9922096.

Pincus G, Enzmann EV. The comparative behavior of mammalian eggs in vivo and in vitro: i. the activation of ovarian eggs. J Exp Med. 1935 Oct 31;62(5):665-75. doi: 10.1084/jem.62.5.665. PMID: 19870440; PMCID: PMC2133299.

Pisarska MD, Carson SA, Casson PR, Tong X, Buster JE, Kieback DG. A mutated progesterone receptor allele is more prevalent in unexplained infertility. Fertil Steril. 2003 Sep;80(3):651-3. doi: 10.1016/s0015-0282(03)00755-6. PMID: 12969718.

Pratt WB, Silverstein AM, Galigniana MD. A model for the cytoplasmic trafficking of signalling proteins involving the hsp90-binding immunophilins and p50cdc37. Cell Signal. 1999 Dec;11(12):839-51. doi: 10.1016/s0898-6568(99)00064-9. PMID: 10659992.

Pratt WB, Toft DO. Steroid receptor interactions with heat shock protein and immunophilin chaperones. Endocr Rev. 1997 Jun;18(3):306-60. doi: 10.1210/edrv.18.3.0303. PMID: 9183567.

Press MF, Greene GL. Localization of progesterone receptor with monoclonal antibodies to the human progestin receptor. Endocrinology. 1988 Mar;122(3):1165-75. doi: 10.1210/endo-122-3-1165. PMID: 3342750.

Rajakoski E. The ovarian follicular system in sexually mature heifers with special reference to seasonal, cyclical, end left-right variations. Acta Endocrinol Suppl (Copenh). 1960;34(Suppl 52):1-68. PMID: 14435925.

Rapoport R, Sklan D, Wolfenson D, Shaham-Albalancy A, Hanukoglu I. Antioxidant capacity is correlated with steroidogenic status of the corpus luteum during the bovine estrous cycle. Biochim Biophys Acta. 1998 Mar 12;1380(1):133-40. doi: 10.1016/s0304-4165(97)00136-0. PMID: 9545562.

Rasband, W.S., ImageJ, U. S. National Institutes of Health, Bethesda, Maryland, USA, https://imagej.net/ij/, 1997-2018.

Revelli A, Pacchioni D, Cassoni P, Bussolati G, Massobrio M. In situ hybridization study of messenger RNA for estrogen receptor and immunohistochemical detection of estrogen and progesterone receptors in the human ovary. Gynecol Endocrinol. 1996 Jun;10(3):177-86. doi: 10.3109/09513599609027986. PMID: 8862493.

Reynier P, May-Panloup P, Chrétien MF, Morgan CJ, Jean M, Savagner F, Barrière P, Malthièry Y. Mitochondrial DNA content affects the fertilizability of human oocytes. Mol Hum Reprod. 2001 May;7(5):425-9. doi: 10.1093/molehr/7.5.425. PMID: 11331664.

Richani D, Dunning KR, Thompson JG, Gilchrist RB. Metabolic co-dependence of the oocyte and cumulus cells: essential role in determining oocyte developmental competence. Hum Reprod Update. 2021 Jan 4;27(1):27-47. doi: 10.1093/humupd/dmaa043. PMID: 33020823.

Rivera FA, Mendonça LG, Lopes G Jr, Santos JE, Perez RV, Amstalden M, Correa-Calderón A, Chebel RC. Reduced progesterone concentration during growth of the first follicular wave

affects embryo quality but has no effect on embryo survival post transfer in lactating dairy cows. Reproduction. 2011 Mar;141(3):333-42. doi: 10.1530/REP-10-0375. Epub 2010 Dec 22. PMID: 21177956.

Rizos D, Ward F, Duffy P, Boland MP, Lonergan P. Consequences of bovine oocyte maturation, fertilization or early embryo development in vitro versus in vivo: implications for blastocyst yield and blastocyst quality. Mol Reprod Dev. 2002 Feb;61(2):234-48. doi: 10.1002/mrd.1153. PMID: 11803560.

Robker RL, Akison LK, Russell DL. Control of oocyte release by progesterone receptor-regulated gene expression. Nucl Recept Signal. 2009 Dec 31;7:e012. doi: 10.1621/nrs.07012. PMID: 20087433; PMCID: PMC2807638.

Robker RL, Russell DL, Espey LL, Lydon JP, O'Malley BW, Richards JS. Progesterone-regulated genes in the ovulation process: ADAMTS-1 and cathepsin L proteases. Proc Natl Acad Sci U S A. 2000 Apr 25;97(9):4689-94. doi: 10.1073/pnas.080073497. PMID: 10781075; PMCID: PMC18294.

Roche JF, Austin EJ, Ryan M, O'Rourke M, Mihm M, Diskin MG. Regulation of follicle waves to maximize fertility in cattle. J Reprod Fertil Suppl. 1999;54:61-71. PMID: 10692845.

Roche JF. Control and regulation of folliculogenesis--a symposium in perspective. Rev Reprod. 1996 Jan;1(1):19-27. doi: 10.1530/ror.0.0010019. PMID: 9414434.

Rodgers RJ, Irving-Rodgers HF. Morphological classification of bovine ovarian follicles. Reproduction. 2010 Feb;139(2):309-18. doi: 10.1530/REP-09-0177. Epub 2009 Sep 28. PMID: 19786400.

Rodríguez-Nuevo A, Torres-Sanchez A, Duran JM, De Guirior C, Martínez-Zamora MA, Böke E. Oocytes maintain ROS-free mitochondrial metabolism by suppressing complex I. Nature. 2022 Jul;607(7920):756-761. doi: 10.1038/s41586-022-04979-5. Epub 2022 Jul 20. PMID: 35859172; PMCID: PMC9329100.

Roh SI, Batten BE, Friedman CI, Kim MH. The effects of progesterone antagonist RU 486 on mouse oocyte maturation, ovulation, fertilization, and cleavage. Am J Obstet Gynecol. 1988 Dec;159(6):1584-9. doi: 10.1016/0002-9378(88)90599-6. PMID: 3207135.

Rubel CA, Lanz RB, Kommagani R, Franco HL, Lydon JP, DeMayo FJ. Research resource: Genome-wide profiling of progesterone receptor binding in the mouse uterus. Mol Endocrinol. 2012 Aug;26(8):1428-42. doi: 10.1210/me.2011-1355. Epub 2012 May 25. PMID: 22638070; PMCID: PMC3404303.

Rueda BR, Hendry IR, Hendry III WJ, Stormshak F, Slayden OD, Davis JS. Decreased progesterone levels and progesterone receptor antagonists promote apoptotic cell death in

bovine luteal cells. Biol Reprod. 2000 Feb;62(2):269-76. doi: 10.1095/biolreprod62.2.269. PMID: 10642562.

Rutter J, Winge DR, Schiffman JD. Succinate dehydrogenase - Assembly, regulation and role in human disease. Mitochondrion. 2010 Jun;10(4):393-401. doi: 10.1016/j.mito.2010.03.001. Epub 2010 Mar 10. PMID: 20226277; PMCID: PMC2874626.

Salehnia M, Zavareh S. The effects of progesterone on oocyte maturation and embryo development. Int J Fertil Steril. 2013 Jul;7(2):74-81. Epub 2013 Jul 31. PMID: 24520467; PMCID: PMC3850344.

Sánchez JM, Simintiras CA, Lonergan P. Aspects of embryo-maternal communication in establishment of pregnancy in cattle. Anim Reprod. 2019 Oct 22;16(3):376-385. doi: 10.21451/1984-3143-AR2019-0075. PMID: 32435281; PMCID: PMC7234086.

Saner KJ, Welter BH, Zhang F, Hansen E, Dupont B, Wei Y, Price TM. Cloning and expression of a novel, truncated, progesterone receptor. Mol Cell Endocrinol. 2003 Feb 28;200(1-2):155-63. doi: 10.1016/s0303-7207(02)00380-5. PMID: 12644308.

Santos JE, Thatcher WW, Chebel RC, Cerri RL, Galvão KN. The effect of embryonic death rates in cattle on the efficacy of estrus synchronization programs. Anim Reprod Sci. 2004 Jul;82-83:513-35. doi: 10.1016/j.anireprosci.2004.04.015. PMID: 15271477.

Savio JD, Keenan L, Boland MP, Roche JF. Pattern of growth of dominant follicles during the oestrous cycle of heifers. J Reprod Fertil. 1988 Jul;83(2):663-71. doi: 10.1530/jrf.0.0830663. PMID: 3045306.

Schally AV, Arimura A, Kastin AJ, Matsuo H, Baba Y, Redding TW, Nair RM, Debeljuk L, White WF. Gonadotropin-releasing hormone: one polypeptide regulates secretion of luteinizing and follicle-stimulating hormones. Science. 1971 Sep 10;173(4001):1036-8. doi: 10.1126/science.173.4001.1036. PMID: 4938639.

Schneider CA, Rasband WS, Eliceiri KW. NIH Image to ImageJ: 25 years of image analysis. Nat Methods. 2012 Jul;9(7):671-5. doi: 10.1038/nmeth.2089. PMID: 22930834; PMCID: PMC5554542.

Schoenfelder M, Schams D, Einspanier R. Steroidogenesis during in vitro maturation of bovine cumulus oocyte complexes and possible effects of tri-butyltin on granulosa cells. J Steroid Biochem Mol Biol. 2003 Feb;84(2-3):291-300. doi: 10.1016/s0960-0760(03)00042-6. PMID: 12711015.

Schuh M, Ellenberg J. Self-organization of MTOCs replaces centrosome function during acentrosomal spindle assembly in live mouse oocytes. Cell. 2007 Aug 10;130(3):484-98. doi: 10.1016/j.cell.2007.06.025. PMID: 17693257.

Shaia KL, Harris BS, Selter JH, Price TM. Reproductive Functions of the Mitochondrial Progesterone Receptor (PR-M). Reprod Sci. 2023 May;30(5):1443-1452. doi: 10.1007/s43032-022-01092-w. Epub 2022 Oct 18. PMID: 36255658.

Shoubridge EA, Wai T. Mitochondrial DNA and the mammalian oocyte. Curr Top Dev Biol. 2007;77:87-111. doi: 10.1016/S0070-2153(06)77004-1. PMID: 17222701.

Sirard MA. Resumption of meiosis: mechanism involved in meiotic progression and its relation with developmental competence. Theriogenology. 2001 Apr 1;55(6):1241-54. doi: 10.1016/s0093-691x(01)00480-0. PMID: 11327682.

Słomczyńska M, Krok M, Pierściński A. Localization of the progesterone receptor in the porcine ovary. Acta Histochem. 2000 May;102(2):183-91. doi: 10.1078/S0065-1281(04)70027-6. PMID: 10824611.

Smith GD. In vitro maturation of oocytes. Curr Womens Health Rep. 2001 Oct;1(2):143-51. PMID: 12112961.

Smith KM, Dinh DT, Akison LK, Nicholls M, Dunning KR, Morimoto A, Lydon JP, Russell DL, Robker RL. Intraovarian, Isoform-Specific Transcriptional Roles of Progesterone Receptor in Ovulation. Cells. 2022 May 5;11(9):1563. doi: 10.3390/cells11091563. PMID: 35563869; PMCID: PMC9105733.

Smith LC, Alcivar AA. Cytoplasmic inheritance and its effects on development and performance. J Reprod Fertil Suppl. 1993;48:31-43. PMID: 8145213.

Sousa JS, D'Imprima E, Vonck J. Mitochondrial Respiratory Chain Complexes. Subcell Biochem. 2018;87:167-227. doi: 10.1007/978-981-10-7757-9_7. PMID: 29464561.

Stevenson JS, Pursley JR, Garverick HA, Fricke PM, Kesler DJ, Ottobre JS, Wiltbank MC. Treatment of cycling and noncycling lactating dairy cows with progesterone during Ovsynch. J Dairy Sci. 2006 Jul;89(7):2567-78. doi: 10.3168/jds.S0022-0302(06)72333-5. PMID: 16772576.

Stevenson JS, Tenhouse DE, Krisher RL, Lamb GC, Larson JE, Dahlen CR, Pursley JR, Bello NM, Fricke PM, Wiltbank MC, Brusveen DJ, Burkhart M, Youngquist RS, Garverick HA. Detection of anovulation by heatmount detectors and transrectal ultrasonography before treatment with progesterone in a timed insemination protocol. J Dairy Sci. 2008 Jul;91(7):2901-15. doi: 10.3168/jds.2007-0856. PMID: 18565948.

Stojkovic M, Machado SA, Stojkovic P, Zakhartchenko V, Hutzler P, Gonçalves PB, Wolf E. Mitochondrial distribution and adenosine triphosphate content of bovine oocytes before and after in vitro maturation: correlation with morphological criteria and developmental capacity after in vitro fertilization and culture. Biol Reprod. 2001 Mar;64(3):904-9. doi: 10.1095/biolreprod64.3.904. PMID: 11207207.

Stricker SA. Structural reorganizations of the endoplasmic reticulum during egg maturation and fertilization. Semin Cell Dev Biol. 2006 Apr;17(2):303-13. doi: 10.1016/j.semcdb.2006.02.002. Epub 2006 Feb 23. PMID: 16546418.

Stroebech L, Gianluca M, Hanne P, Kristine F, Haja K, Henrik C, Hyttel, P. In vitro production of bovine embryos: revisiting oocyte development and application of systems biology. Animal reproduction. 2015 12. 465-472.

Sun F, Huo X, Zhai Y, Wang A, Xu J, Su D, Bartlam M, Rao Z. Crystal structure of mitochondrial respiratory membrane protein complex II. Cell. 2005 Jul 1;121(7):1043-57. doi: 10.1016/j.cell.2005.05.025. PMID: 15989954.

Sun QY, Schatten H. Regulation of dynamic events by microfilaments during oocyte maturation and fertilization. Reproduction. 2006 Feb;131(2):193-205. doi: 10.1530/rep.1.00847. PMID: 16452714.

Sun QY, Schatten H. Regulation of dynamic events by microfilaments during oocyte maturation and fertilization. Reproduction. 2006 Feb;131(2):193-205. doi: 10.1530/rep.1.00847. PMID: 16452714.

Sunderland SJ, Crowe MA, Boland MP, Roche JF, Ireland JJ. Selection, dominance and atresia of follicles during the oestrous cycle of heifers. J Reprod Fertil. 1994 Aug;101(3):547-55.

Susor A, Jansova D, Anger M, Kubelka M. Translation in the mammalian oocyte in space and time. Cell Tissue Res. 2016 Jan;363(1):69-84. doi: 10.1007/s00441-015-2269-6. Epub 2015 Sep 4. PMID: 26340983.

Suzuki T, Sasano H, Kimura N, Tamura M, Fukaya T, Yajima A, Nagura H. Immunohistochemical distribution of progesterone, androgen and oestrogen receptors in the human ovary during the menstrual cycle: relationship to expression of steroidogenic enzymes. Hum Reprod. 1994 Sep;9(9):1589-95. doi: 10.1093/oxfordjournals.humrep.a138757. PMID: 7836505.

Svensson EC, Markström E, Andersson M, Billig H. Progesterone receptor-mediated inhibition of apoptosis in granulosa cells isolated from rats treated with human chorionic gonadotropin. Biol Reprod. 2000 Nov;63(5):1457-64. doi: 10.1095/biolreprod63.5.1457. PMID: 11058552.

Svensson EC, Markström E, Shao R, Andersson M, Billig H. Progesterone receptor antagonists Org 31710 and RU 486 increase apoptosis in human periovulatory granulosa cells. Fertil Steril. 2001 Dec;76(6):1225-31. doi: 10.1016/s0015-0282(01)02891-6. PMID: 11730755.

Szabo I, Szewczyk A. Mitochondrial Ion Channels. Annu Rev Biophys. 2023 May 9;52:229-254. doi: 10.1146/annurev-biophys-092622-094853. PMID: 37159294.

Tamassia M, Nuttinck F, May-Panloup P, Reynier P, Heyman Y, Charpigny G, Stojkovic M, Hiendleder S, Renard JP, Chastant-Maillard S. In vitro embryo production efficiency in cattle and its association with oocyte adenosine triphosphate content, quantity of mitochondrial DNA, and mitochondrial DNA haplogroup. Biol Reprod. 2004 Aug;71(2):697-704. doi: 10.1095/biolreprod.103.026104. Epub 2004 Apr 14. PMID: 15084486.

Tarazona AM, Rodríguez JI, Restrepo LF, Olivera-Angel M. Mitochondrial activity, distribution and segregation in bovine oocytes and in embryos produced in vitro. Reprod Domest Anim. 2006 Feb;41(1):5-11. doi: 10.1111/j.1439-0531.2006.00615.x. PMID: 16420320.

Teilmann SC, Clement CA, Thorup J, Byskov AG, Christensen ST. Expression and localization of the progesterone receptor in mouse and human reproductive organs. J Endocrinol. 2006 Dec;191(3):525-35. doi: 10.1677/joe.1.06565. PMID: 17170211.

Telfer EE, Grosbois J, Odey YL, Rosario R, Anderson RA. Making a good egg: human oocyte health, aging, and in vitro development. Physiol Rev. 2023 Oct 1;103(4):2623-2677. doi: 10.1152/physrev.00032.2022. Epub 2023 May 12. PMID: 37171807; PMCID: PMC10625843.

Terzaghi L, Tessaro I, Raucci F, Merico V, Mazzini G, Garagna S, Zuccotti M, Franciosi F, Lodde V. PGRMC1 participates in late events of bovine granulosa cells mitosis and oocyte meiosis. Cell Cycle. 2016 Aug 2;15(15):2019-32.

Tetsuka M, Tanakadate M. Activation of HSD11B1 in the bovine cumulus-oocyte complex during IVM and IVF. Endocr Connect. 2019 Jul;8(7):1029-1039. doi: 10.1530/EC-19-0188. PMID: 31252401; PMCID: PMC6652248.

Thackray VG, Toft DO, Nordeen SK. Novel activation step required for transcriptional competence of progesterone receptor on chromatin templates. Mol Endocrinol. 2003 Dec;17(12):2543-53. doi: 10.1210/me.2003-0200. Epub 2003 Oct 9. PMID: 14551264.

Timón-Gómez A, Nývltová E, Abriata LA, Vila AJ, Hosler J, Barrientos A. Mitochondrial cytochrome c oxidase biogenesis: Recent developments. Semin Cell Dev Biol. 2018 Apr;76:163-178. doi: 10.1016/j.semcdb.2017.08.055. Epub 2017 Sep 8. PMID: 28870773; PMCID: PMC5842095.

Thomas P. Membrane Progesterone Receptors (mPRs, PAQRs): Review of Structural and Signaling Characteristics. Cells. 2022 May 30;11(11):1785. doi: 10.3390/cells11111785. PMID: 35681480; PMCID: PMC9179843.Trounson A, Anderiesz C, Jones G. Maturation of human oocytes in vitro and their developmental competence. Reproduction. 2001 Jan;121(1):51-75. doi: 10.1530/rep.0.1210051. PMID: 11226029.

Uzbekova S, Arlot-Bonnemains Y, Dupont J, Dalbiès-Tran R, Papillier P, Pennetier S, Thélie A, Perreau C, Mermillod P, Prigent C, Uzbekov R. Spatio-temporal expression patterns of aurora kinases a, B, and C and cytoplasmic polyadenylation-element-binding protein in bovine oocytes during meiotic maturation. Biol Reprod. 2008 Feb;78(2):218-33. doi: 10.1095/biolreprod.107.061036. Epub 2007 Aug 8. PMID: 17687118.

Van Blerkom J, Davis P, Alexander S. Differential mitochondrial distribution in human pronuclear embryos leads to disproportionate inheritance between blastomeres: relationship to microtubular organization, ATP content and competence. Hum Reprod. 2000 Dec;15(12):2621-33. doi: 10.1093/humrep/15.12.2621. PMID: 11098036.

Van Blerkom J. Mitochondria in human oogenesis and preimplantation embryogenesis: engines of metabolism, ionic regulation and developmental competence. Reproduction. 2004 Sep;128(3):269-80. doi: 10.1530/rep.1.00240. PMID: 15333778.

Van den Broeck W, D'haeseleer M, Coryn M, Simoens P. Cell-specific distribution of progesterone receptors in the bovine ovary. Reprod Domest Anim. 2002 Oct;37(5):314-20. doi: 10.1046/j.1439-0531.2002.00366.x. PMID: 12354187.

van der Reest J, Nardini Cecchino G, Haigis MC, Kordowitzki P. Mitochondria: Their relevance during oocyte ageing. Ageing Res Rev. 2021 Sep;70:101378. doi: 10.1016/j.arr.2021.101378. Epub 2021 Jun 4. PMID: 34091076.

Vermeirsch H, Simoens P, Lauwers H. Immunohistochemical detection of the estrogen receptor-alpha and progesterone receptor in the canine pregnant uterus and placental labyrinth. Anat Rec. 2000 Sep 1;260(1):42-50. doi: 10.1002/1097-0185(20000901)260:1<42::AID-AR50>3.0.CO;2-8. PMID: 10967535.

Vicent GP, Ballaré C, Nacht AS, Clausell J, Subtil-Rodríguez A, Quiles I, Jordan A, Beato M. Induction of progesterone target genes requires activation of Erk and Msk kinases and phosphorylation of histone H3. Mol Cell. 2006 Nov 3;24(3):367-81. doi: 10.1016/j.molcel.2006.10.011. PMID: 17081988.

Vicent GP, Nacht AS, Font-Mateu J, Castellano G, Gaveglia L, Ballaré C, Beato M. Four enzymes cooperate to displace histone H1 during the first minute of hormonal gene activation. Genes Dev. 2011 Apr 15;25(8):845-62. doi: 10.1101/gad.621811. Epub 2011 Mar 29. PMID: 21447625; PMCID: PMC3078709.

Vicent GP, Nacht AS, Zaurin R, Font-Mateu J, Soronellas D, Le Dily F, Reyes D, Beato M. Unliganded progesterone receptor-mediated targeting of an RNA-containing repressive complex silences a subset of hormone-inducible genes. Genes Dev. 2013 May 15;27(10):1179-97. doi: 10.1101/gad.215293.113. PMID: 23699411; PMCID: PMC3672650.

Vicent GP, Zaurin R, Nacht AS, Font-Mateu J, Le Dily F, Beato M. Nuclear factor 1 synergizes with progesterone receptor on the mouse mammary tumor virus promoter wrapped around a histone H3/H4 tetramer by facilitating access to the central hormone-responsive elements. J Biol Chem. 2010 Jan 22;285(4):2622-31. doi: 10.1074/jbc.M109.060848. Epub 2009 Nov 24. PMID: 19940123; PMCID: PMC2807319.

Vicent GP, Zaurin R, Nacht AS, Li A, Font-Mateu J, Le Dily F, Vermeulen M, Mann M, Beato M. Two chromatin remodeling activities cooperate during activation of hormone responsive promoters. PLoS Genet. 2009 Jul;5(7):e1000567. doi: 10.1371/journal.pgen.1000567. Epub 2009 Jul 17. PMID: 19609353; PMCID: PMC2704372.

Wai T, Teoli D, Shoubridge EA. The mitochondrial DNA genetic bottleneck results from replication of a subpopulation of genomes. Nat Genet. 2008 Dec;40(12):1484-8. doi: 10.1038/ng.258. PMID: 19029901.

Walsh SW, Williams EJ, Evans AC. A review of the causes of poor fertility in high milk producing dairy cows. Anim Reprod Sci. 2011 Feb;123(3-4):127-38. doi: 10.1016/j.anireprosci.2010.12.001. Epub 2010 Dec 30. PMID: 21255947; PMCID: PMC7125520.

Wang L, Tang J, Wang L, Tan F, Song H, Zhou J, Li F. Oxidative stress in oocyte aging and female reproduction. J Cell Physiol. 2021 Dec;236(12):7966-7983. doi: 10.1002/jcp.30468. Epub 2021 Jun 14. PMID: 34121193.

Weck J, Fallest PC, Pitt LK, Shupnik MA. Differential gonadotropin-releasing hormone stimulation of rat luteinizing hormone subunit gene transcription by calcium influx and mitogen-activated protein kinase-signaling pathways. Mol Endocrinol. 1998 Mar;12(3):451-7. doi: 10.1210/mend.12.3.0070. PMID: 9514161.

Wen DX, Xu YF, Mais DE, Goldman ME, McDonnell DP. The A and B isoforms of the human progesterone receptor operate through distinct signaling pathways within target cells. Mol Cell Biol. 1994 Dec;14(12):8356-64. doi: 10.1128/mcb.14.12.8356-8364.1994. PMID: 7969170; PMCID: PMC359374.

Wen DX, Xu YF, Mais DE, Goldman ME, McDonnell DP. The A and B isoforms of the human progesterone receptor operate through distinct signaling pathways within target cells. Mol Cell Biol. 1994 Dec;14(12):8356-64. doi: 10.1128/mcb.14.12.8356-8364.1994. PMID: 7969170; PMCID: PMC359374.

Wiltbank MC, Belfiore CJ, Niswender GD. Steroidogenic enzyme activity after acute activation of protein kinase (PK) A and PKC in ovine small and large luteal cells. Mol Cell Endocrinol. 1993 Nov;97(1-2):1-7. doi: 10.1016/0303-7207(93)90205-x. PMID: 8143891.

Wiltbank MC, Souza AH, Carvalho PD, Bender RW, Nascimento AB. Improving fertility to timed artificial insemination by manipulation of circulating progesterone concentrations in

lactating dairy cattle. Reprod Fertil Dev. 2011;24(1):238-43. doi: 10.1071/RD11913. PMID: 22394964.

Wright RH, Castellano G, Bonet J, Le Dily F, Font-Mateu J, Ballaré C, Nacht AS, Soronellas D, Oliva B, Beato M. CDK2-dependent activation of PARP-1 is required for hormonal gene regulation in breast cancer cells. Genes Dev. 2012 Sep 1;26(17):1972-83. doi: 10.1101/gad.193193.112. PMID: 22948662; PMCID: PMC3435499.

Wu YK, Fan HY. Revisiting ZAR proteins: the understudied regulator of female fertility and beyond. Cell Mol Life Sci. 2022 Jan 24;79(2):92. doi: 10.1007/s00018-022-04141-4. PMID: 35072788; PMCID: PMC11071961.

Xin QL, Qiu JT, Cui S, Xia GL, Wang HB. Transcriptional activation of nuclear estrogen receptor and progesterone receptor and its regulation. Sheng Li Xue Bao. 2016 Aug 25;68(4):435-54. PMID: 27546504.

Yadav PK, Tiwari M, Gupta A, Sharma A, Prasad S, Pandey AN, Chaube SK. Germ cell depletion from mammalian ovary: possible involvement of apoptosis and autophagy. J Biomed Sci. 2018 Apr 23;25(1):36. doi: 10.1186/s12929-018-0438-0. PMID: 29681242; PMCID: PMC5911955.

Yang X, Zaurin R, Beato M, Peterson CL. Swi3p controls SWI/SNF assembly and ATP-dependent H2A-H2B displacement. Nat Struct Mol Biol. 2007 Jun;14(6):540-7. doi: 10.1038/nsmb1238. Epub 2007 May 13. PMID: 17496903.

Young JM, McNeilly AS. Theca: the forgotten cell of the ovarian follicle. Reproduction. 2010 Oct;140(4):489-504. doi: 10.1530/REP-10-0094. Epub 2010 Jul 13. PMID: 20628033.

Yu XJ, Yi Z, Gao Z, Qin D, Zhai Y, Chen X, Ou-Yang Y, Wang ZB, Zheng P, Zhu MS, Wang H, Sun QY, Dean J, Li L. The subcortical maternal complex controls symmetric division of mouse zygotes by regulating F-actin dynamics. Nat Commun. 2014 Sep 11;5:4887. doi: 10.1038/ncomms5887. PMID: 25208553; PMCID: PMC6529946.

Zaffagnini G, Cheng S, Salzer MC, Pernaute B, Duran JM, Irimia M, Schuh M, Böke E. Mouse oocytes sequester aggregated proteins in degradative super-organelles. Cell. 2024 Feb 29;187(5):1109-1126.e21. doi: 10.1016/j.cell.2024.01.031. Epub 2024 Feb 20. PMID: 38382525.

Zhang KH, Zou YJ, Shan MM, Pan ZN, Ju JQ, Liu JC, Ji YM, Sun SC. Arf1 GTPase Regulates Golgi-Dependent G2/M Transition and Spindle Organization in Oocyte Meiosis. Adv Sci (Weinh). 2024 Jan;11(4):e2303009. doi: 10.1002/advs.202303009. Epub 2023 Nov 28. PMID: 38014604; PMCID: PMC10811507.

Zhang M, Su YQ, Sugiura K, Xia G, Eppig JJ. Granulosa cell ligand NPPC and its receptor NPR2 maintain meiotic arrest in mouse oocytes. Science. 2010 Oct 15;330(6002):366-9. doi: 10.1126/science.1193573. PMID: 20947764; PMCID: PMC3056542.

Zhao RZ, Jiang S, Zhang L, Yu ZB. Mitochondrial electron transport chain, ROS generation and uncoupling (Review). Int J Mol Med. 2019 Jul;44(1):3-15. doi: 10.3892/ijmm.2019.4188. Epub 2019 May 8. PMID: 31115493; PMCID: PMC6559295.

Zhu Y, Bond J, Thomas P. Identification, classification, and partial characterization of genes in humans and other vertebrates homologous to a fish membrane progestin receptor. Proc Natl Acad Sci U S A. 2003 Mar 4;100(5):2237-42. doi: 10.1073/pnas.0436133100. Epub 2003 Feb 24. PMID: 12601167; PMCID: PMC151324.